

UNCLASSIFIED

AD NUMBER

AD832710

LIMITATION CHANGES

TO:

Approved for public release; distribution is unlimited.

FROM:

Distribution authorized to U.S. Gov't. agencies and their contractors; Critical Technology; MAY 1968. Other requests shall be referred to Ogden Air Materiel Area, Attn: OOEYEC, Hill AFB, UT 84401. This document contains export-controlled technical data.

AUTHORITY

OOY USAF ltr, 22 Jul 1971

THIS PAGE IS UNCLASSIFIED



STATIC STABILITY TESTS OF THE M-117 BOMB AT MACH NUMBERS FROM 0.55 TO 1.30 WITH SEVEN TAIL FIN CONFIGURATIONS

Paul Lehner

ARO, Inc.

May 1968

~~This document is subject to special export controls and such transmittal to foreign governments or foreign nationals may be made only with prior approval of Ogden Air Materiel Area (OOYEC), Hill AFB, Utah 84101.~~

APPROVED FOR PUBLIC RELEASE: DISTRIBUTION
UNLIMITED (PER DDC-TAB-71-21, 1 Nov 71)

**PROPULSION WIND TUNNEL FACILITY
ARNOLD ENGINEERING DEVELOPMENT CENTER
AIR FORCE SYSTEMS COMMAND
ARNOLD AIR FORCE STATION, TENNESSEE**

PROPERTY OF U. S. AIR FORCE
AEDC LIBRARY
AF 40(600)1200

AEDC TECHNICAL LIBRARY



S 0720 00031 7356

NOTICES

When U. S. Government drawings specifications, or other data are used for any purpose other than a definitely related Government procurement operation, the Government thereby incurs no responsibility nor any obligation whatsoever, and the fact that the Government may have formulated, furnished, or in any way supplied the said drawings, specifications, or other data, is not to be regarded by implication or otherwise, or in any manner licensing the holder or any other person or corporation, or conveying any rights or permission to manufacture, use, or sell any patented invention that may in any way be related thereto.

Qualified users may obtain copies of this report from the Defense Documentation Center.

References to named commercial products in this report are not to be considered in any sense as an endorsement of the product by the United States Air Force or the Government.

STATIC STABILITY TESTS OF THE M-117 BOMB AT
MACH NUMBERS FROM 0.55 TO 1.30 WITH
SEVEN TAIL FIN CONFIGURATIONS

Paul Lehner
ARO, Inc.

~~This document is subject to special export controls and each transmittal to foreign governments or foreign nationals may be made only with prior approval of Ogden Air Materiel Area (OOYEC), Hill AFB, Utah 84001.~~

APPROVED FOR PUBLIC RELEASE: DISTRIBUTION
UNLIMITED (PER DDC-TAB-71-21, 1 Nov 71)

FOREWORD

The test reported herein was sponsored by the Air Force Logistics Command (AFLC) under Program Element 6441514F.

The results of the test were obtained by ARO, Inc. (a subsidiary of Sverdrup & Parcel and Associates, Inc.), contract operator of the Arnold Engineering Development Center (AEDC), AFSC, Arnold Air Force Station, Tennessee, under Contract AF40(600)-1200. The tests were conducted from February 26 through March 1, 1968, under ARO Project No. PC0871, and the manuscript was submitted for publication on April 15, 1968.

Information in this report is embargoed under the Department of State International Traffic in Arms Regulations. This report may be released to foreign governments by departments or agencies of the U. S. Government subject to approval of Ogden Air Materiel Area (OOYEC), or higher authority within the Department of the Air Force. Private individuals or firms require a Department of State export license.

This technical report has been reviewed and is approved.

Richard W. Bradley
Lt Col, USAF
Directorate of Test

Roy R. Croy, Jr.
Colonel, USAF
Director of Test

ABSTRACT

Wind tunnel tests at Mach numbers from 0.55 to 1.30 and angles of attack from -4 to 20 deg were conducted on a 0.18-scale model of the M-117 Bomb with seven tail fin configurations to determine the static stability characteristics of the bomb. The seven tail fin configurations consisted of the M131A1, MAU-103/B, and five variations of the MAU-103/B fin. The five variations were represented by changes in fin span, chord length, and planform shape. The stability characteristics of the seven tail fin configurations were compared on the basis of neutral-point location with respect to the center-of-gravity location. A suitable fin configuration was found that was stable throughout the range of conditions tested.

~~This document is subject to special export controls and each transmittal to foreign governments or foreign nationals may be made only with prior approval of Ogden Air Materiel Area (OOYEC), Hill AFB, Utah 84401.~~

CONTENTS

	<u>Page</u>
ABSTRACT	iii
NOMENCLATURE	viii
I. INTRODUCTION	1
II. APPARATUS	
2.1 Test Facility	1
2.2 Test Article	2
2.3 Instrumentation	2
III. TEST DESCRIPTION	
3.1 Test Conditions and Procedures	3
3.2 Corrections	3
3.3 Precision of Measurements	3
IV. RESULTS AND DISCUSSION	4
V. CONCLUSIONS	6

APPENDIX

Illustrations

Figure

1. Schematic of the Tunnel Test Section Showing Model Location	9
2. Photograph of the M-117 Bomb with Configuration D-2 Fins Installed in the Tunnel Test Section	10
3. Details and Dimensions of Models	
a. M-117 Bomb with Configuration A Fins (M131A1 Fin)	11
b. Configuration B Fin (MAU-103/B Fin)	12
c. Configuration C and C-1 Fins (see Note A)	12
d. Configuration D Fin	13
e. Configuration D-1 and D-2 Fins (see Note B)	13
4. Photographs of the Models Tested	
a. M-117 Bomb with Configuration A Fins (M131A1 Fin)	14
b. M-117 Bomb with Configuration B Fins (MAU-103/B Fin)	15
c. M-117 Bomb with Configuration C Fins	16

<u>Figure</u>	<u>Page</u>
4. Continued	
d. Configuration C-1 Fins	17
e. Configuration D Fins	18
f. Configuration D-1 Fins	19
g. Configuration D-2 Fins	20
5. Variation of Dynamic Pressure and Reynolds Number with Mach Number	21
6. Reference Axis System	22
7. Normal-Force Coefficient versus Angle of Attack	
a. Configuration A.	23
b. Configuration B.	24
c. Configuration C.	25
d. Configuration C-1.	26
e. Configuration D.	27
f. Configuration D-1.	28
g. Configuration D-2.	29
8. Normal-Force Coefficient Slope versus Mach Number	
a. Configurations A, B, C, and C-1	30
b. Configurations A, D, D-1, and D-2	30
9. Pitching-Moment Coefficient versus Angle of Attack	
a. Configuration A.	31
b. Configuration B.	32
c. Configuration C.	33
d. Configuration C-1.	34
e. Configuration D.	35
f. Configuration D-1.	36
g. Configuration D-2.	37
10. Pitching-Moment Coefficient Slope versus Mach Number	
a. Configurations A, B, C, and C-1	38
b. Configurations A, D, D-1, and D-2	38
11. Angle of Attack versus Forebody Axial-Force Coefficient	
a. Configuration A.	39
b. Configuration B.	40
c. Configuration C.	41
d. Configuration C-1.	42

<u>Figure</u>	<u>Page</u>
11. Continued	
e. Configuration D.	43
f. Configuration D-1.	44
g. Configuration D-2.	45
12. Forebody Axial-Force Coefficient $\alpha = 0$ versus Mach Number for Configuration D-2	46
13. Angle of Attack versus Base Axial-Force Coefficient	
a. Configuration A.	47
b. Configuration B.	48
c. Configuration C.	49
d. Configuration C-1.	50
e. Configuration D.	51
f. Configuration D-1.	52
g. Configuration D-2.	53
14. Angle of Attack versus Center-of-Pressure Location	
a. Configuration A.	54
b. Configuration B.	55
c. Configuration C.	56
d. Configuration C-1.	57
e. Configuration D.	58
f. Configuration D-1.	59
g. Configuration D-2.	60
15. Neutral-Point Location versus Mach Number Comparing Configurations B, C, C-1, and A	61
16. Neutral-Point Location versus Mach Number Comparing Configurations D, D-1, D-2, and A	62
17. Neutral-Point Location versus Mach Number Comparing Configurations B, D-2, and A	63

NOMENCLATURE

A_b	Projected model base area measured in a plane perpendicular to the model x-axis, 0.003922 ft ² , for Configuration A, 0.00511 ft ² for Configurations B through D-2
C_A	Axial-force coefficient, axial force/ $q_\infty S$
$C_{A, b}$	Base axial-force coefficient, $\frac{p_\infty - p_b}{q_\infty} \left(\frac{A_b}{S} \right)$
$C_{A, F}$	Forebody axial-force coefficient, $C_A - C_{A, b}$
C_m	Pitching-moment coefficient, pitching moment/ $q_\infty S D$ moment referenced to cg location
C_{m_α}	Pitching-moment coefficient slope, $dC_m/d\alpha$ at $\alpha = 0$ deg
C_N	Normal-force coefficient, normal force/ $q_\infty S$
C_{N_α}	Normal-force coefficient slope, $dC_N/d\alpha$ at $\alpha = 0$ deg
cg	Full-scale center-of-gravity location (see Fig. 3)
D	Model reference diameter, 0.242 ft (see Fig. 3)
M_∞	Free-stream Mach number
p_b	Model base pressure, psfa
p_∞	Free-stream static pressure, psfa
q_∞	Free-stream dynamic pressure, psf
S	Model reference area, $\pi D^2/4$
x_{cp}	Center-of-pressure location expressed in body diameters from cg, C_m/C_N , positive forward of the cg location
x_{np}	Neutral-point location expressed in body diameters from the cg, dC_m/dC_N at $\alpha = 0$, positive forward of the cg location
α	Angle of attack, deg - angle between model longitudinal axis and the wind direction (see Fig. 6)
ϕ	Roll angle, deg - angle between plane of pitch motion and the model longitudinal plane of symmetry, with zero roll corresponding to having two fins in the pitch plane (see Fig. 6)

SECTION I INTRODUCTION

The M-117 Bomb was introduced approximately 25 years ago with the M131A1 tail fin and was aerodynamically and structurally acceptable for the aircraft velocities of that era. With today's high speed aircraft, the M131A1 tail fin has proved to be aerodynamically acceptable but structurally unsound when attached to the M-117 bomb shell. To correct this structural deficiency, the MAU-103/B tail fin was introduced in place of the M131A1 tail fin. Flight tests subsequently proved the structural integrity of this modification, but aerodynamic instability at high speeds resulted. This investigation was conducted to determine the static stability characteristics of various tail fin configurations proposed for the M-117 Bomb in order to provide both an aerodynamically and a structurally acceptable fin.

To accomplish this objective, force and moment data were obtained for seven tail fin configurations of a 0.18-scale model of the M-117 Bomb at Mach numbers from 0.55 to 1.30 in the angle-of-attack range from -4 to 22 deg.

SECTION II APPARATUS

2.1 TEST FACILITY

The Aerodynamic Wind Tunnel, Transonic (4T) is a closed-loop, continuous flow, variable density tunnel. It is capable of operating at Mach numbers from 0.20 to 1.30 with a variable stagnation pressure from 300 to 3900 psf at all Mach numbers. The test section is 4 ft square and 12.5 ft long with variable porosity walls (0.5 to 10 percent) and top and bottom walls that can be diverged or converged (± 0.5 deg). The test section is completely enclosed in a plenum chamber from which the air can be evacuated, thus allowing part of the tunnel airflow to be removed through the test section walls. This design allows control of wave attenuation and blockage effects. The tunnel model-support system consists of a pitch sector, boom, and sting and provides a pitch capability of from -12 to 28 deg with respect to the tunnel centerline. A temporary tunnel modification restricted the positive pitch angle to 12 deg during this test so that an 8-deg offset adapter was required in order to obtain angles of attack on the order of 20 deg. A schematic of the test section showing the location of the test model is shown in Fig. 1. A photograph of the test installation is shown in Fig. 2.

2.2 TEST ARTICLE

The test article was a 0.18-scale model of the M-117 Bomb. The basic bomb consisted of a round nose fuse, a contoured nose section, cylindrical midsection, and a conical afterbody with four fins spaced at 90-deg intervals.

The tail cone and the base of the fins were altered slightly to accommodate an 0.675-in. -diam sting. Provisions were made to manually rotate the tail assembly about the model body longitudinal axis to obtain roll angles at preset 11.25-deg increments. Details of the bomb model tested and the seven tail fin configurations are shown in Fig. 3. The basic differences are listed below:

Configuration	Model Span, in.	Full-Scale Span, in.	Comments
A	4.028	22.40	M131A1 Fin
B	3.420	19.00	MAU-103/B Fin
C	3.600	20.00	Configuration B with increased span
C-1	3.600	20.00	Configuration C with part of rib removed
D	3.600	20.00	Configuration C-1 with increased chord
D-1	3.792	21.07	Configuration D with increased span
D-2	3.792	21.07	Configuration D-1 with part of rib removed

Photographs of the models are shown in Fig. 4.

2.3 INSTRUMENTATION

A six-component strain-gage balance was used to obtain the force and moment data during the test. Base pressure measurements were obtained with a pressure transducer connected to an orifice located inside the tail cone cavity of the model.

SECTION III TEST DESCRIPTION

3.1 TEST DESCRIPTION AND PROCEDURES

The models were tested at nine Mach numbers from 0.55 to 1.30. Tunnel stagnation pressure ranged from 3500 psf at $M_\infty = 0.55$ to 1850 psf at $M_\infty = 1.30$, and the total temperature ranged from 65 to 85°F. Reynolds number and dynamic pressure variations with Mach number are presented in Fig. 5. The test section wall porosity and the top and bottom test section wall angles were set to provide optimum flow for each test condition.

The tunnel conditions were held constant at the prescribed Mach number and total pressure, while the angle of attack was varied through the prescribed range of -4 to 20 deg. Data were recorded at each of several angles of attack. At some test conditions, the maximum angle of attack was restricted to less than 20 deg because of the aerodynamic loads exceeding the capacity of the balance.

3.2 CORRECTIONS

Balance and sting deflections caused by the aerodynamic loads on the model were accounted for in the data reduction program to determine the true model angle of attack and roll angle. Corrections were also made for model weight tares to calculate net aerodynamic forces on the models.

3.3 PRECISION OF MEASUREMENTS

Uncertainties in the data were calculated taking into consideration probable inaccuracies in balance measurements and tunnel conditions. The uncertainties in coefficients are based on a 95-percent confidence level and are listed below for each quantity:

C_N	$C_{A, F}$	$C_{A, b}$	C_m	x_{cp}
± 0.008	± 0.008	± 0.001	± 0.015	± 0.012

Values of x_{cp} within the angle-of-attack range ± 2 deg are not reliable data because of the small values of C_m and C_N and the uncertainties stated above. These values of x_{cp} are thus deleted and are replaced with the neutral point, x_{np} , at $\alpha = 0$ deg.

The estimated uncertainty in setting Mach number was no greater than ± 0.005 , and the uncertainty in angle of attack was estimated to be ± 0.1 deg. Tunnel calibrations indicate that the Mach number variation in the area of the tunnel occupied by the model was no greater than ± 0.004 for $M_\infty \leq 1.0$ and ± 0.014 for $M_\infty > 1.0$.

SECTION IV RESULTS AND DISCUSSION

The primary purpose of this investigation was to obtain aerodynamic data concerning the static stability characteristics for various tail fin configurations attached to the M-117 Bomb. Basic stability data are presented for each configuration tested. The coefficients are presented for the body-axis system, and the pitching moments are referenced to the full-scale center of gravity. The coordinate system for the coefficients is shown in Fig. 6.

The normal-force coefficient data for each Mach number and configuration are presented in Fig. 7. Figure 8 shows the effect of fin span, chord length, and planform on the normal-force coefficient slope for the Mach number range 0.55 to 1.30. Increasing the span and chord length increases the normal-force coefficient slope, but removing a portion of the forward part of the tail fin tends to decrease the normal-force coefficient slope.

The pitching-moment coefficient data for each Mach number and configuration are presented in Fig. 9. Figure 10 presents the pitching-moment coefficient slope versus Mach number for all configurations and shows that increasing the fin span, chord length, and removing a portion of the forward part of the tail fin all produce increases in the pitching-moment coefficient slope.

Figure 11 presents the forebody axial-force coefficient data for all Mach numbers and configurations. The trend of the data for Configuration A differs slightly from that of the other configurations, with the effect being most notable at high angles of attack and at Mach numbers near 1.0. Figure 12 presents the variation of forebody axial-force coefficient with Mach number for Configuration D-2 at 0-deg angle of attack. All configurations tested exhibited approximately the same axial-force coefficient versus Mach number.

The base axial-force coefficient data are presented in Fig. 13. Because of the small base area, these values are quite small compared

to the forebody axial-force coefficients. The negative values experienced at low angles of attack correspond to high base pressures resulting from the fin and afterbody geometries and the presence of the sting. Removal of the sting (as in free flight) would generally result in lower base pressures and thus higher base axial-force coefficients.

Figure 14 presents the center-of-pressure locations for all Mach numbers and configurations. Also shown on these plots are the neutral-point locations. Configuration A is seen to be stable (negative x_{cp}) at all angles of attack throughout the Mach number range. However, Configuration B shows instability at low angles for Mach numbers 0.9 and above. The other configurations had stability margins between these two extremes, and all configurations were stable at angles of attack greater than ± 4 deg.

The stability data are summarized in Figs. 15 and 16 which show neutral-point location versus Mach number. Configurations B, C, and C-1 are compared to Configuration A in Fig. 15. The increase in span of Configuration C over that of Configuration B results in a substantial movement of the neutral point aft of the cg except in the vicinity of Mach number 1.0. Configuration C-1 produced a further aft movement of the neutral point. All the changes were in the direction of increasing stability with respect to Configuration B. Configurations D, D-1, and D-2 are compared to Configuration A in Fig. 16. Configurations D, D-1, and D-2 have a longer chord length than Configurations B, C, and C-1. The extension of the chord length was achieved by adding to the aft end of the fin, resulting in an overall increase in model length. This increase in length resulted in a stable configuration, although the margin of stability near Mach number 1.0 was very small. Configuration D had the same span as Configuration C-1, and the span was further increased to produce Configuration D-1. This moved the neutral point generally aft, but did not help at Mach number 1.0. Further improvement in stability was achieved with Configuration D-2. This configuration had a minimum positive margin of stability of 0.28 cal at Mach number 1.0. Although this is still less than the stability of Configuration A, it is considered to represent an acceptable compromise.

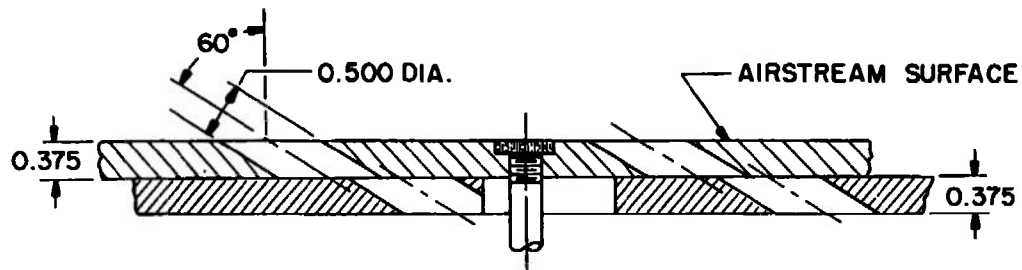
Figure 17 shows the effect of roll attitude on the neutral-point location for Configuration D-2. It can be seen that this configuration remains stable even at the roll angle of minimum fin effectiveness ($\phi = 45$ deg). This figure also shows improvement of Configuration D-2 over Configuration B.

SECTION V CONCLUSIONS

The following conclusions were made from the results of this investigation:

1. The MAU-103/B fin is unstable at low angles of attack for Mach numbers of 0.9 and higher.
2. Increasing the fin span increases the stability.
3. Moving the fin further aft increases the stability.
4. Configuration D-2 proved to be stable throughout the Mach number range of the test at roll angles of both 0 and 45 deg.

**APPENDIX
ILLUSTRATIONS**



TYPICAL PERFORATED WALL CROSS SECTION

NOTE: All dimensions in inches

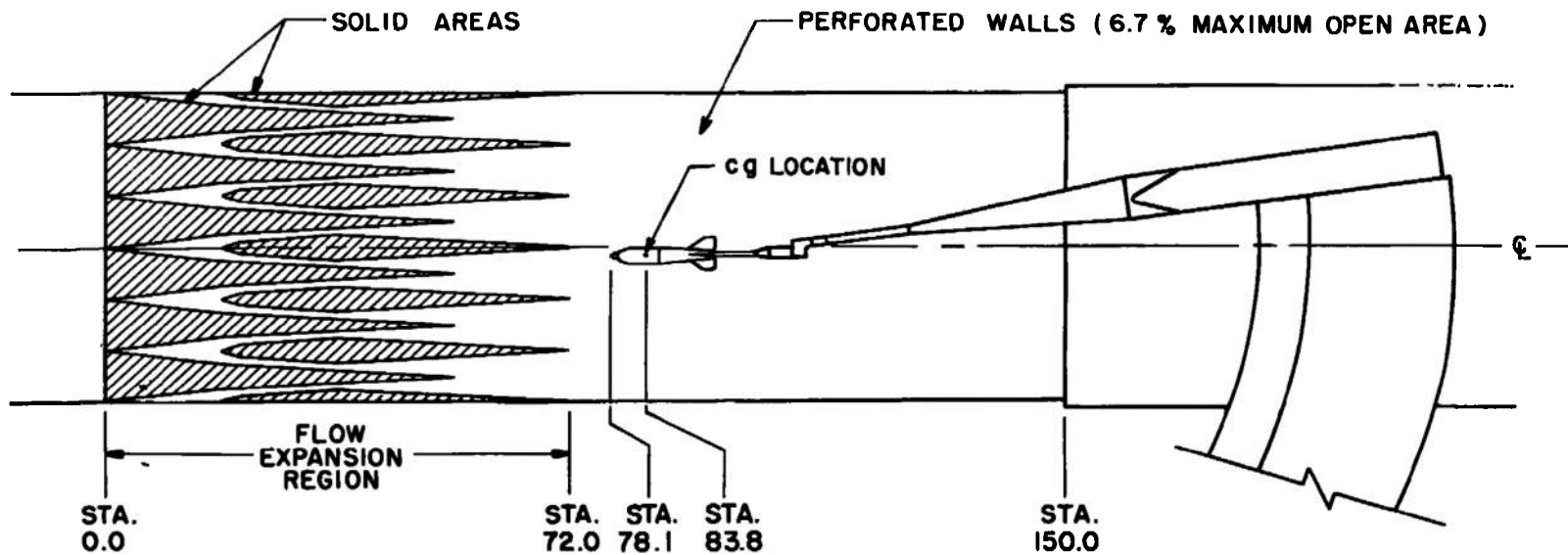


Fig. 1 Schematic of the Tunnel Test Section Showing Model Location

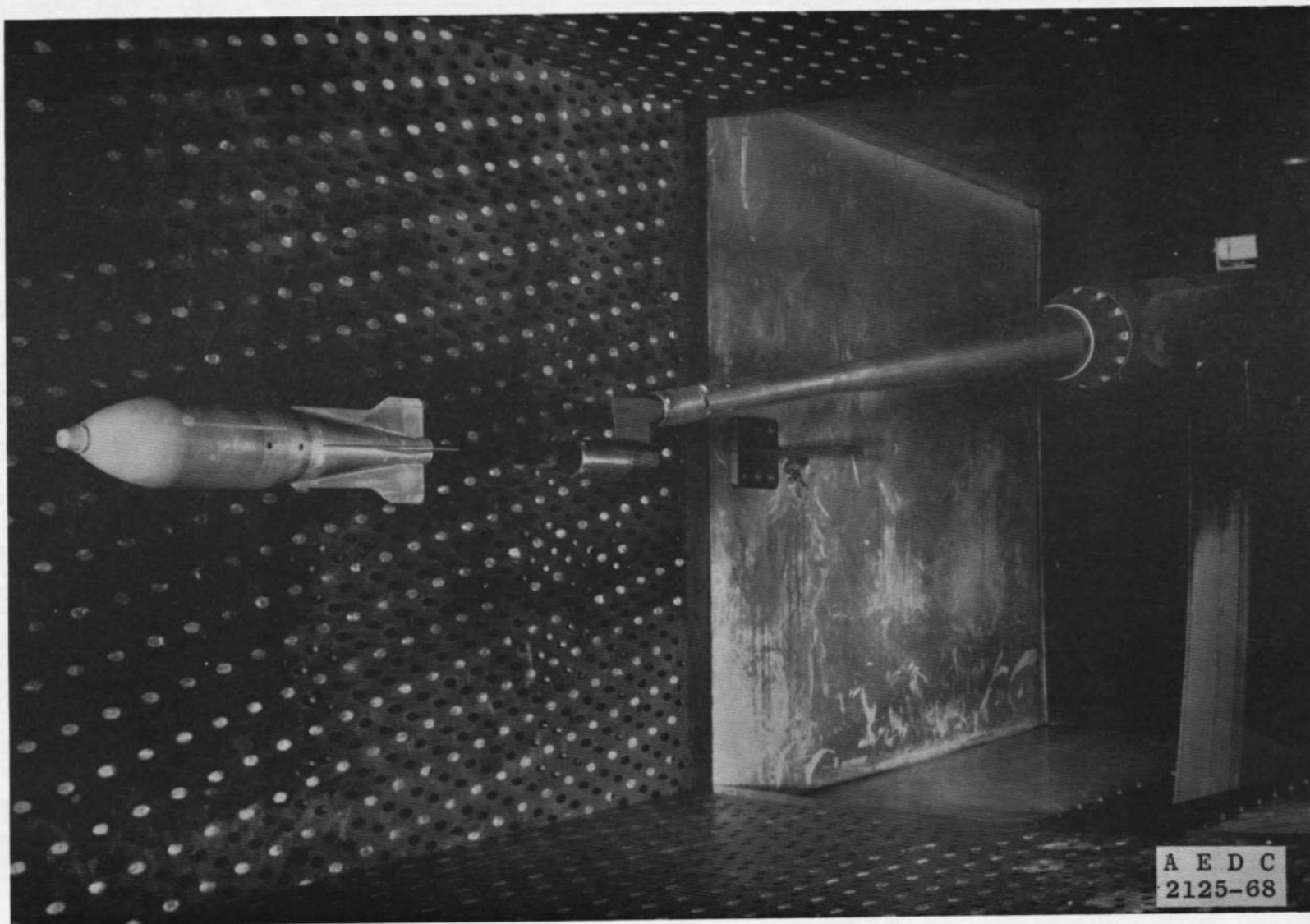
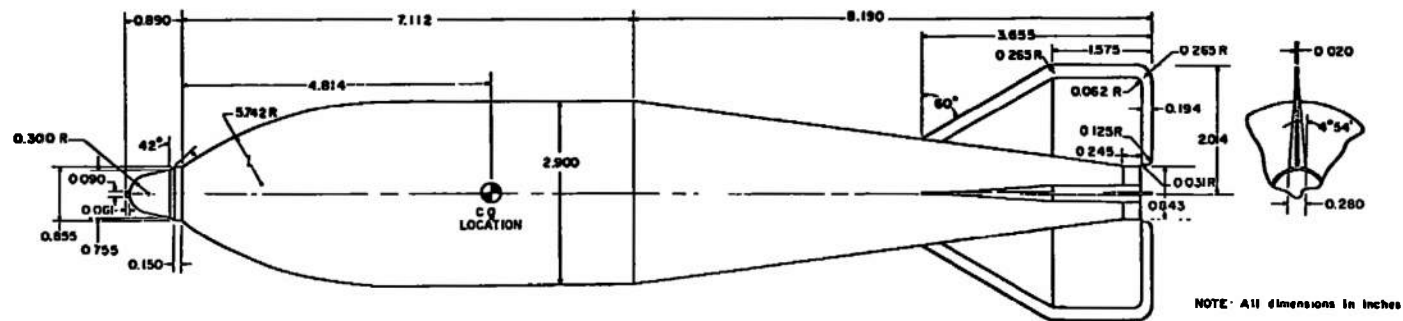
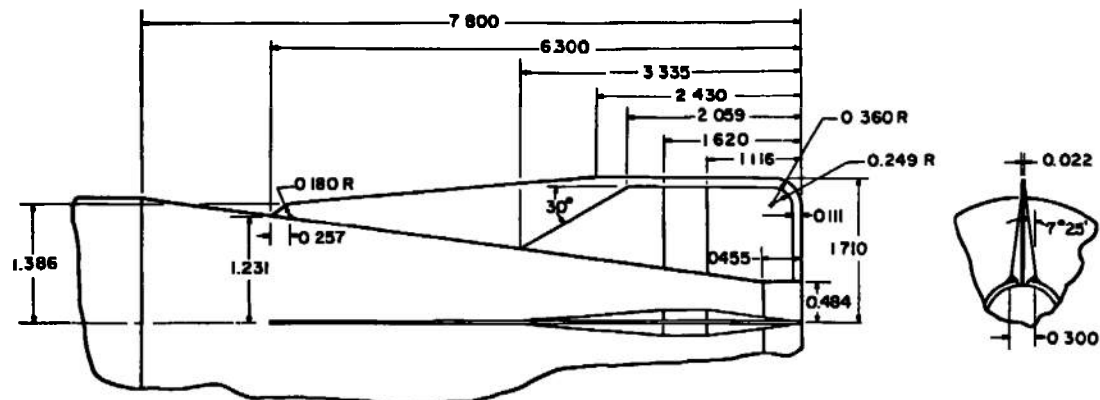


Fig. 2 Photograph of the M-117 Bomb with Configuration D-2 Fins Installed in the Tunnel Test Section



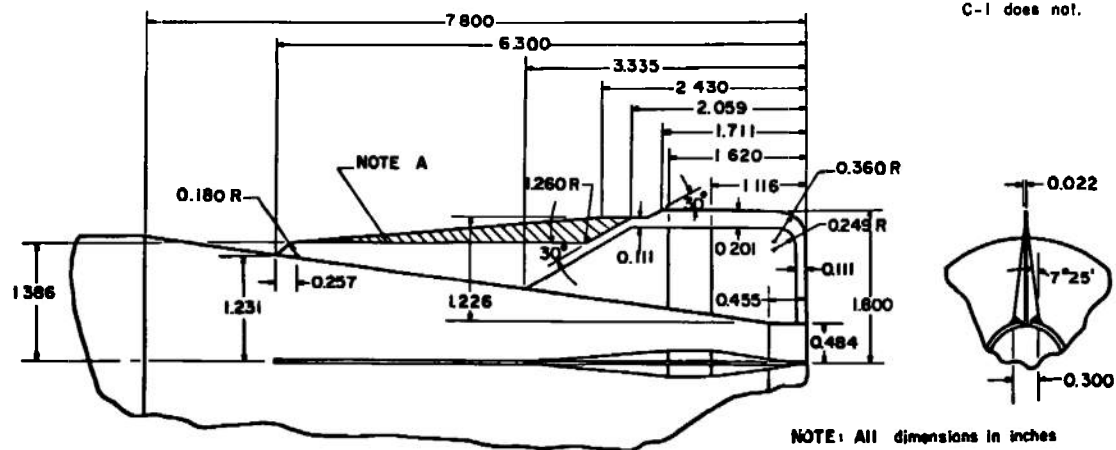
a. M-117 Bomb with Configuration A Fins (M131A1 Fin)

Fig. 3 Details and Dimensions of Models



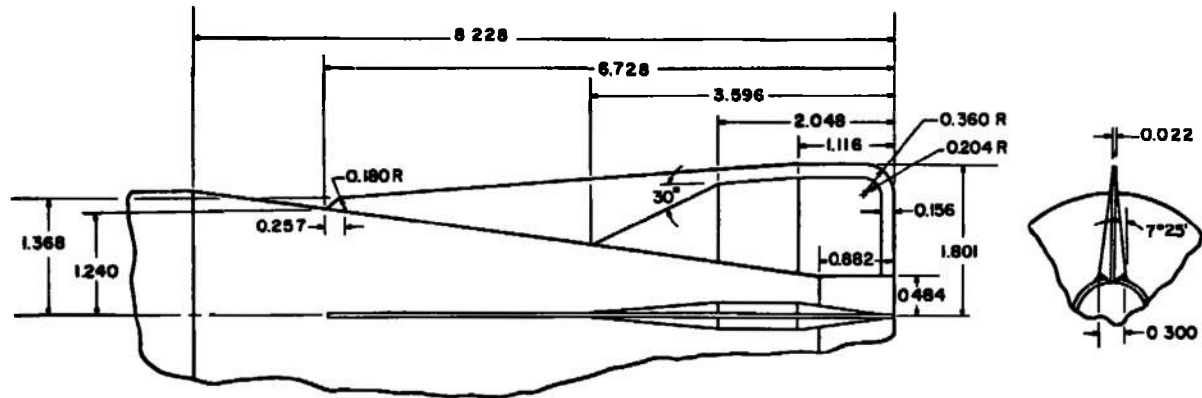
b. Configuration B Fin (MAU-103/B Fin)

NOTE A Configuration C includes cross hatched area, Configuration C-1 does not.



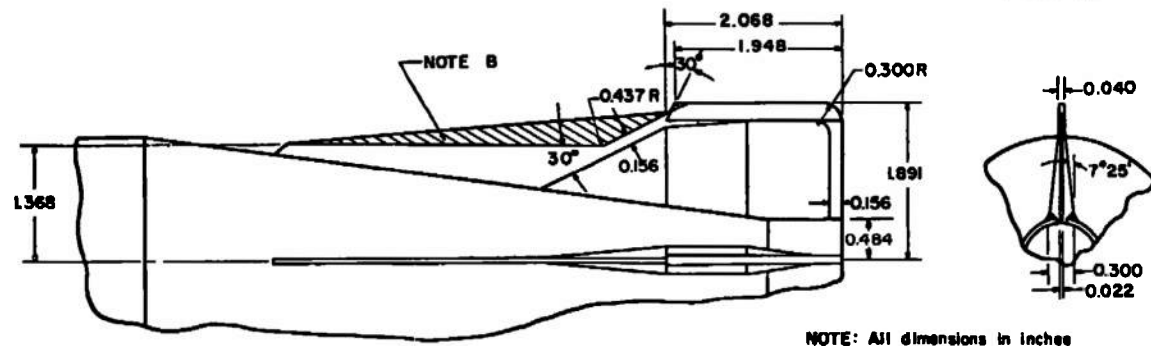
c. Configuration C and C-1 Fins (see Note A)

Fig. 3 Continued



d. Configuration D Fin

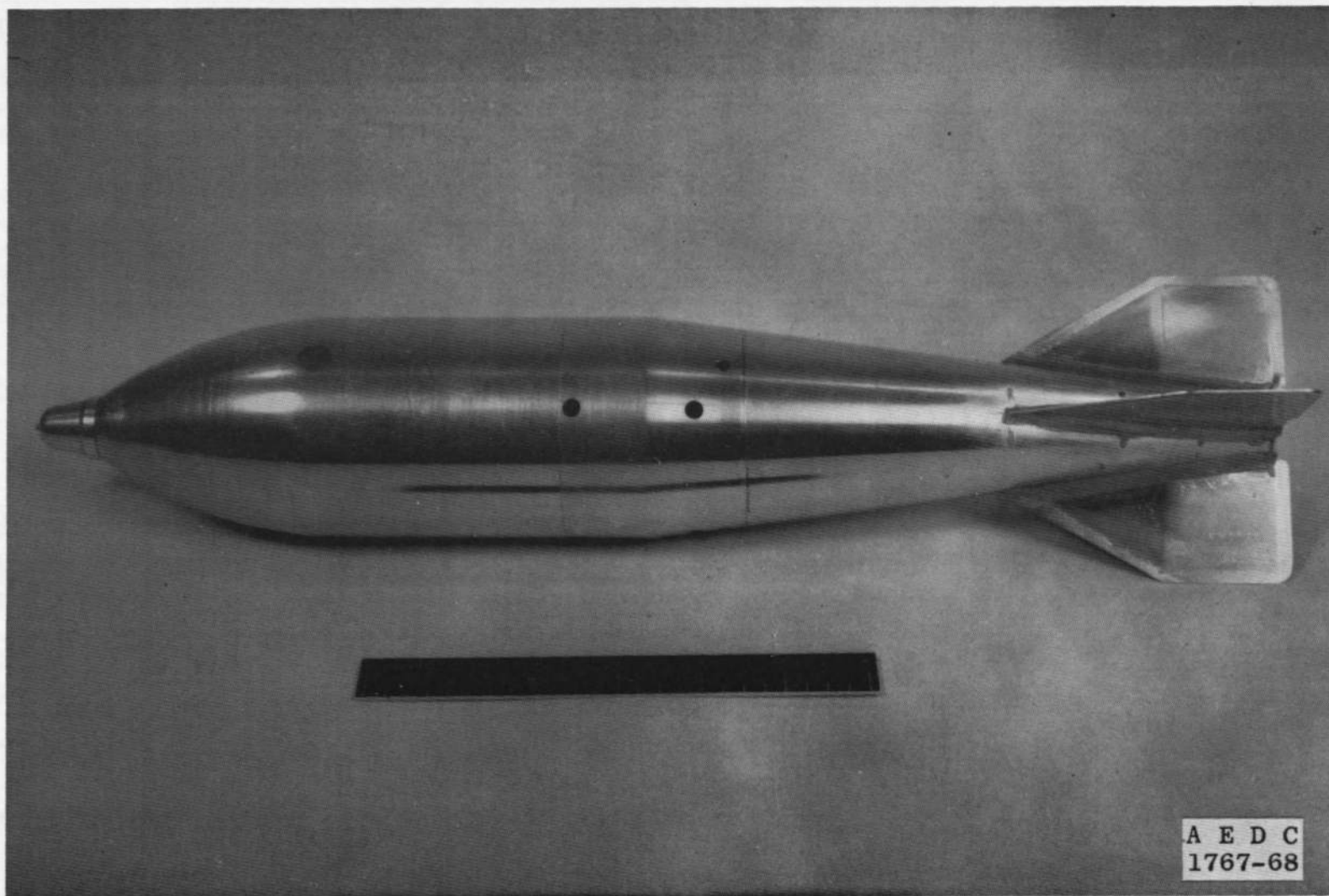
NOTE B: Configuration D-1 includes cross hatched area, Configuration D-2 does not



e. Configuration D-1 and D-2 Fins (see Note B)

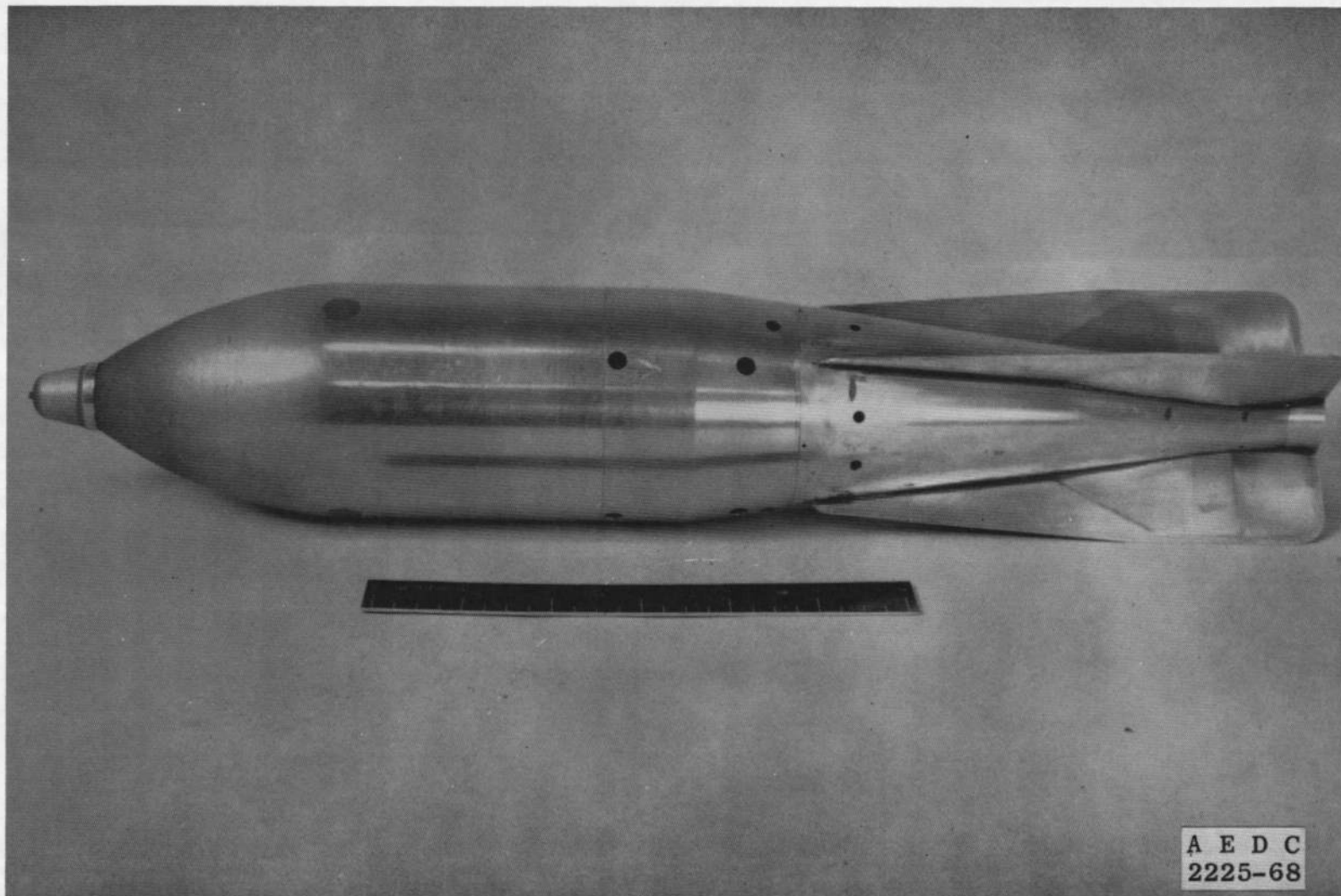
Fig. 3 Concluded

NOTE: All dimensions in inches



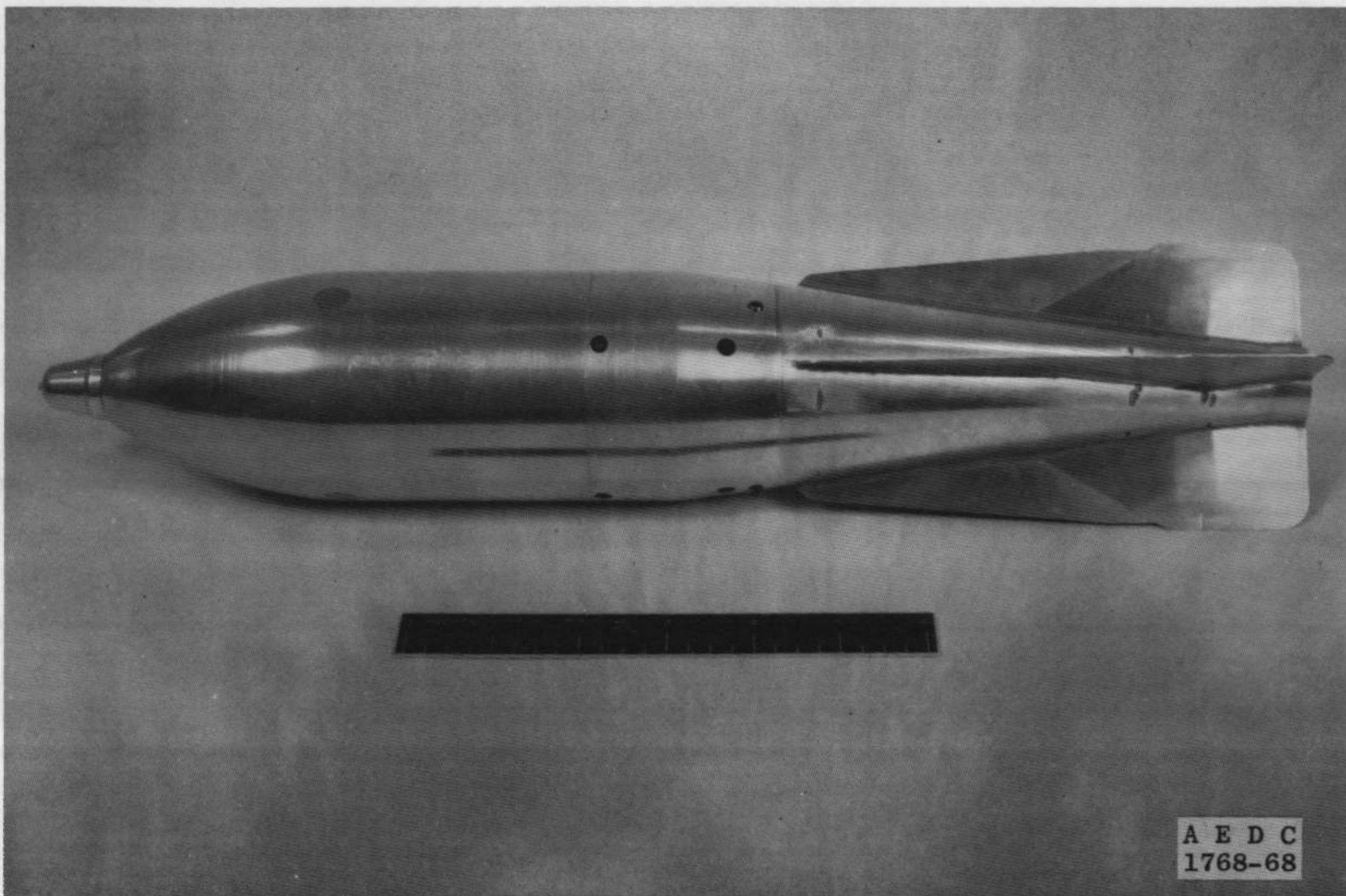
a. M-117 Bomb with Configuration A Fins (M131A1 Fin)

Fig. 4 Photographs of the Models Tested

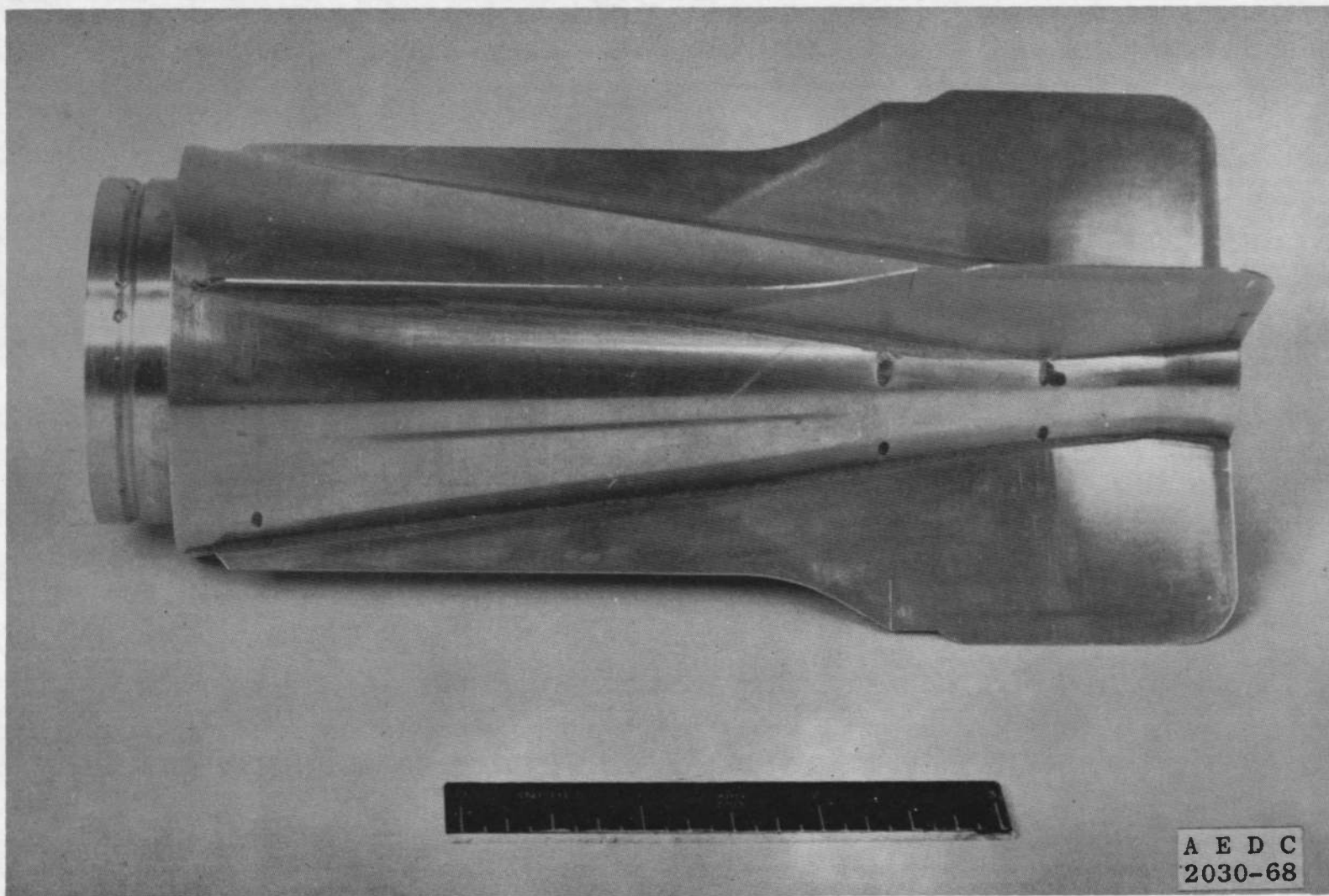


b. M-117 Bomb with Configuration B Fins (MAU-103/B Fin)

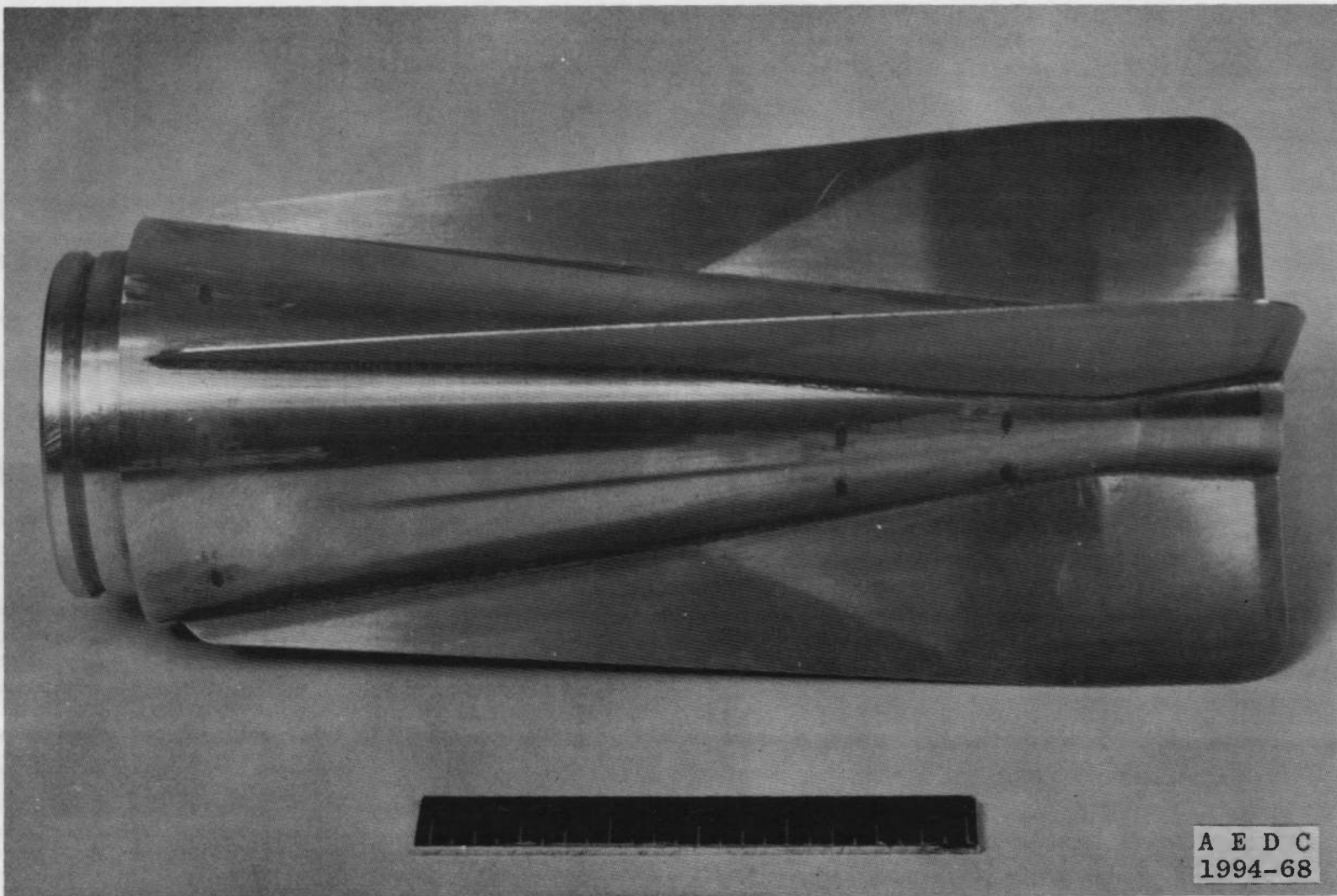
Fig. 4 Continued



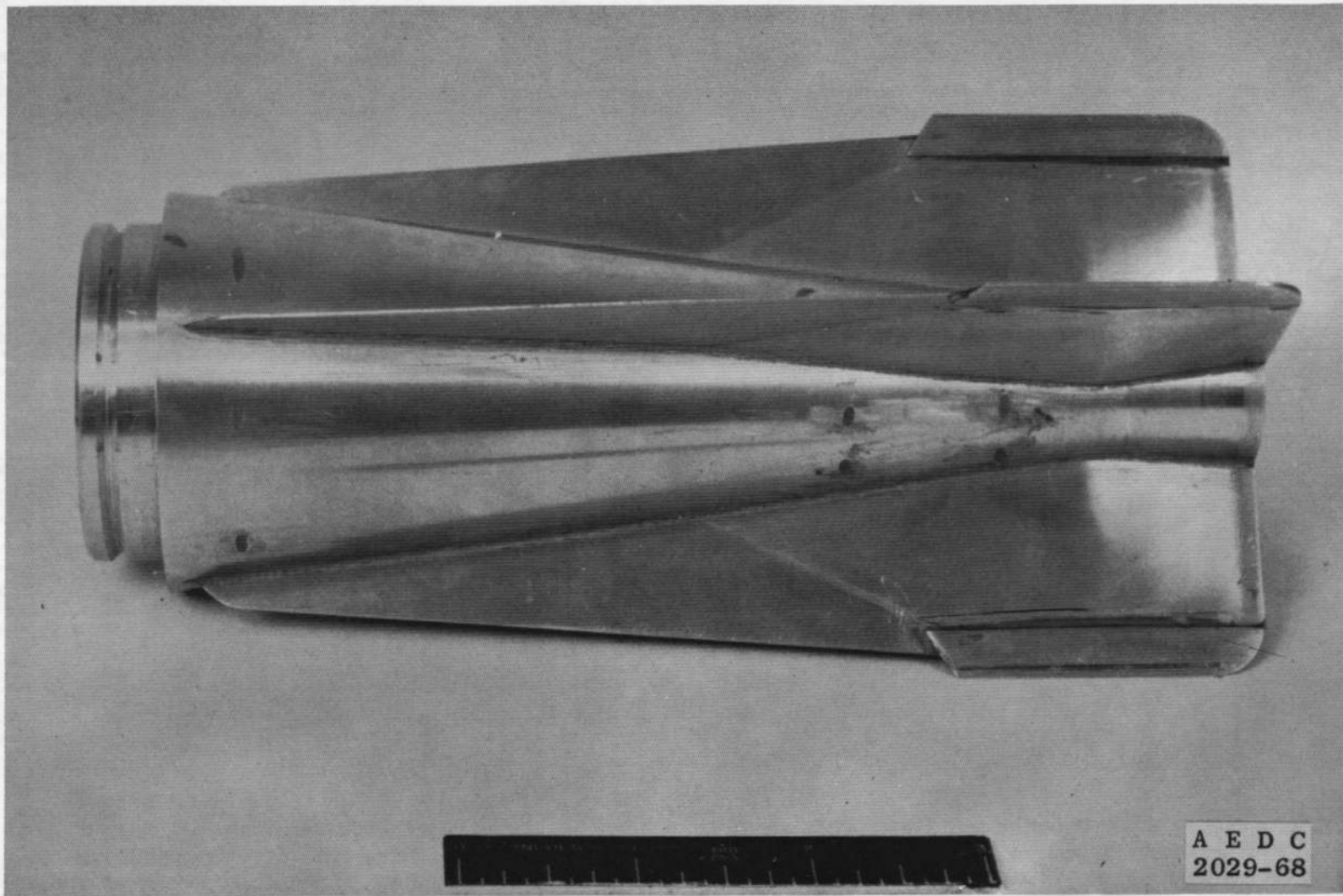
c. M-117 Bomb with Configuration C Fins
Fig. 4 Continued



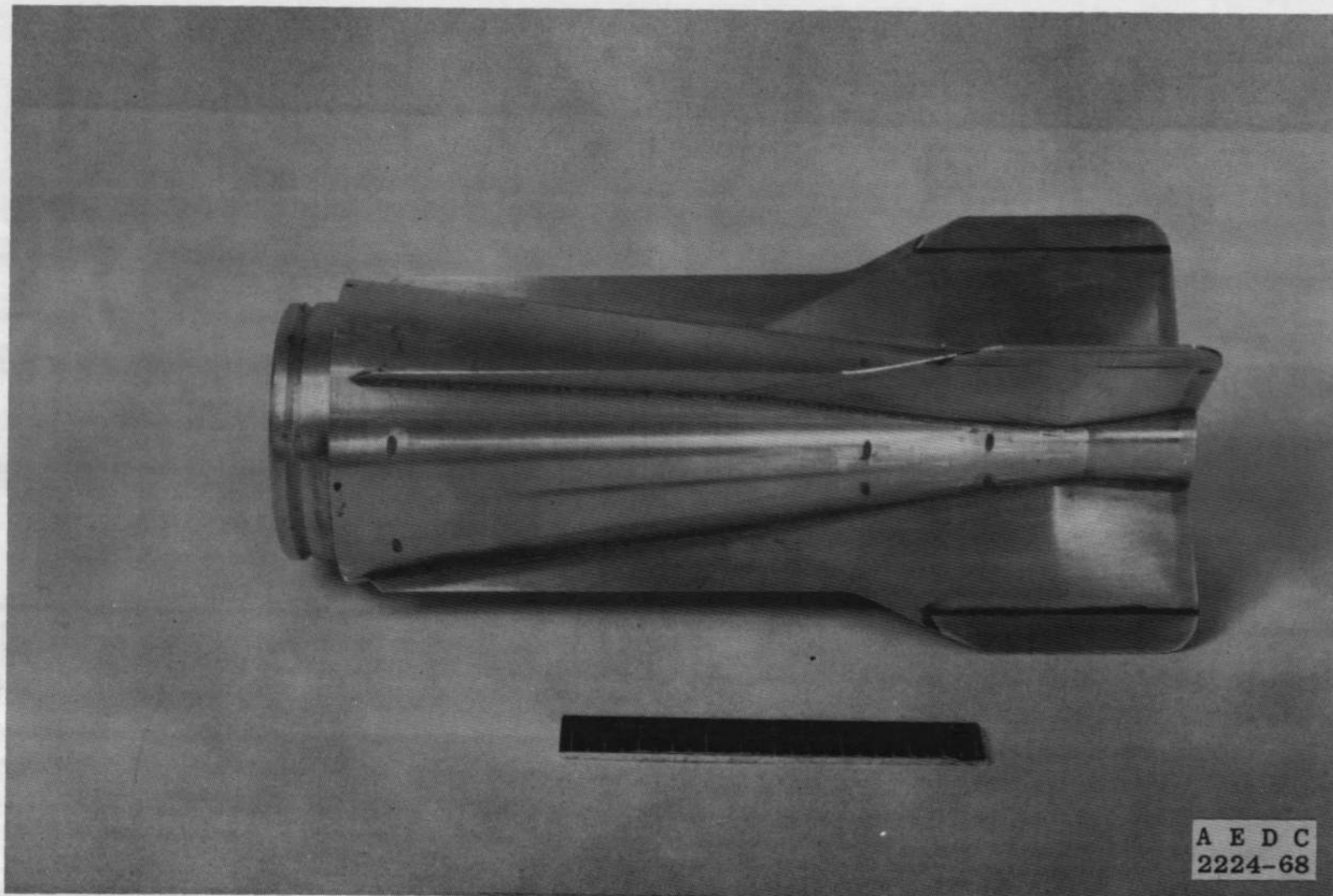
d. Configuration C-1 Fins
Fig. 4 Continued



e. Configuration D Fins
Fig. 4 Continued



f. Configuration D-1 Fins
Fig. 4 Continued



g. Configuration D-2 Fins
Fig. 4 Concluded

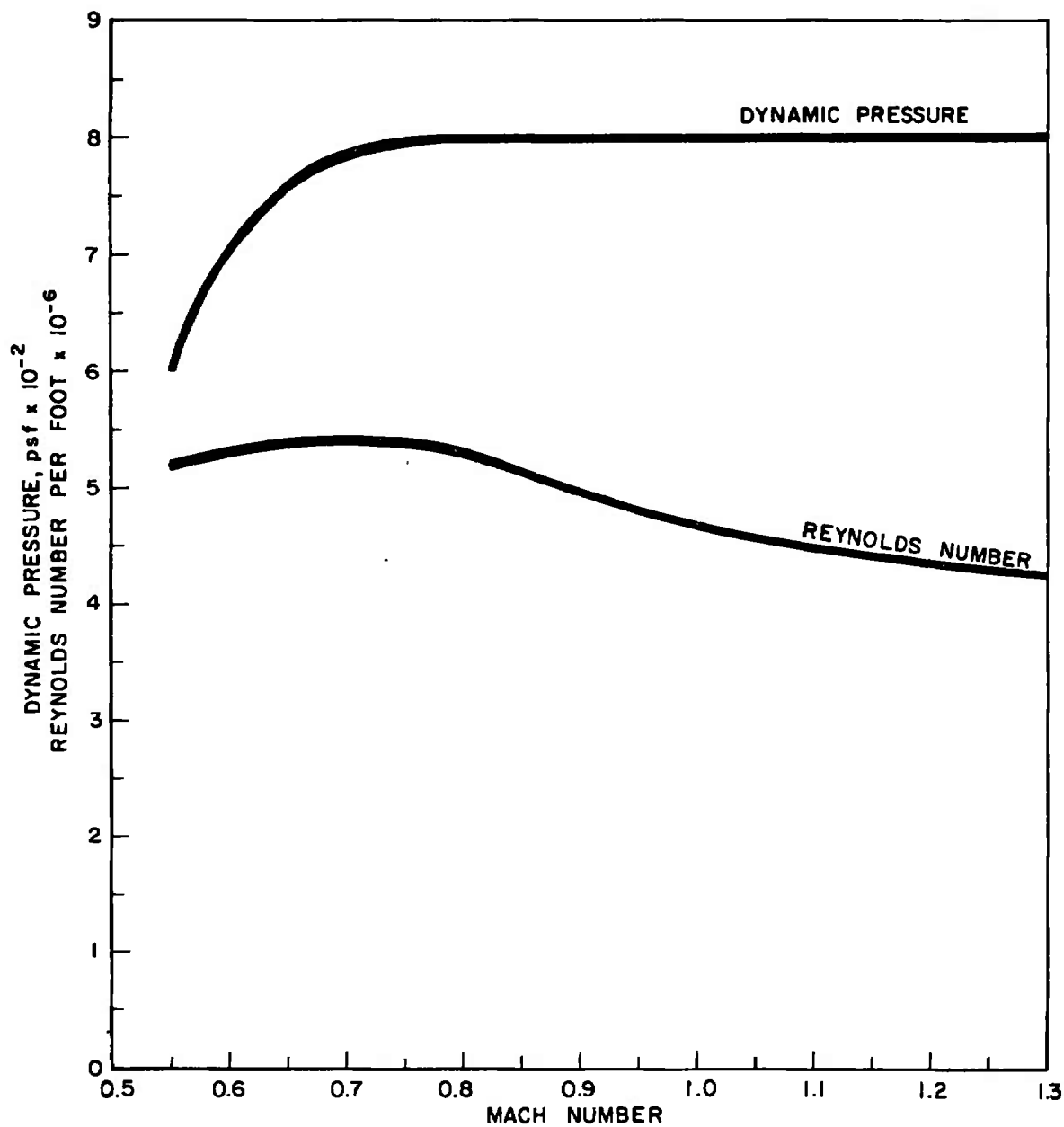


Fig. 5 Variation of Dynamic Pressure and Reynolds Number with Mach Number

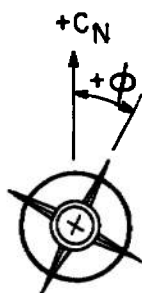
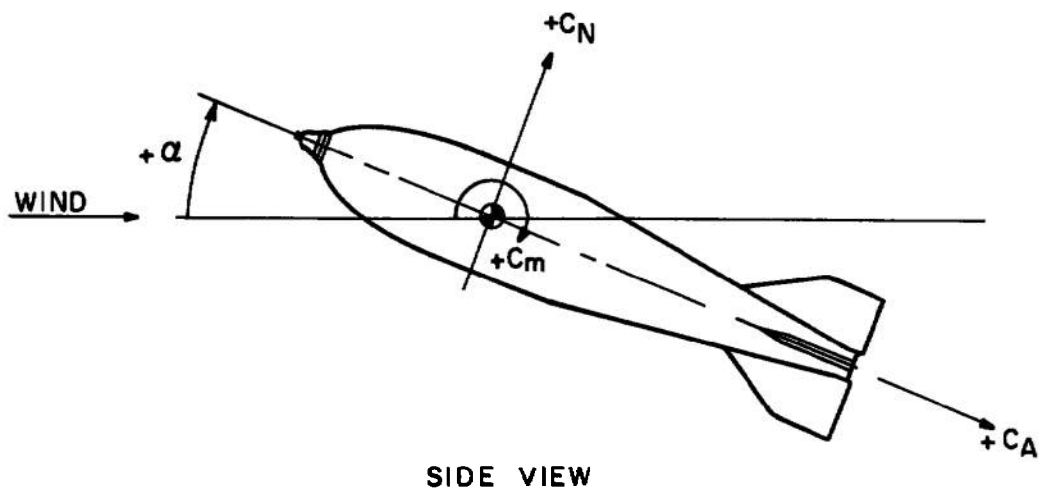
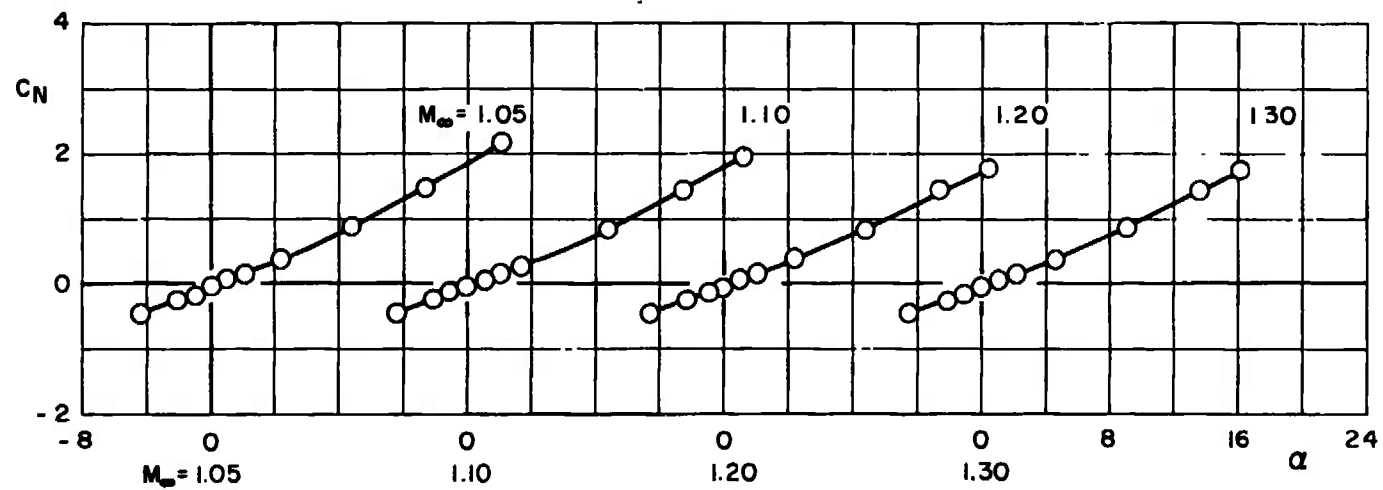
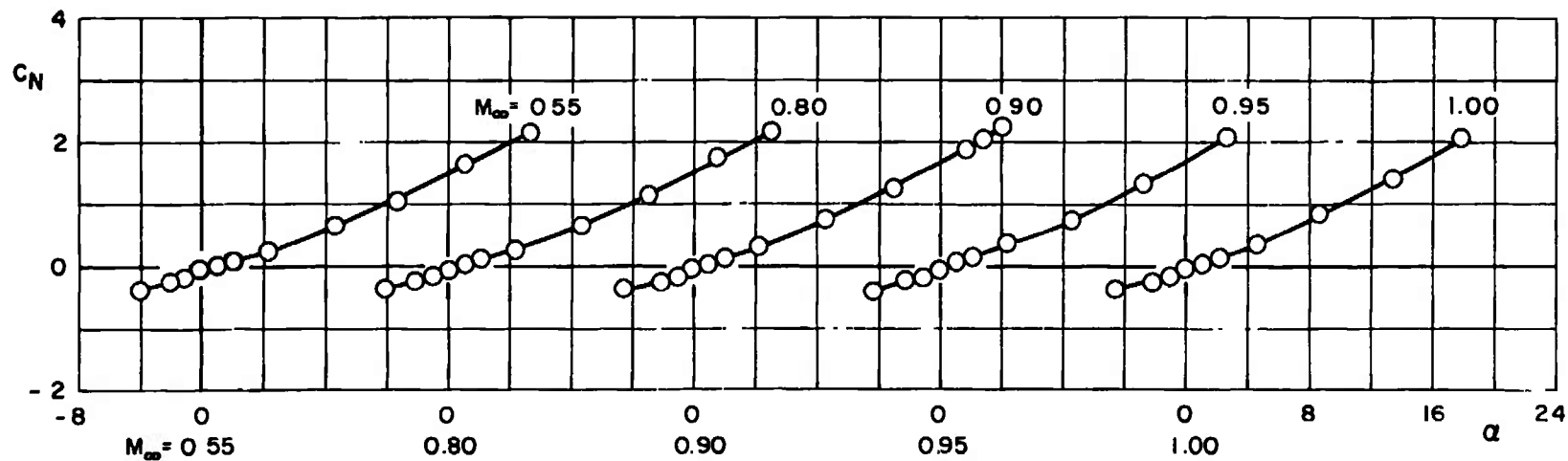
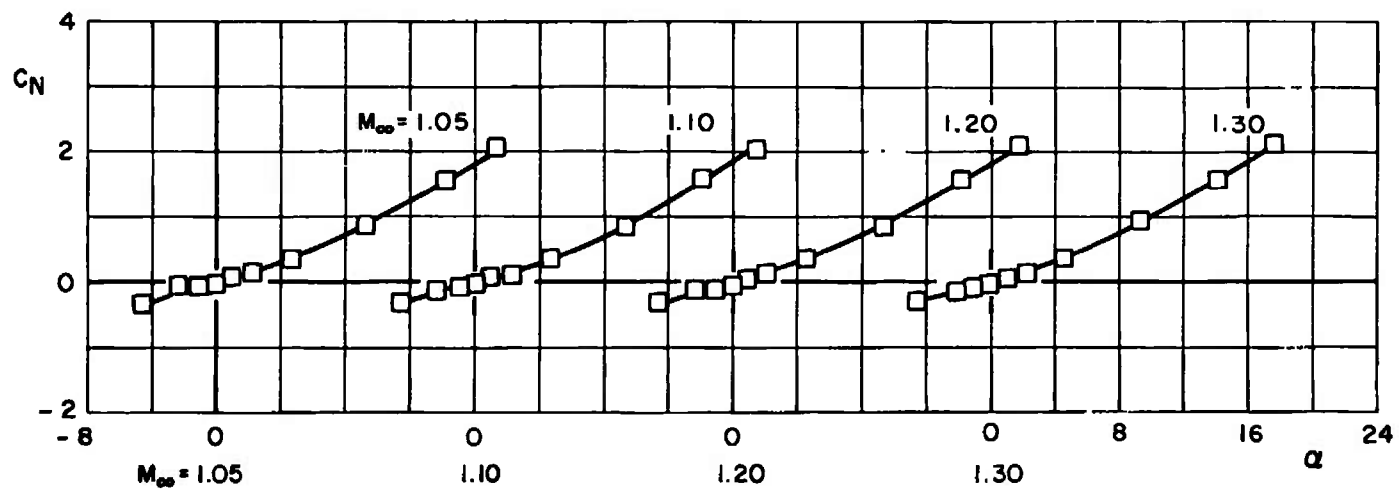
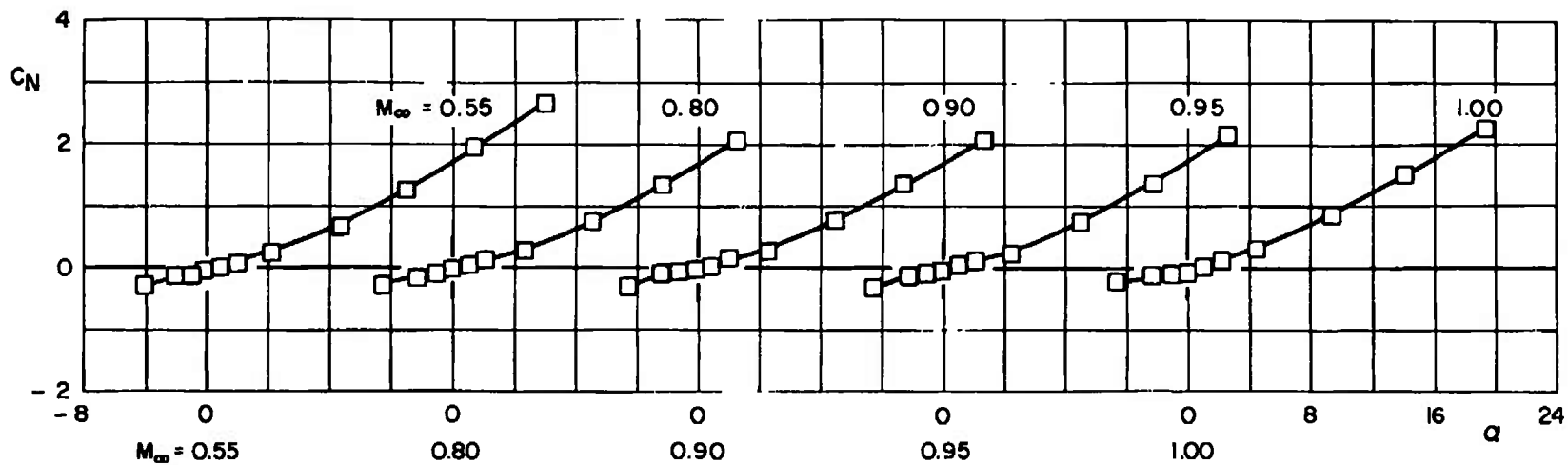


Fig. 6 Reference Axis System

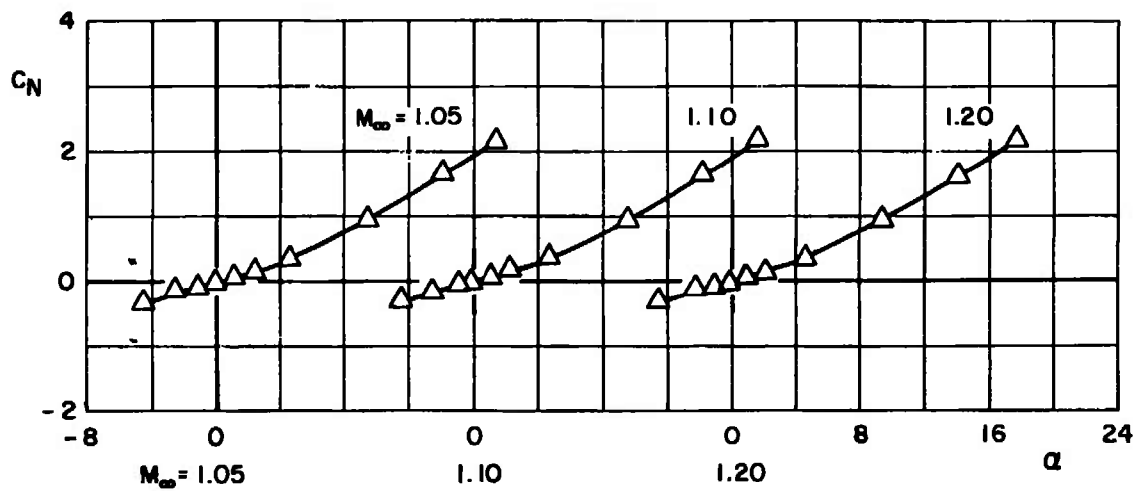
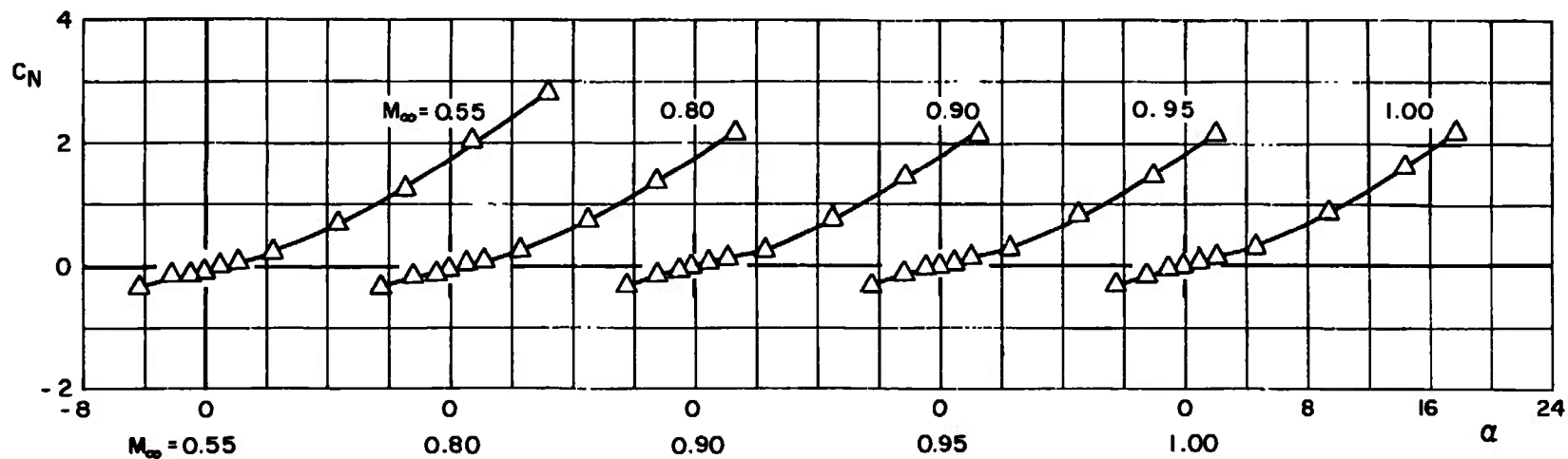


o. Configuration A

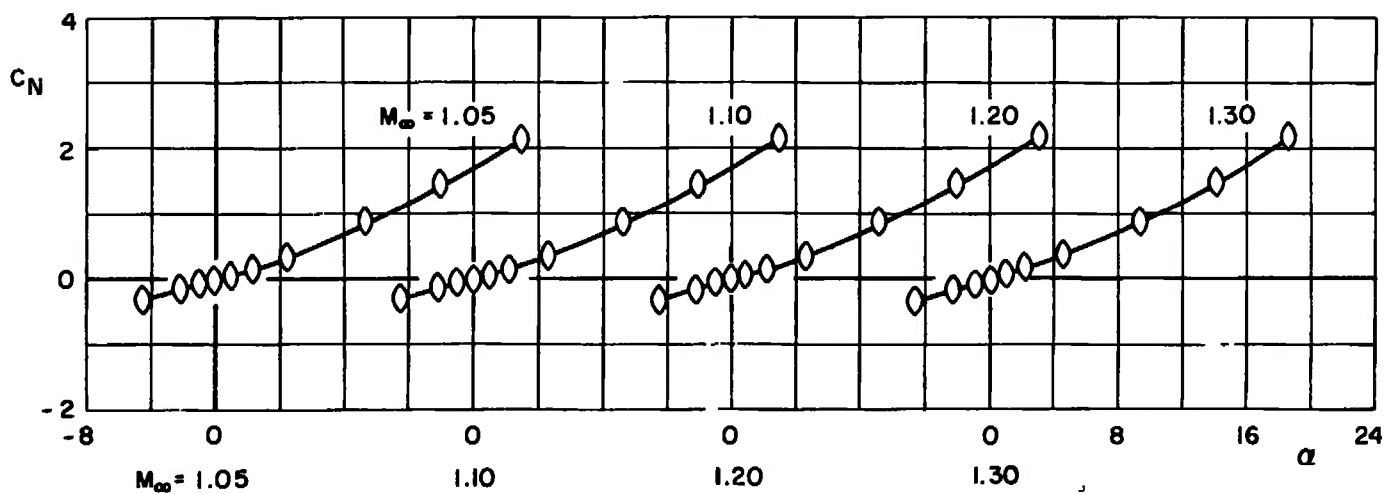
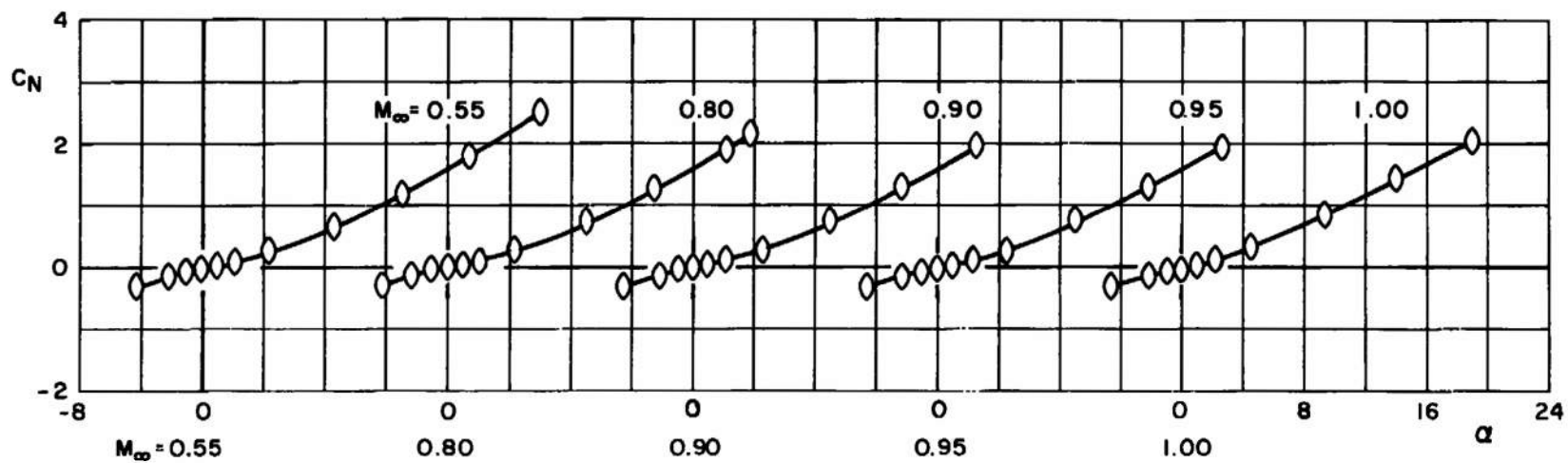
Fig. 7 Normal-Force Coefficient versus Angle of Attack



b. Configuration B
Fig. 7 Continued

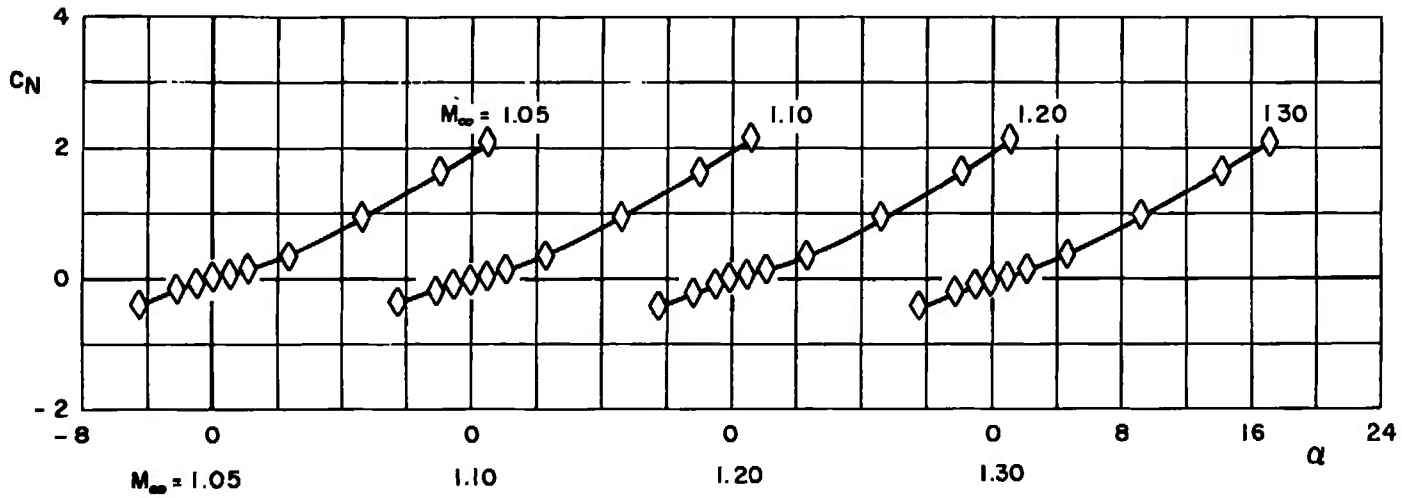
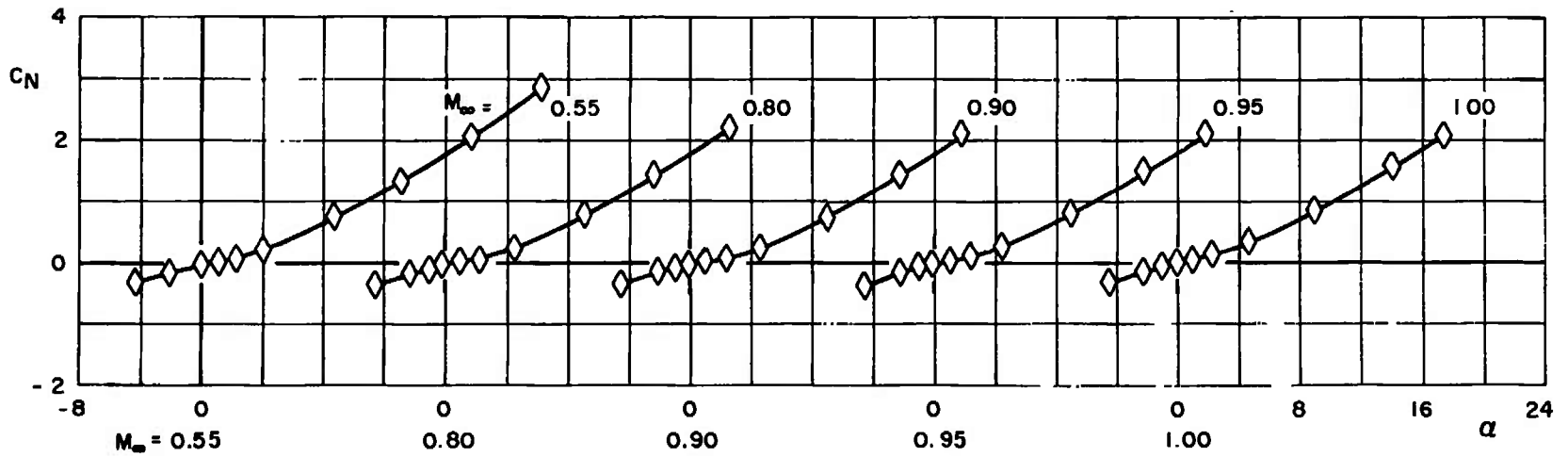


c. Configuration C
Fig. 7 Continued

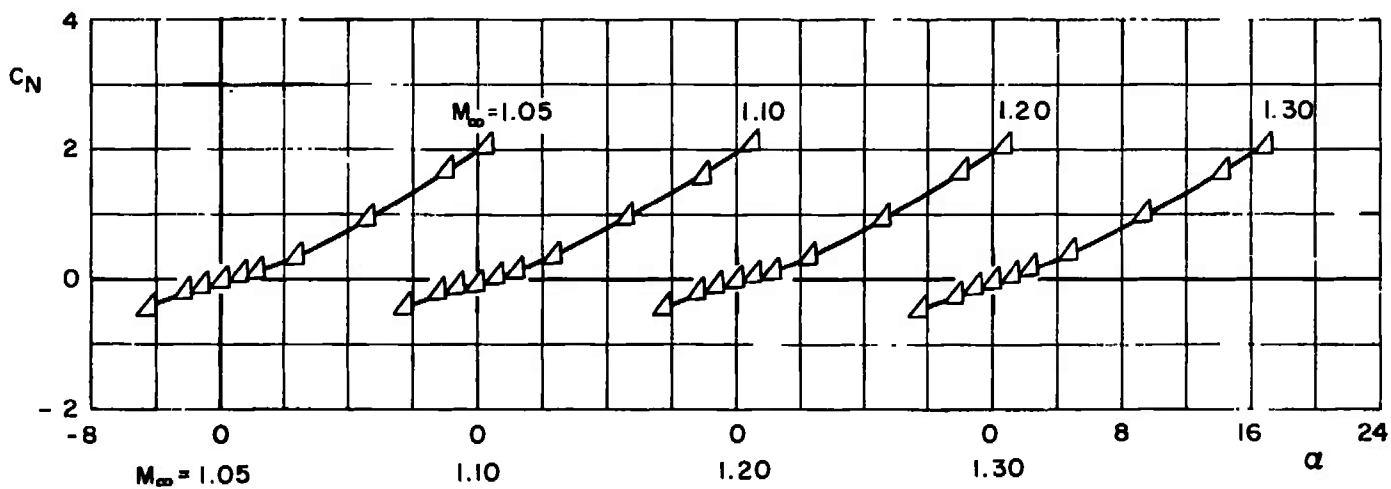
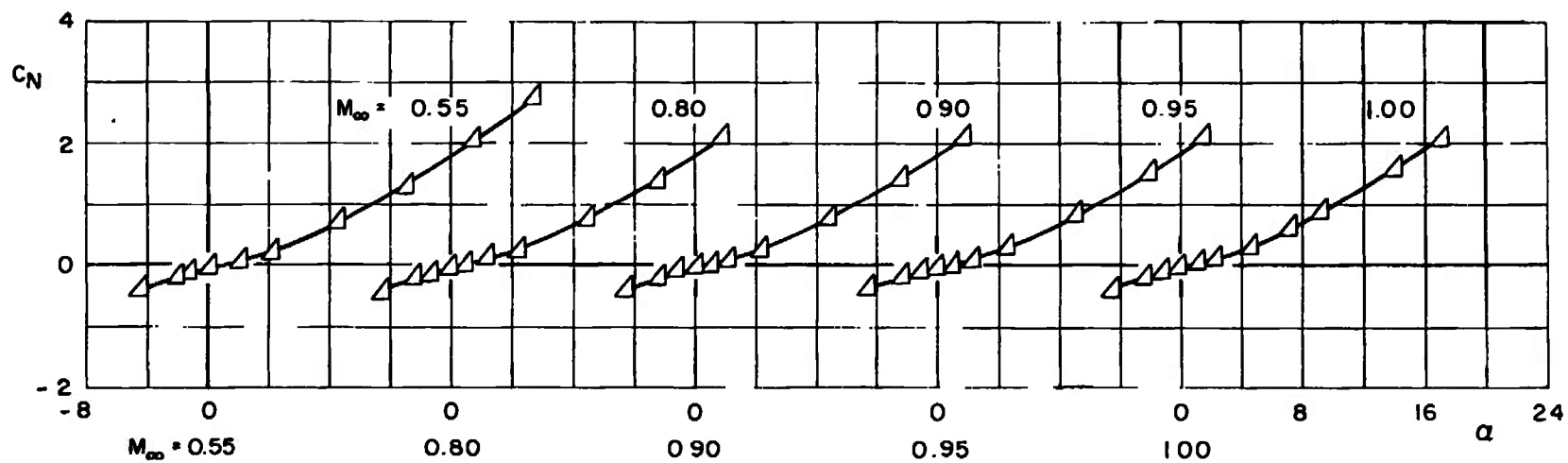


d. Configuration C-1

Fig. 7 Continued

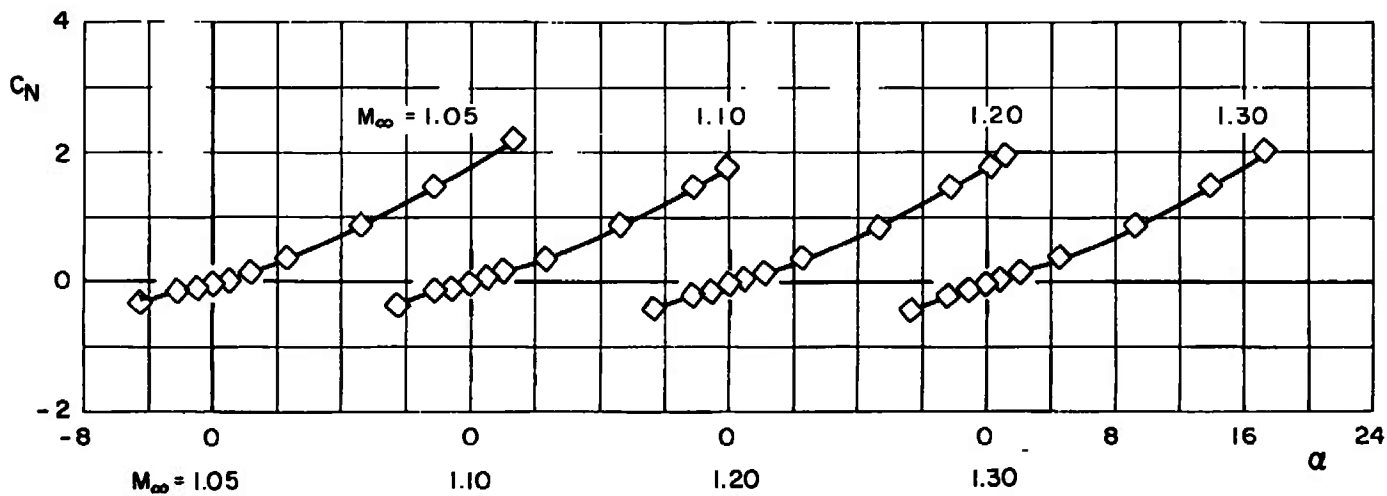
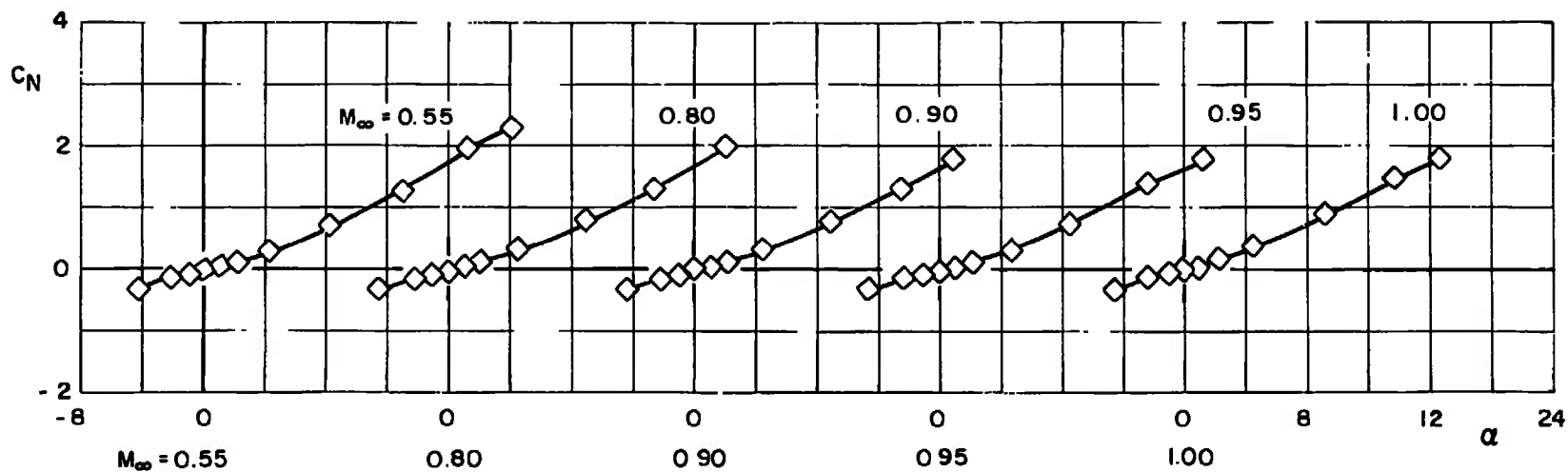


e. Configuration D
Fig. 7 Continued



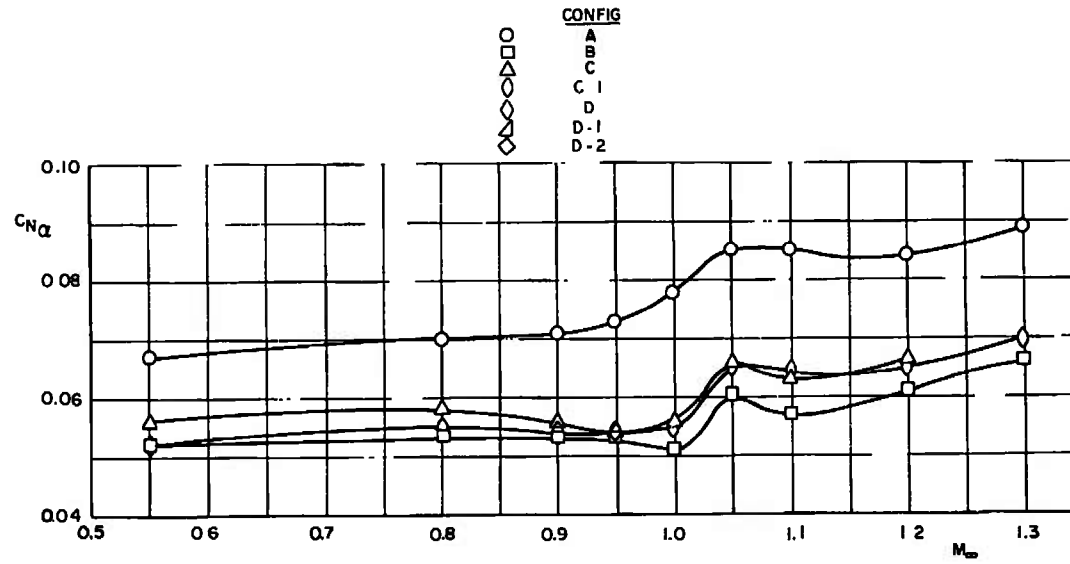
f. Configuration D-1

Fig. 7 Continued

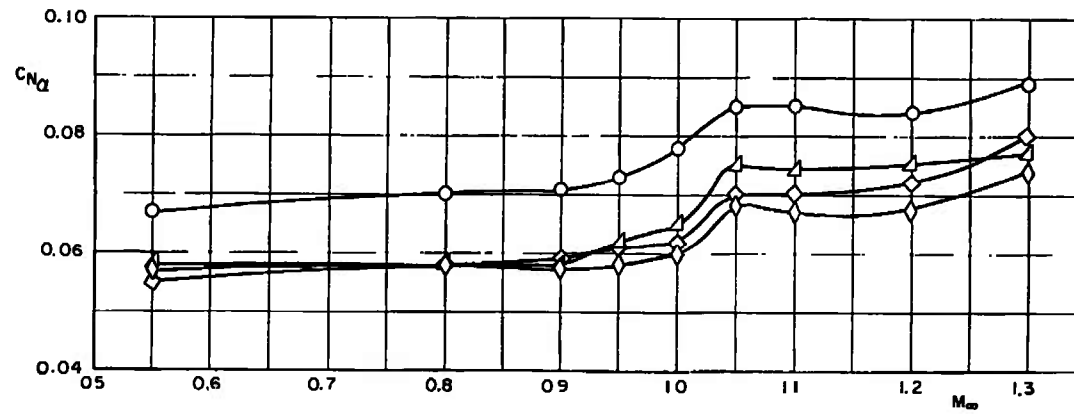


g. Configuration D-2

Fig. 7 Concluded

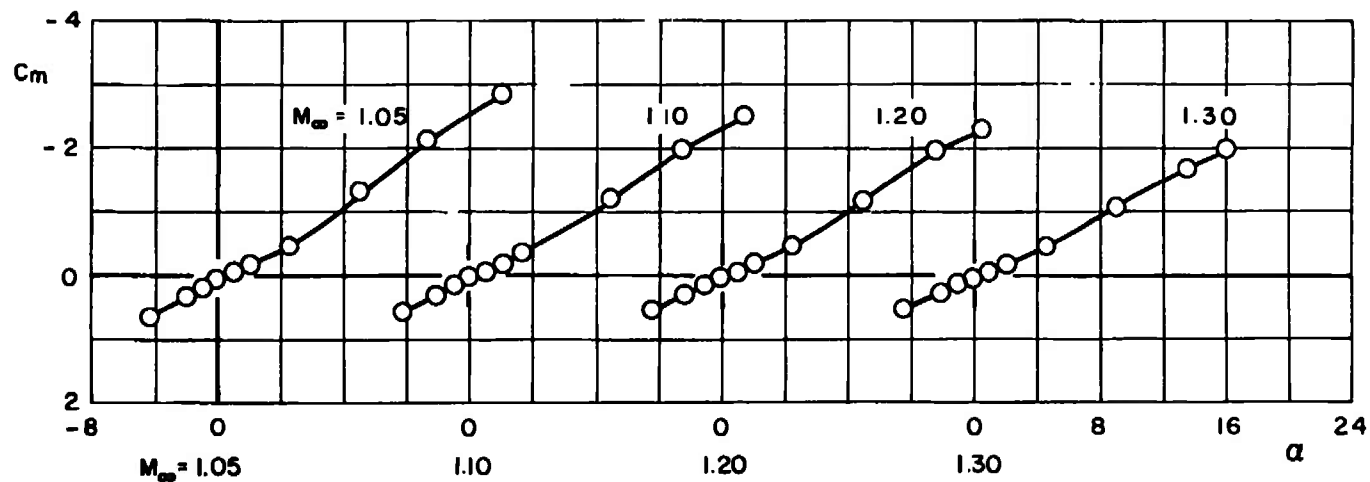
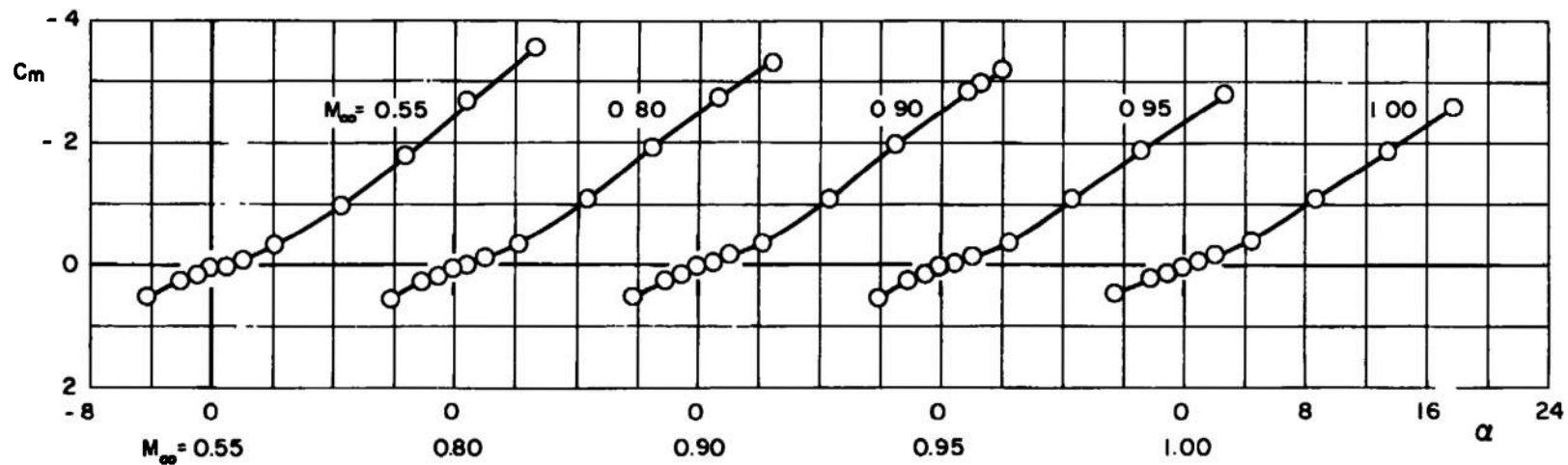


a. Configurations A, B, C, and C-1



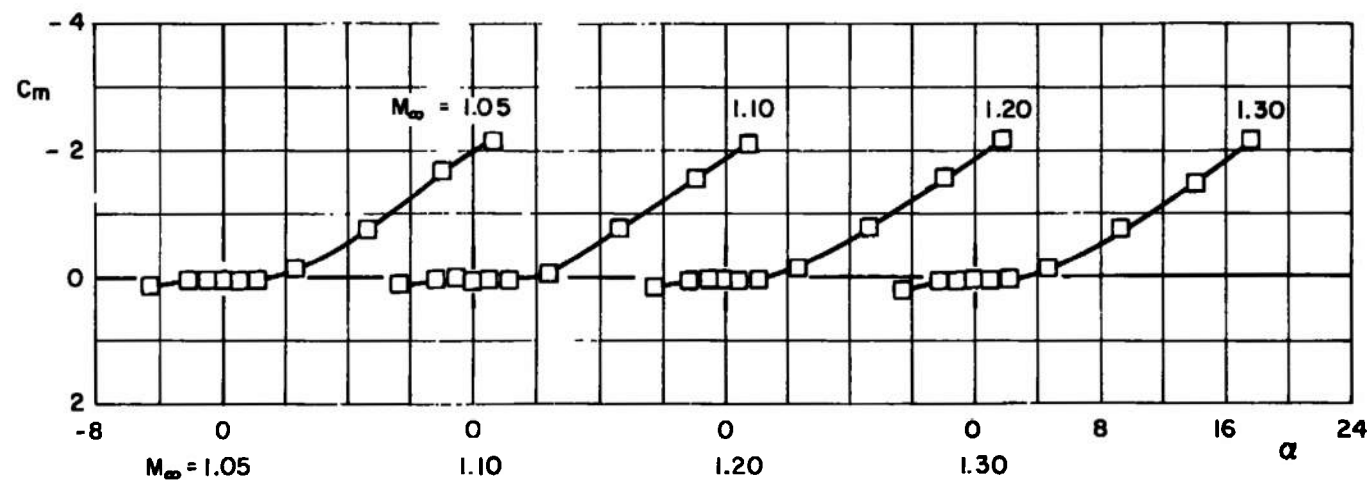
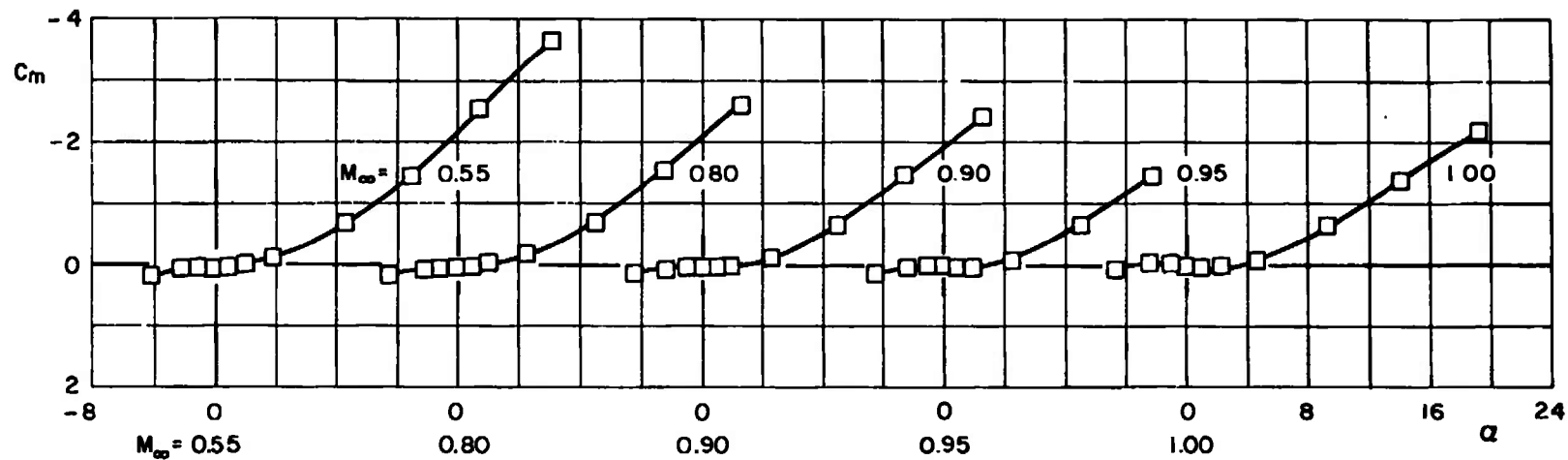
b. Configurations A, D, D-1, and D-2

Fig. 8 Normal-Force Coefficient Slope versus Mach Number

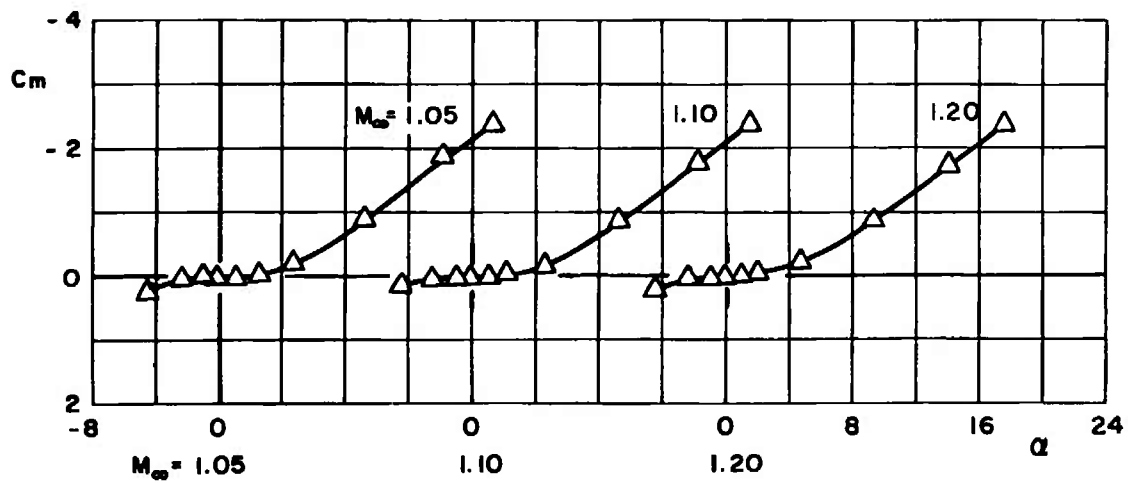
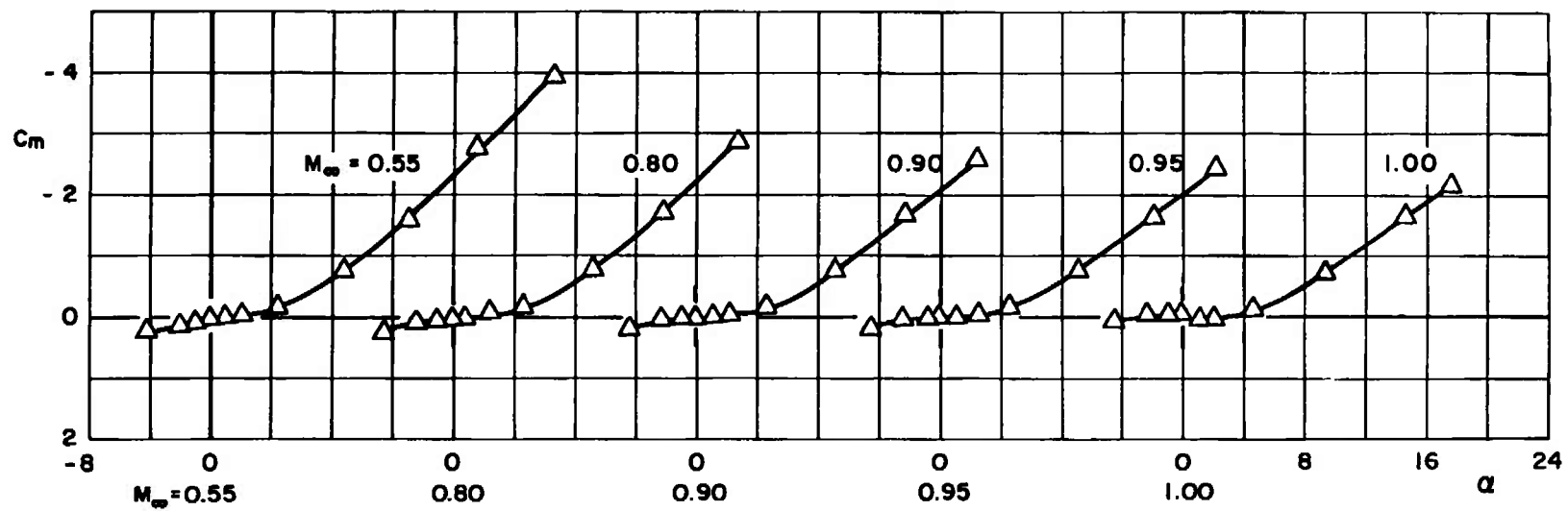


a. Configuration A

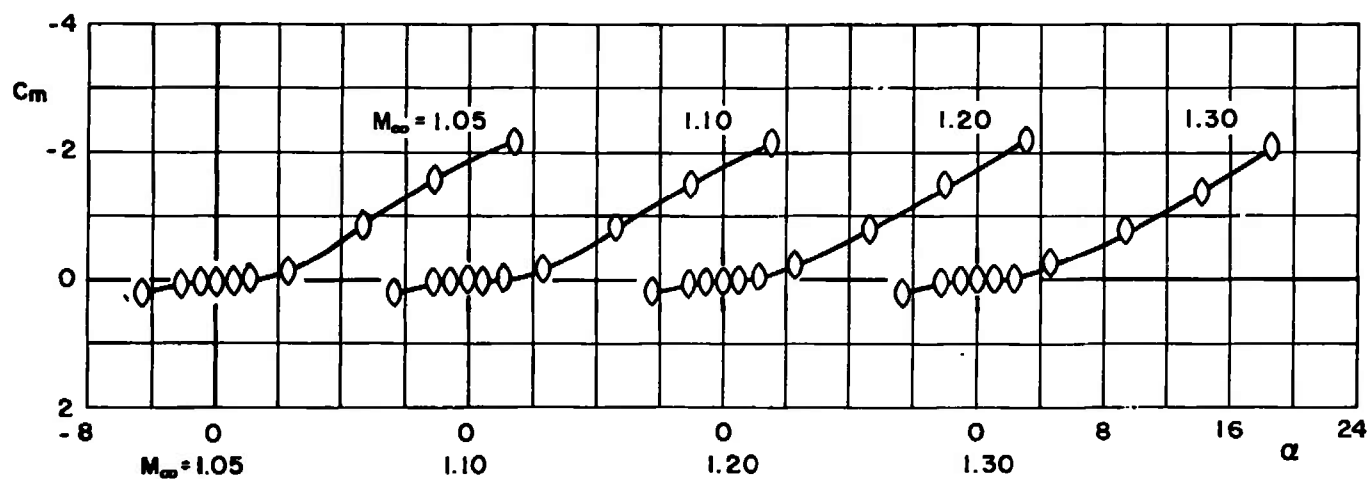
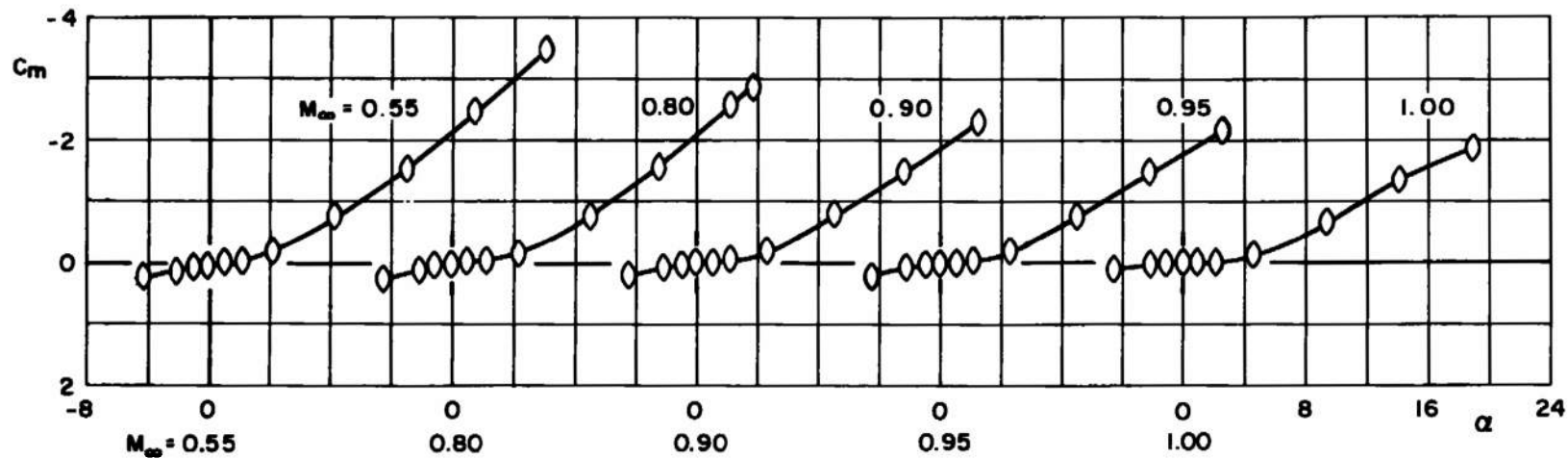
Fig. 9 Pitching-Moment Coefficient versus Angle of Attack



b. Configuration B
Fig. 9 Continued

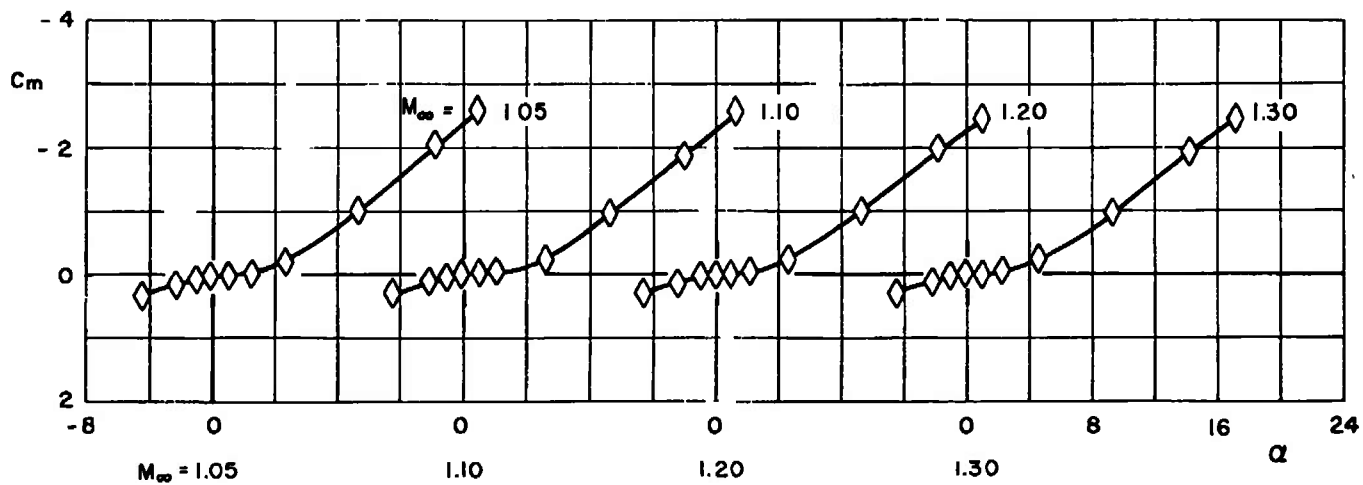
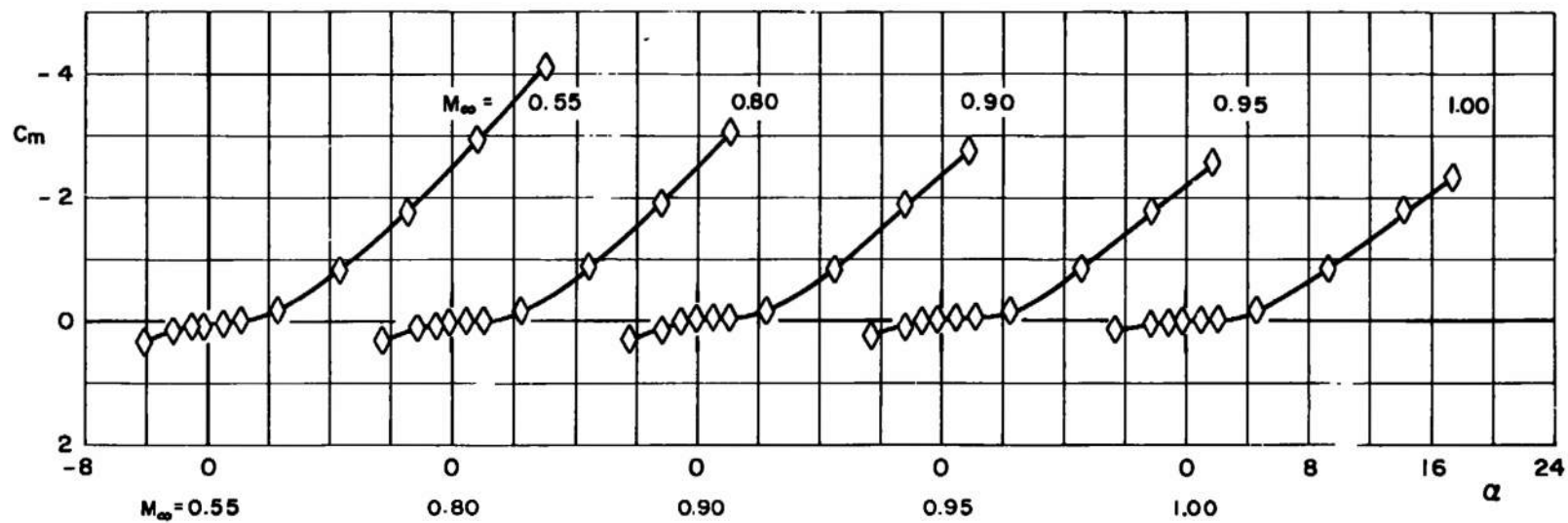


c. Configuration C
Fig. 9 Continued

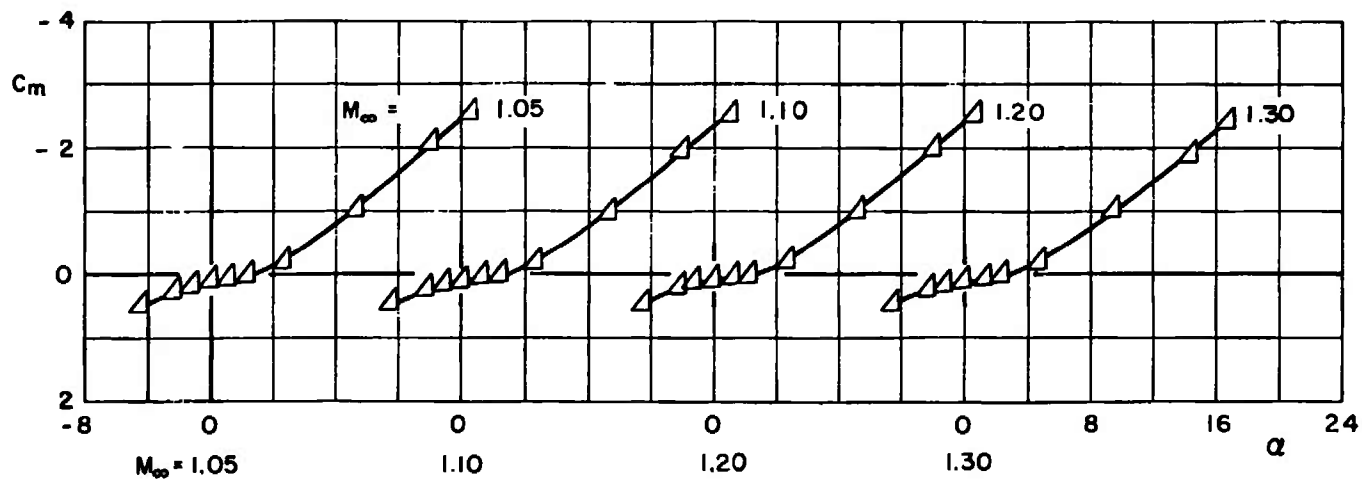
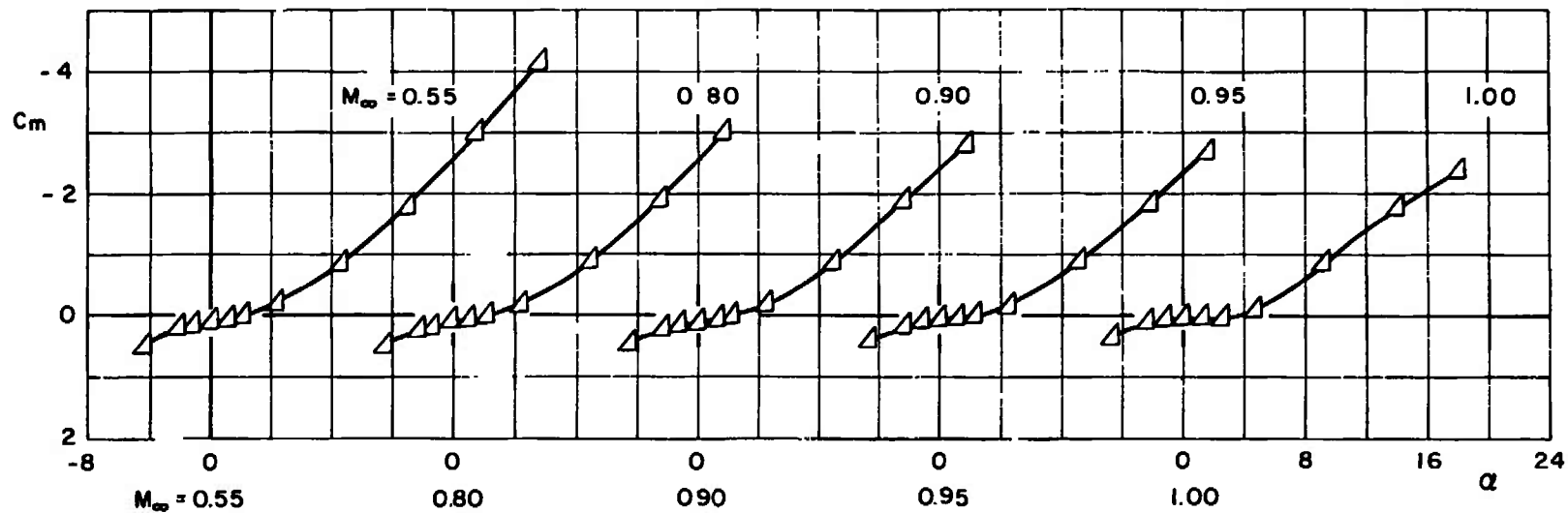


d. Configuration C-1

Fig. 9 Continued

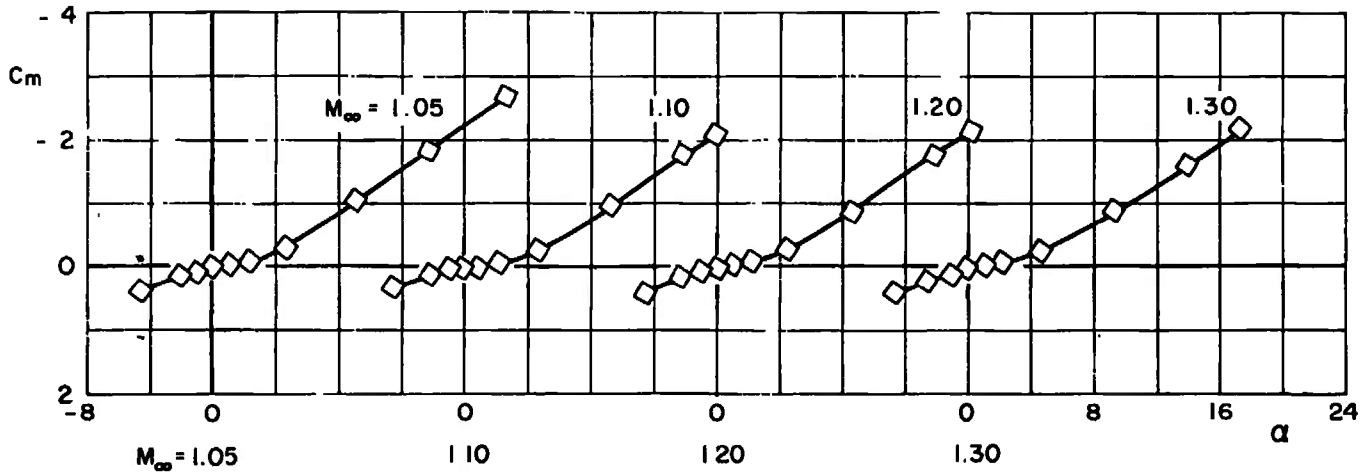
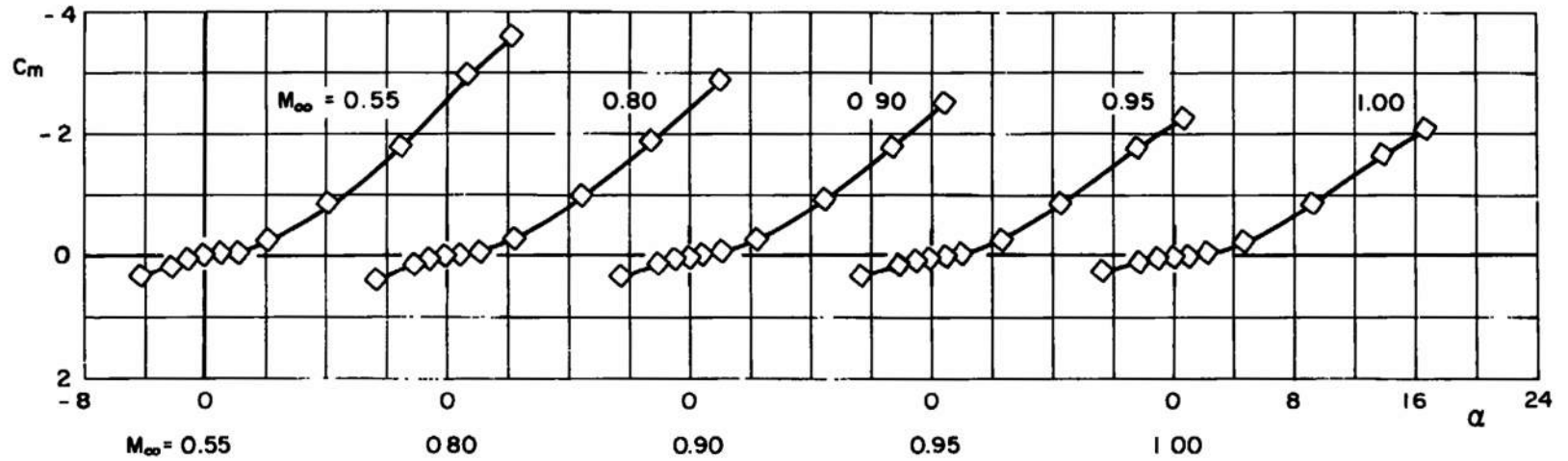


e. Configuration D
Fig. 9 Continued

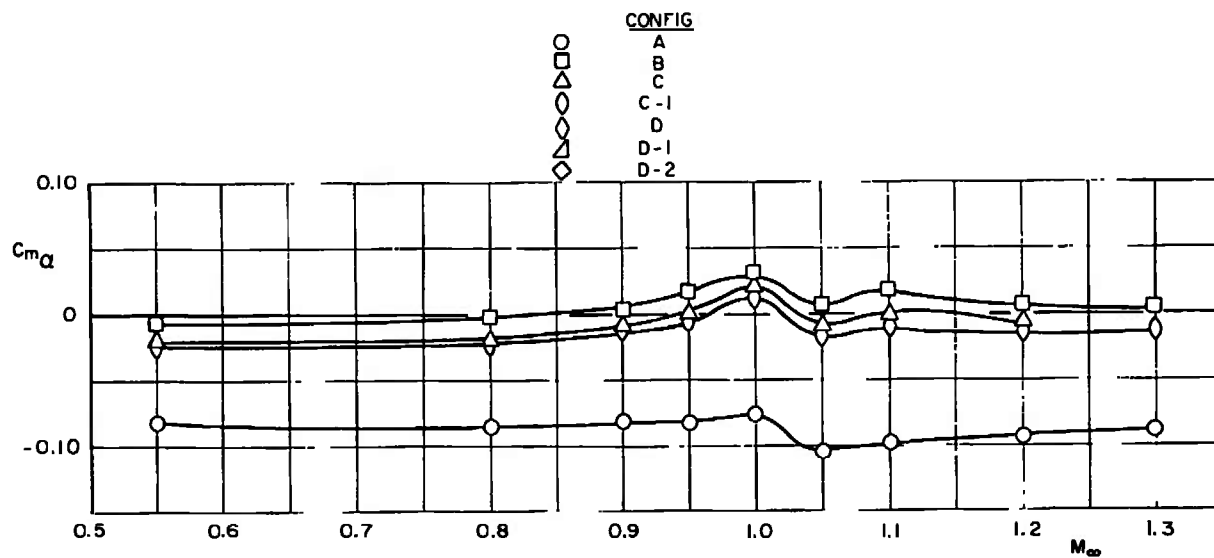


f. Configuration D-1

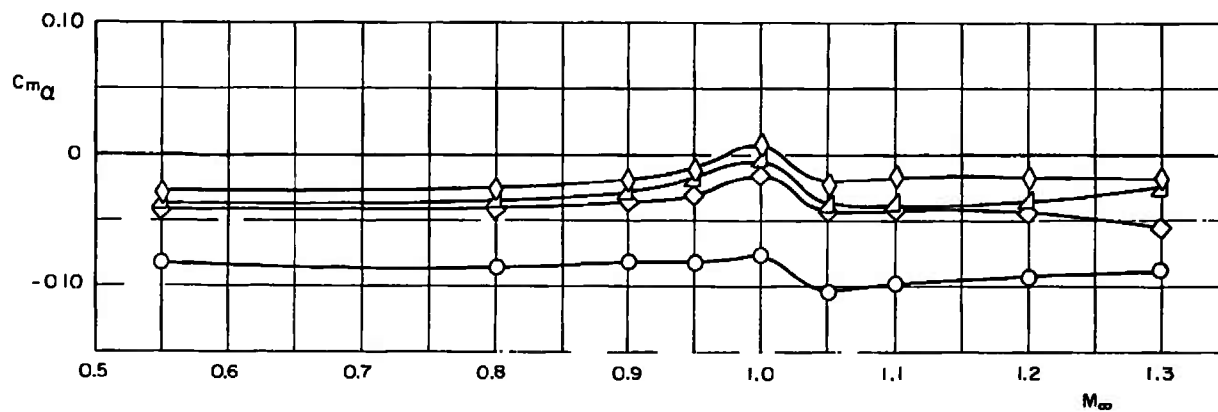
Fig. 9 Continued



g. Configuration D-2
Fig. 9 Concluded

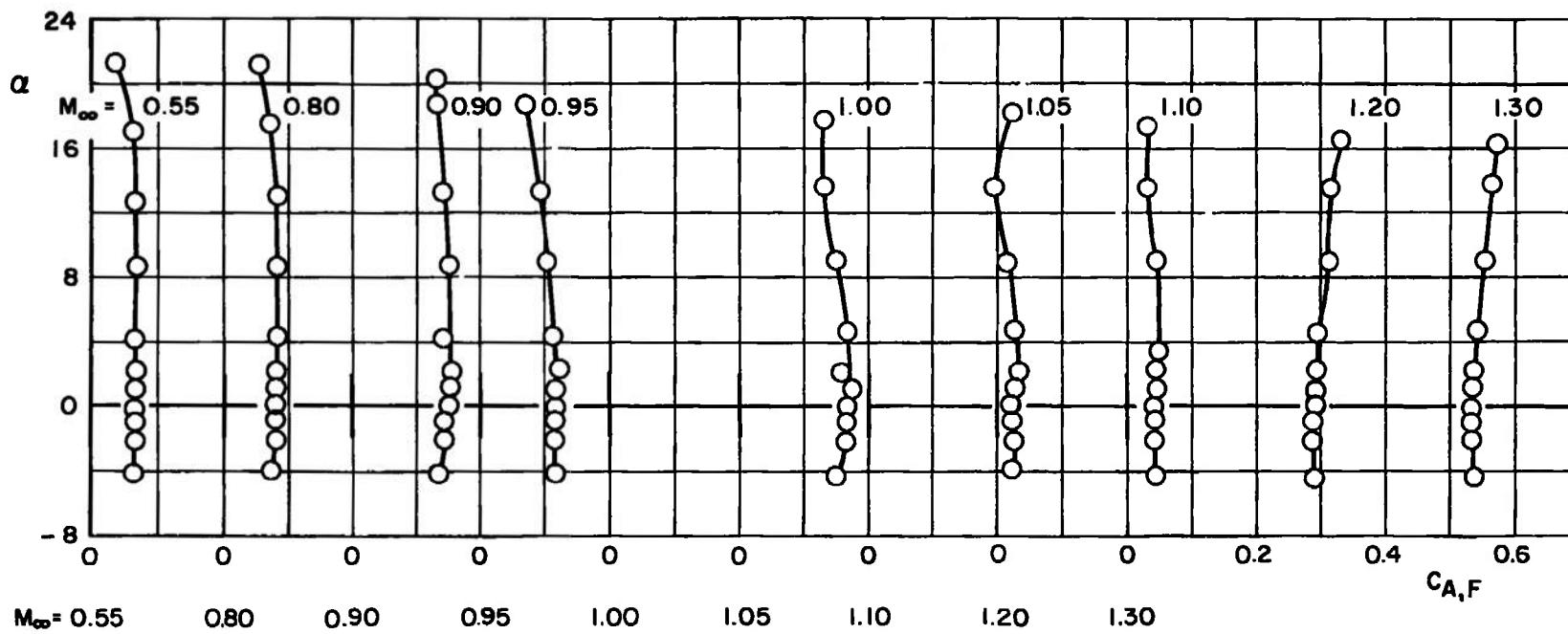


a. Configurations A, B, C, and C-1



b. Configurations A, D, D-1, and D-2

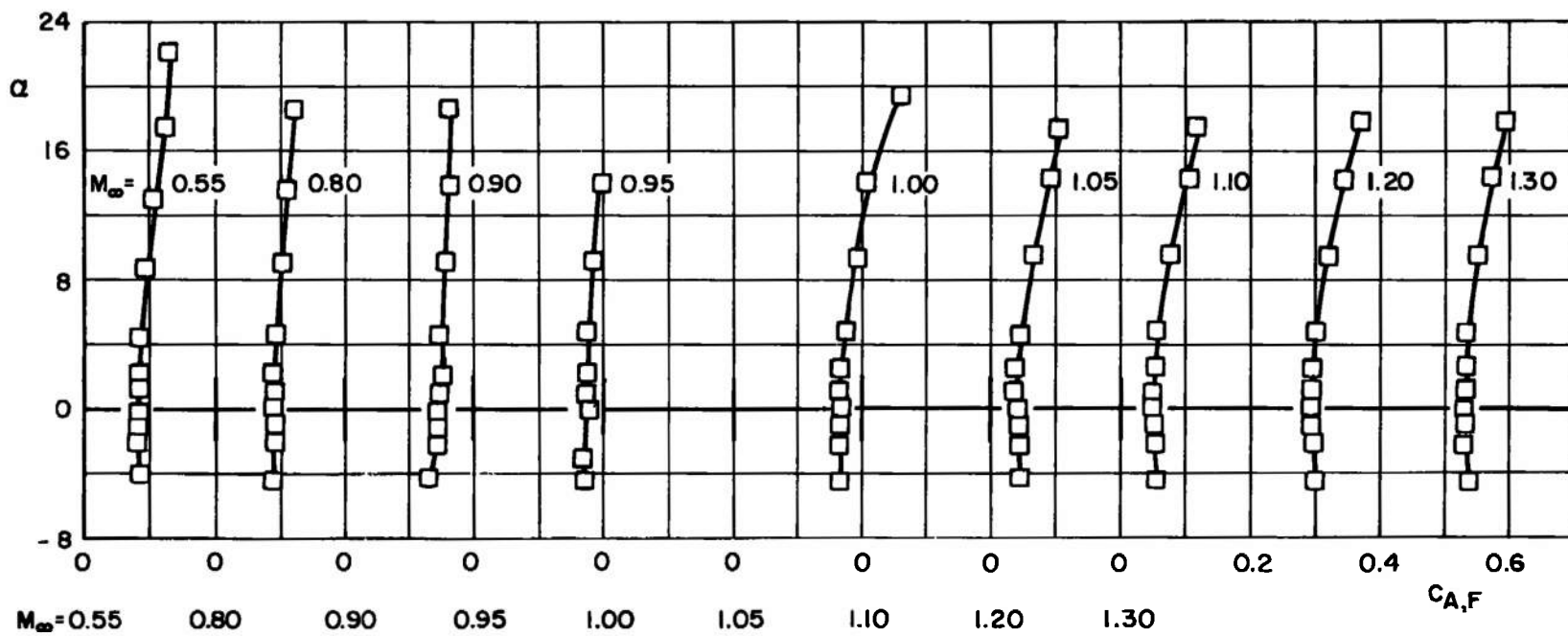
Fig. 10 Pitching-Moment Coefficient Slope versus Mach Number



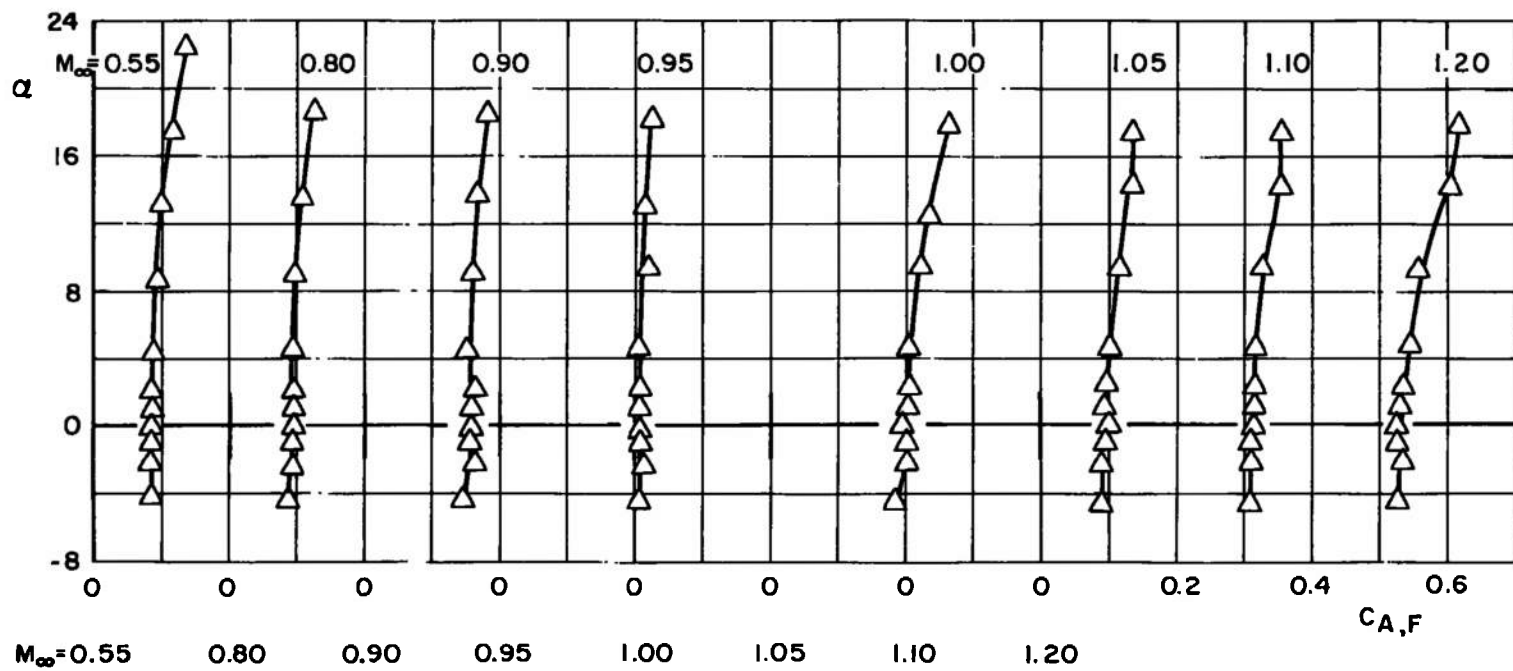
a. Configuration A

Fig. 11 Angle of Attack versus Forebody Axial-Force Coefficient

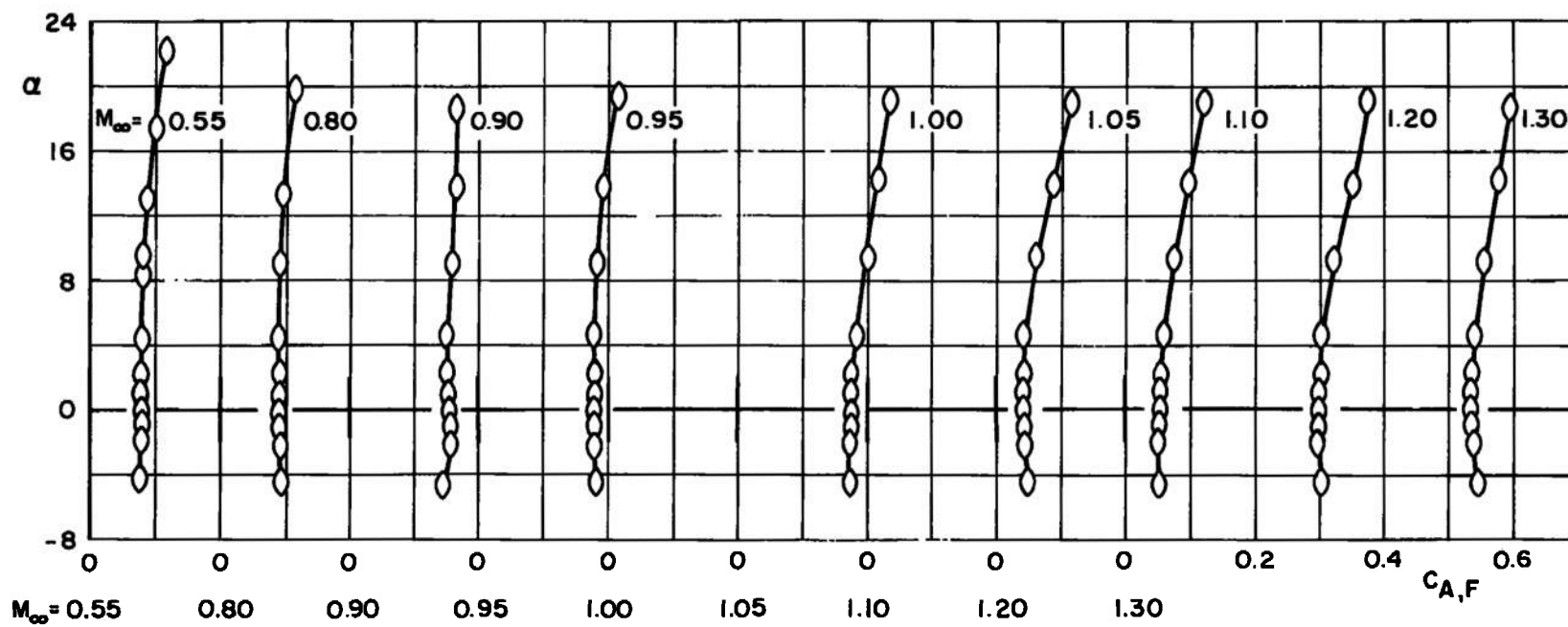
40



b. Configuration B
Fig. 11 Continued

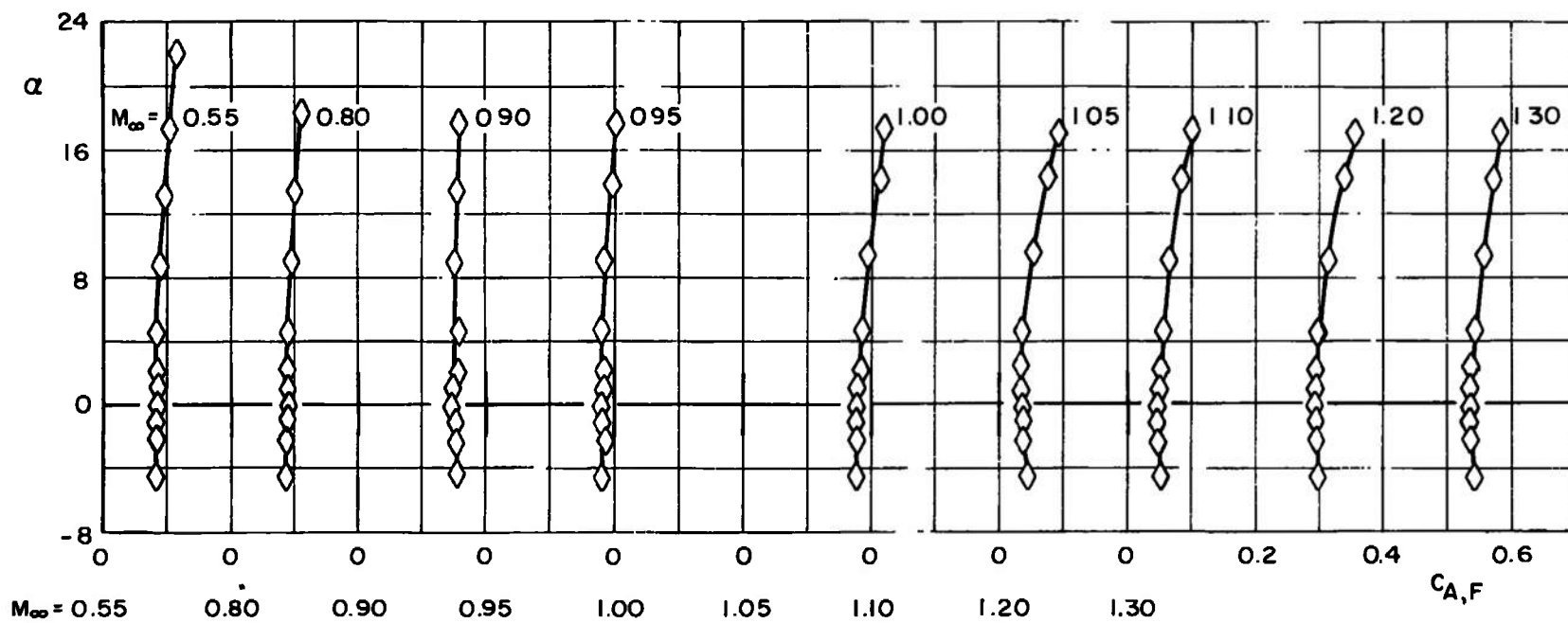


c. Configuration C
Fig. 11 Continued

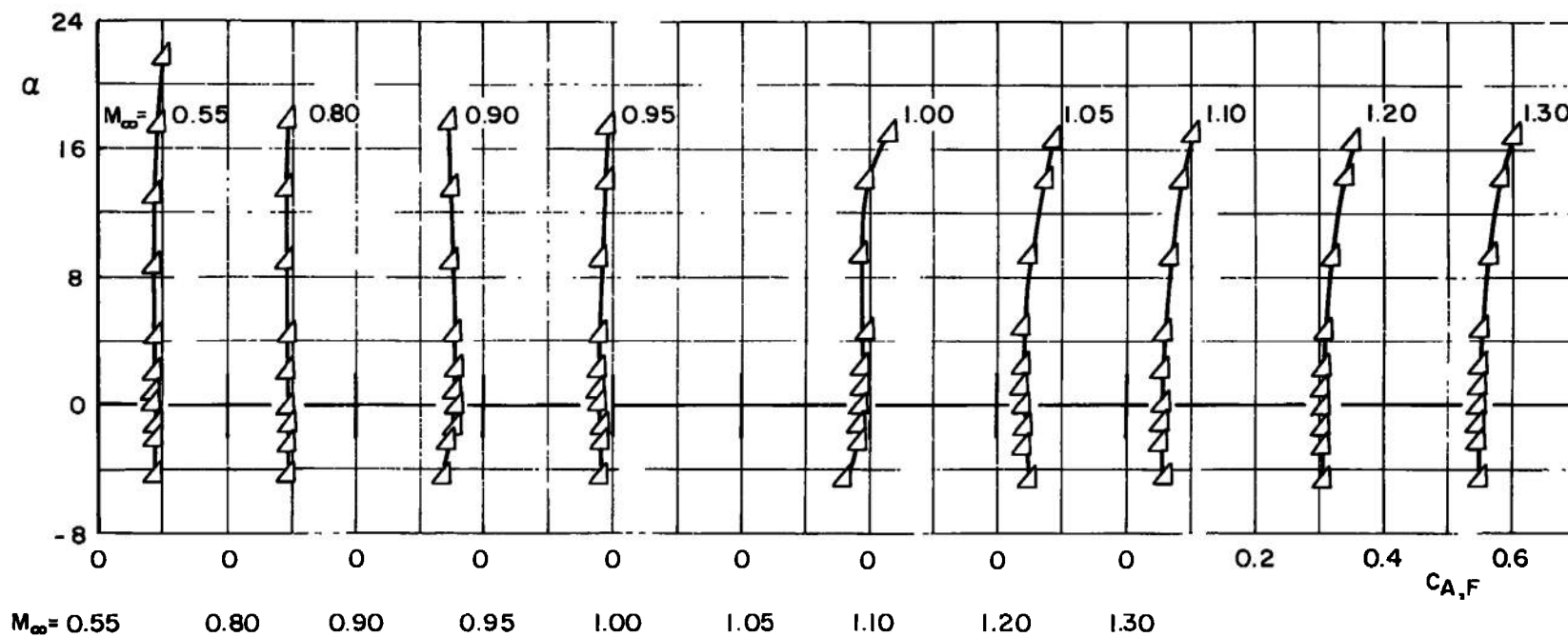


d. Configuration C-1

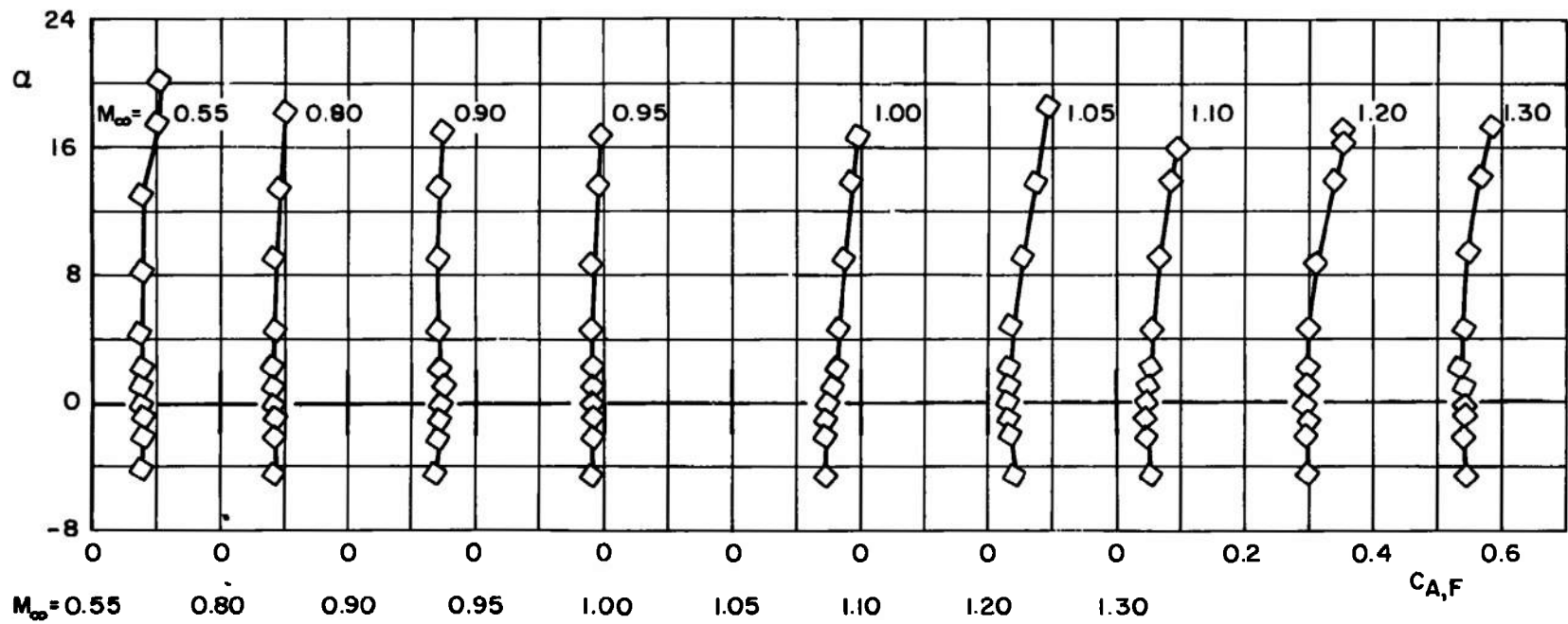
Fig. 11 Continued



e. Configuration D
Fig. 11 Continued



f. Configuration D-1
Fig. 11 Continued



g. Configuration D-2

Fig. 11 Concluded

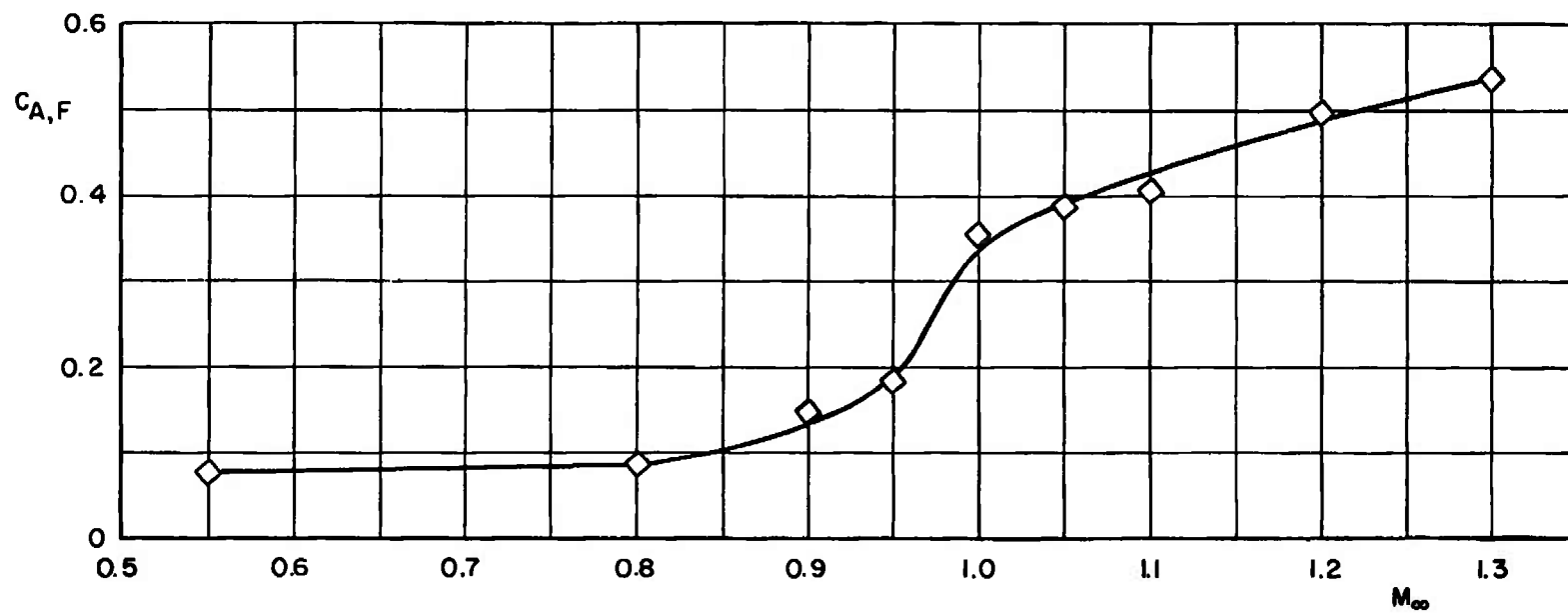
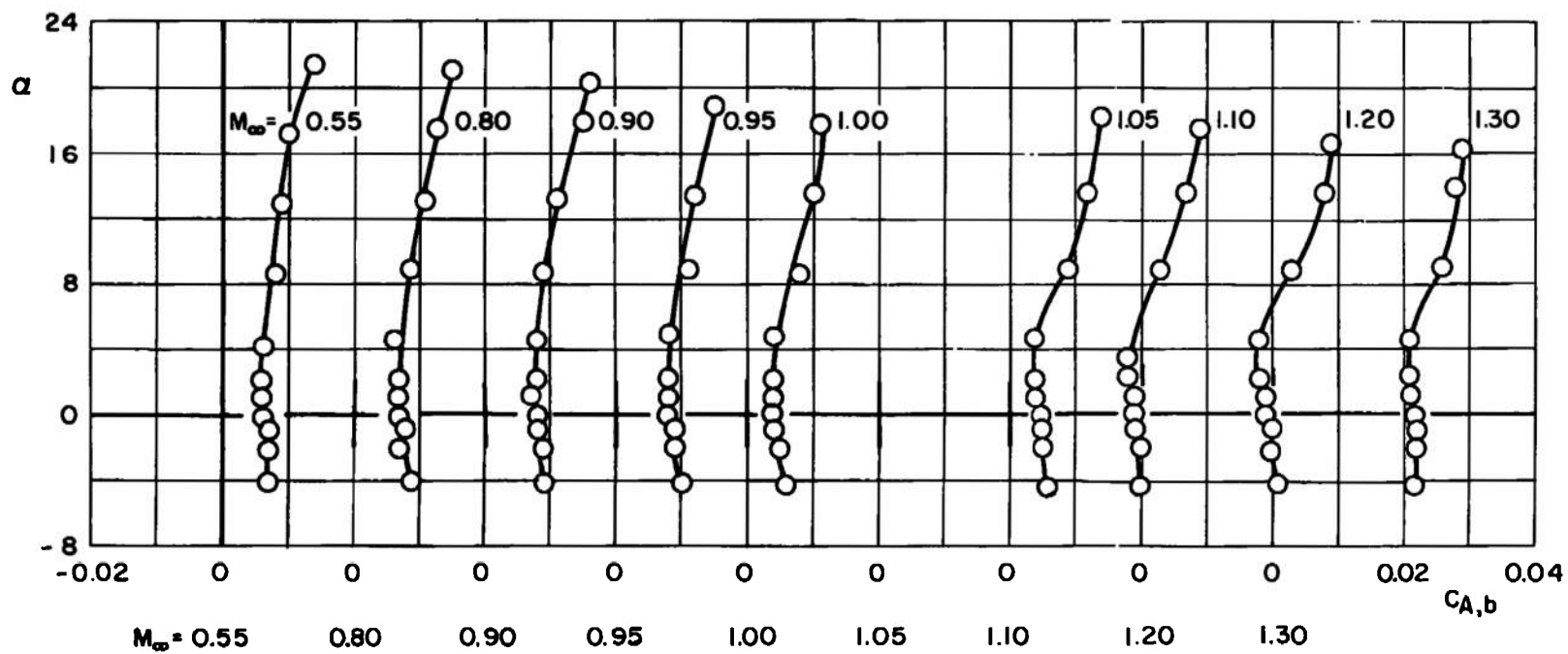
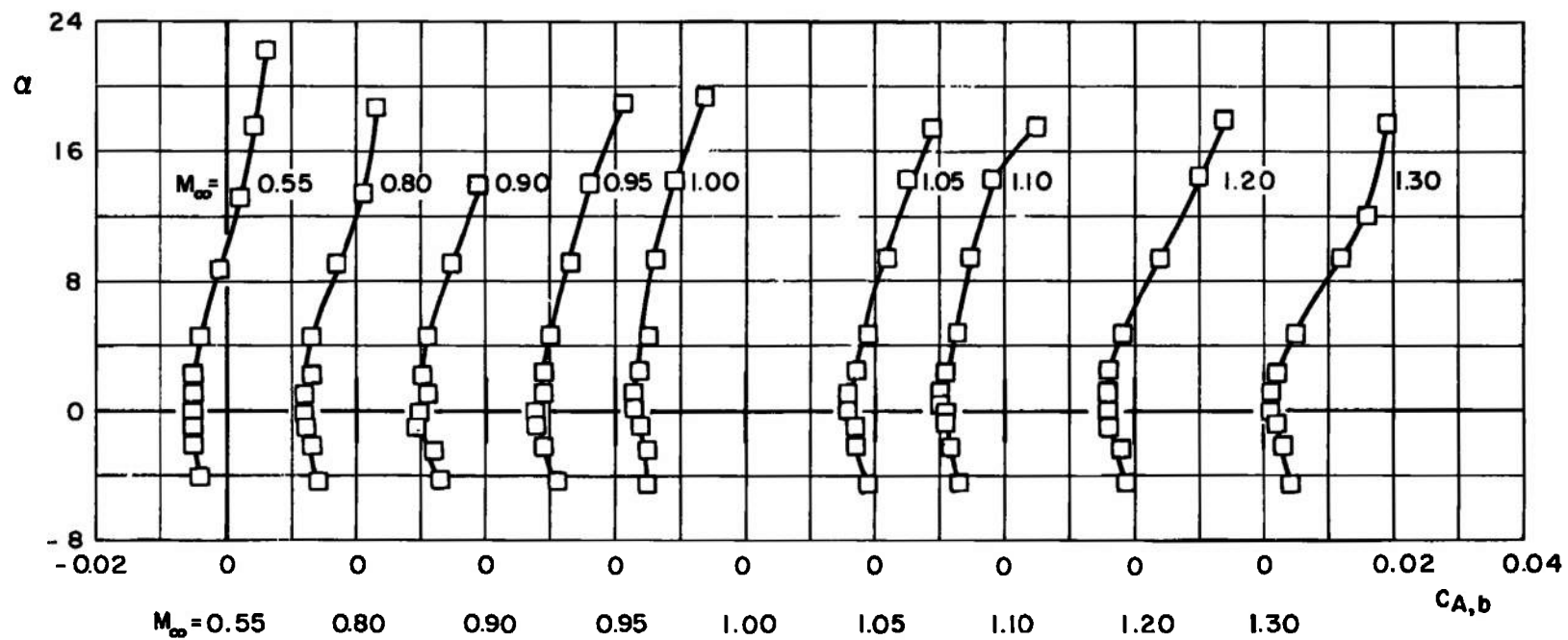


Fig. 12 Forebody Axial-Force Coefficient $\alpha = 0$ versus Mach Number for Configuration D-2

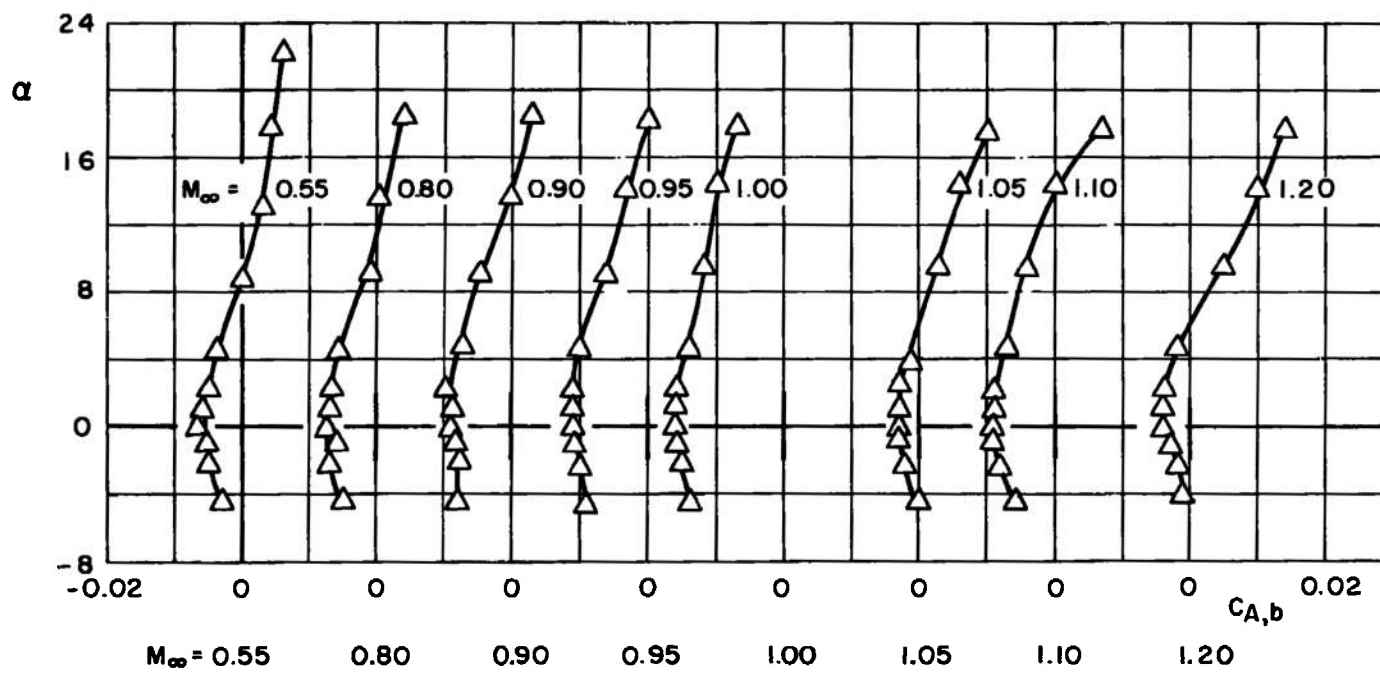


o. Configuration A

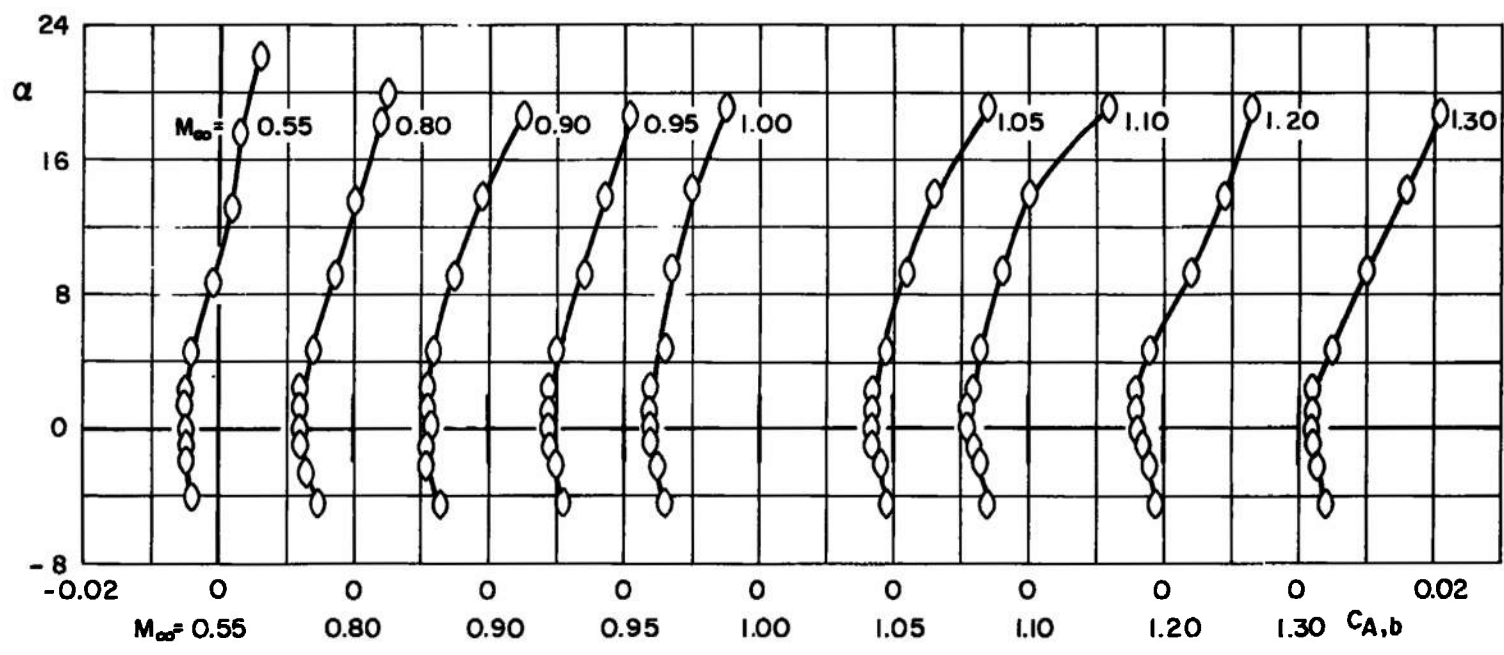
Fig. 13 Angle of Attack versus Base Axial-Force Coefficient



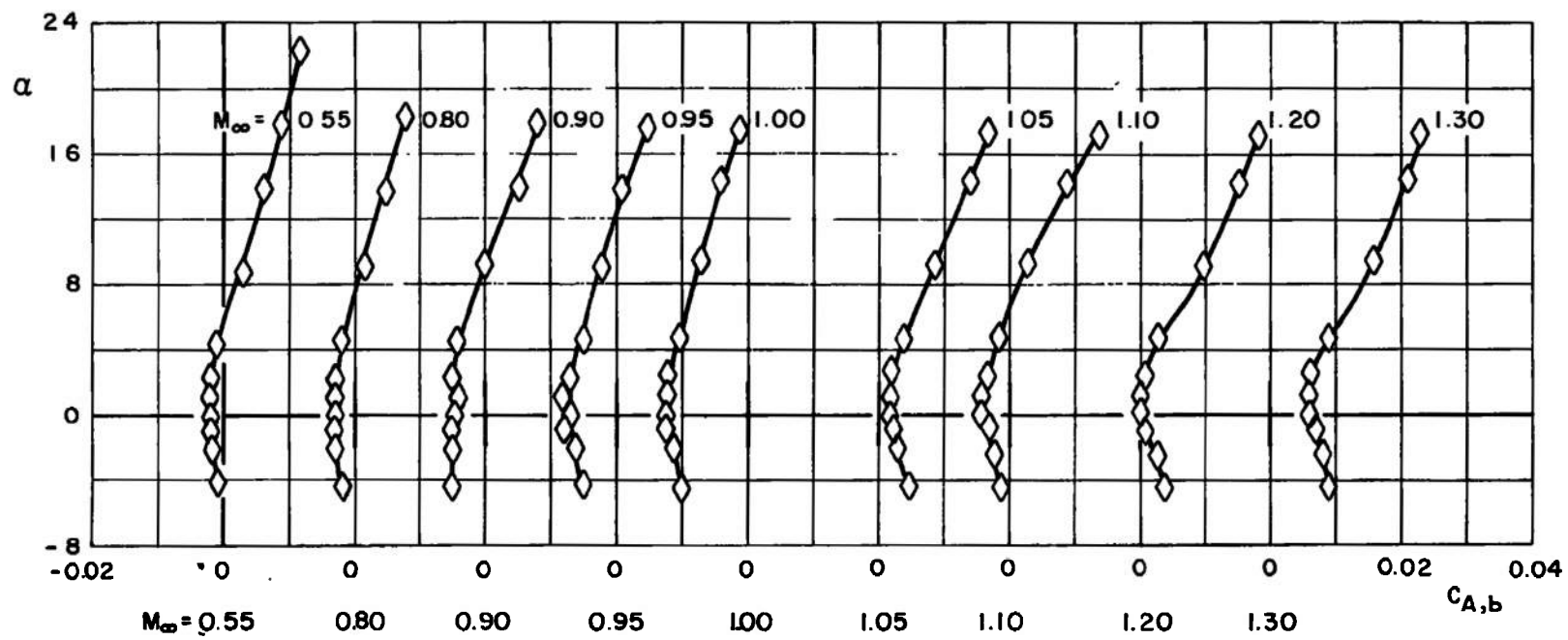
b. Configuration B
Fig. 13 Continued



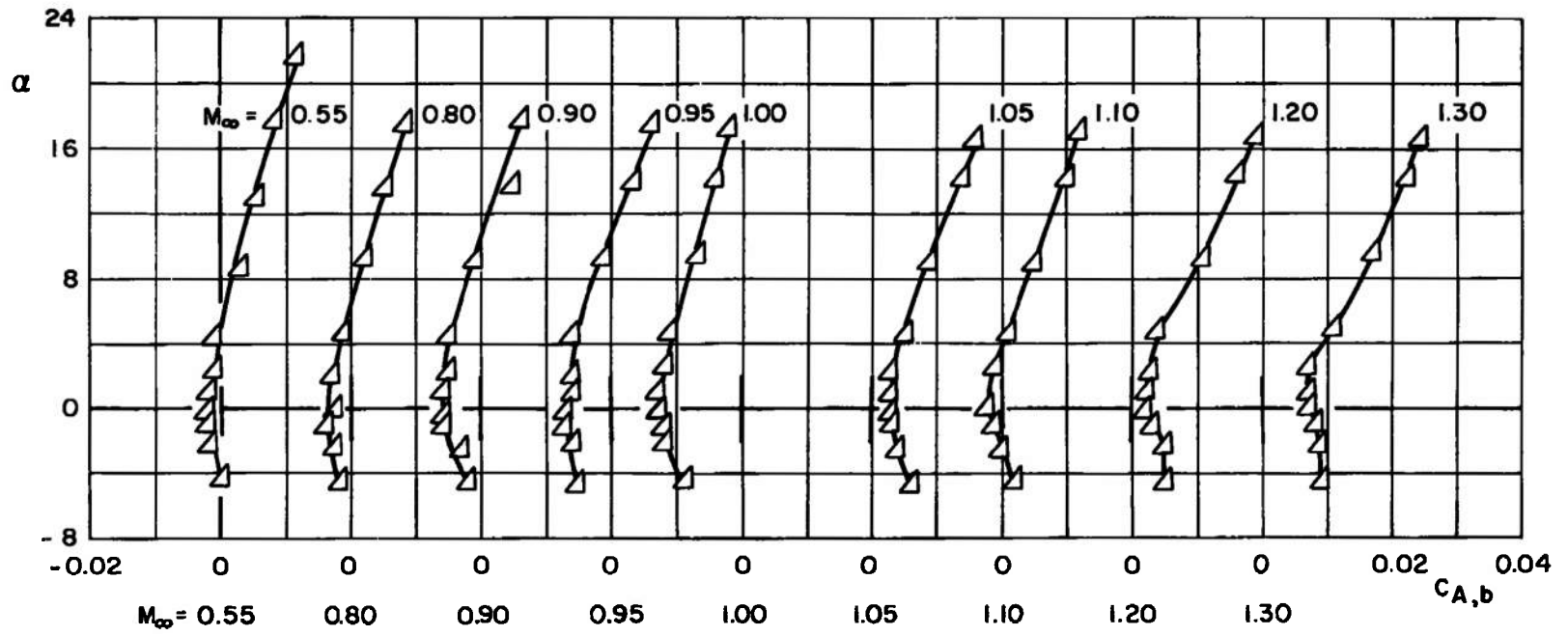
c. Configuration C
Fig. 13 Continued



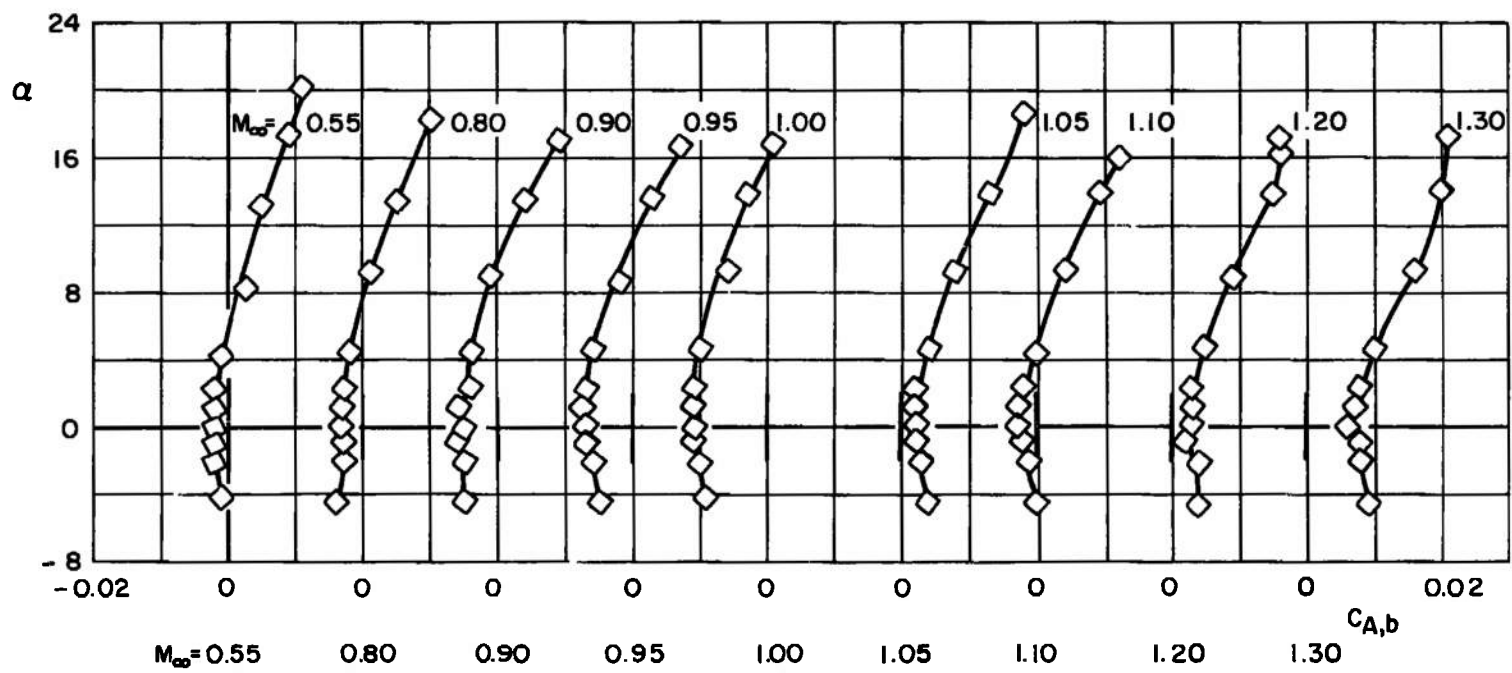
d. Configuration C-1
Fig. 13 Continued



e. Configuration D
Fig. 13 Continued

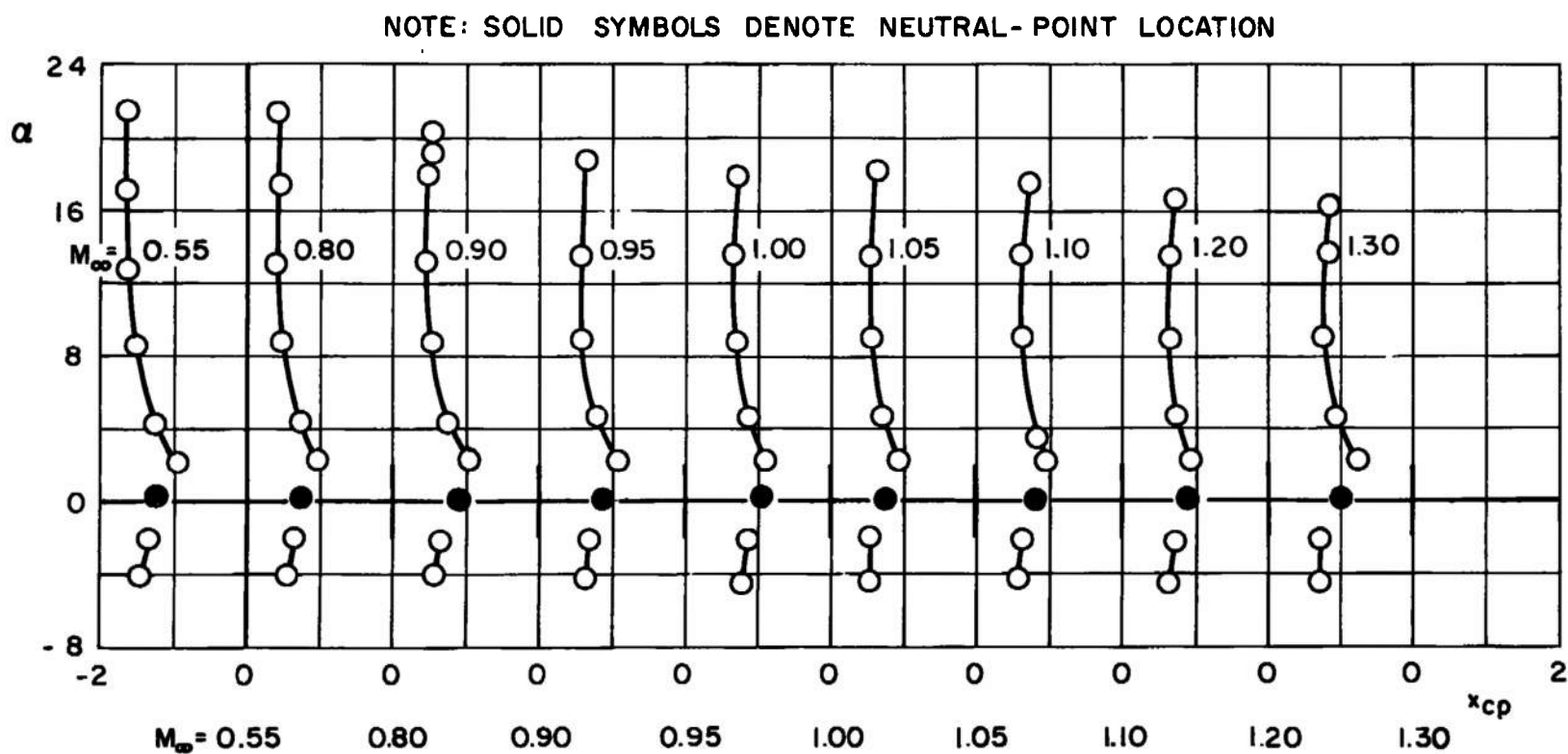


f. Configuration D-1
Fig. 13 Continued



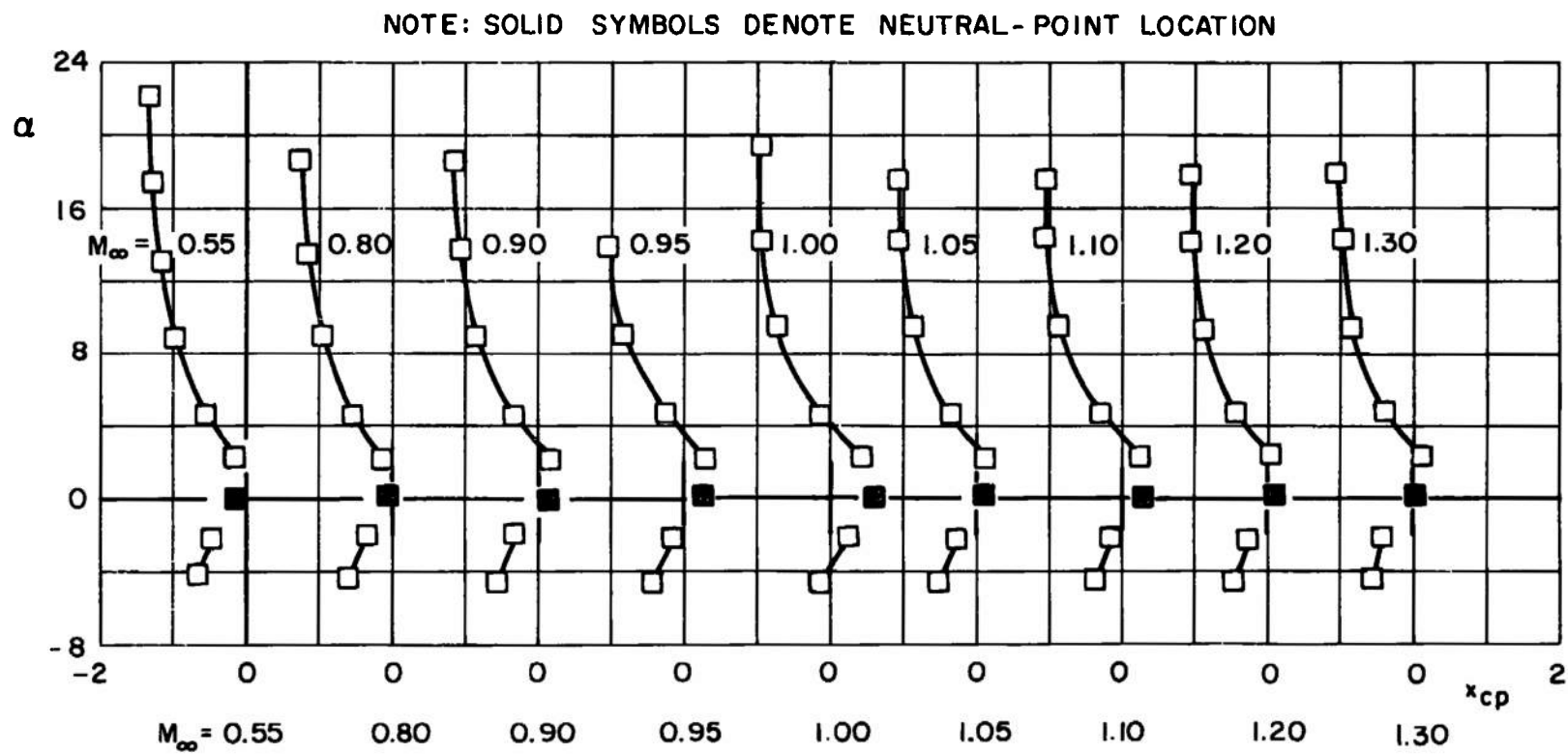
g. Configuration D-2

Fig. 13 Concluded



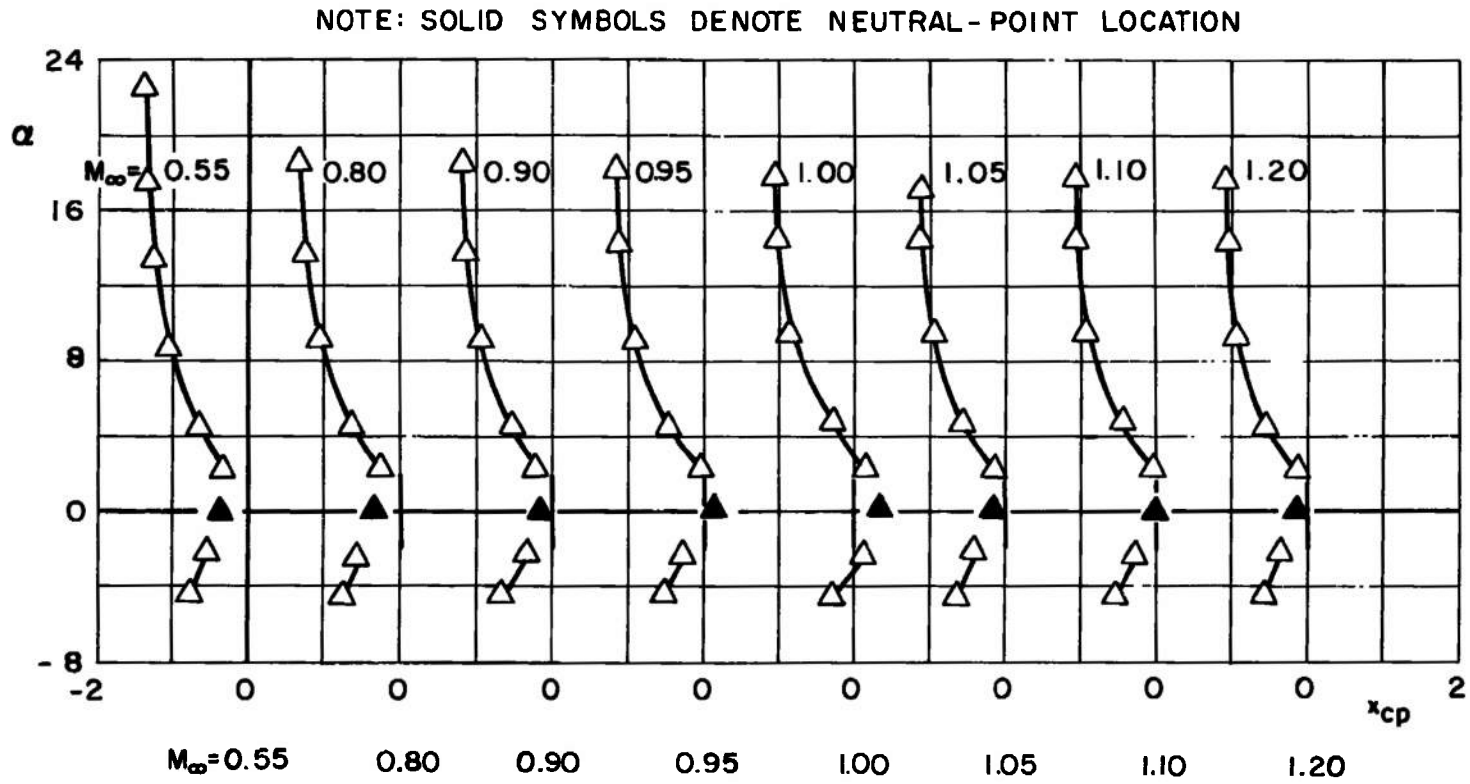
a. Configuration A

Fig. 14 Angle of Attack versus Center-of-Pressure Location

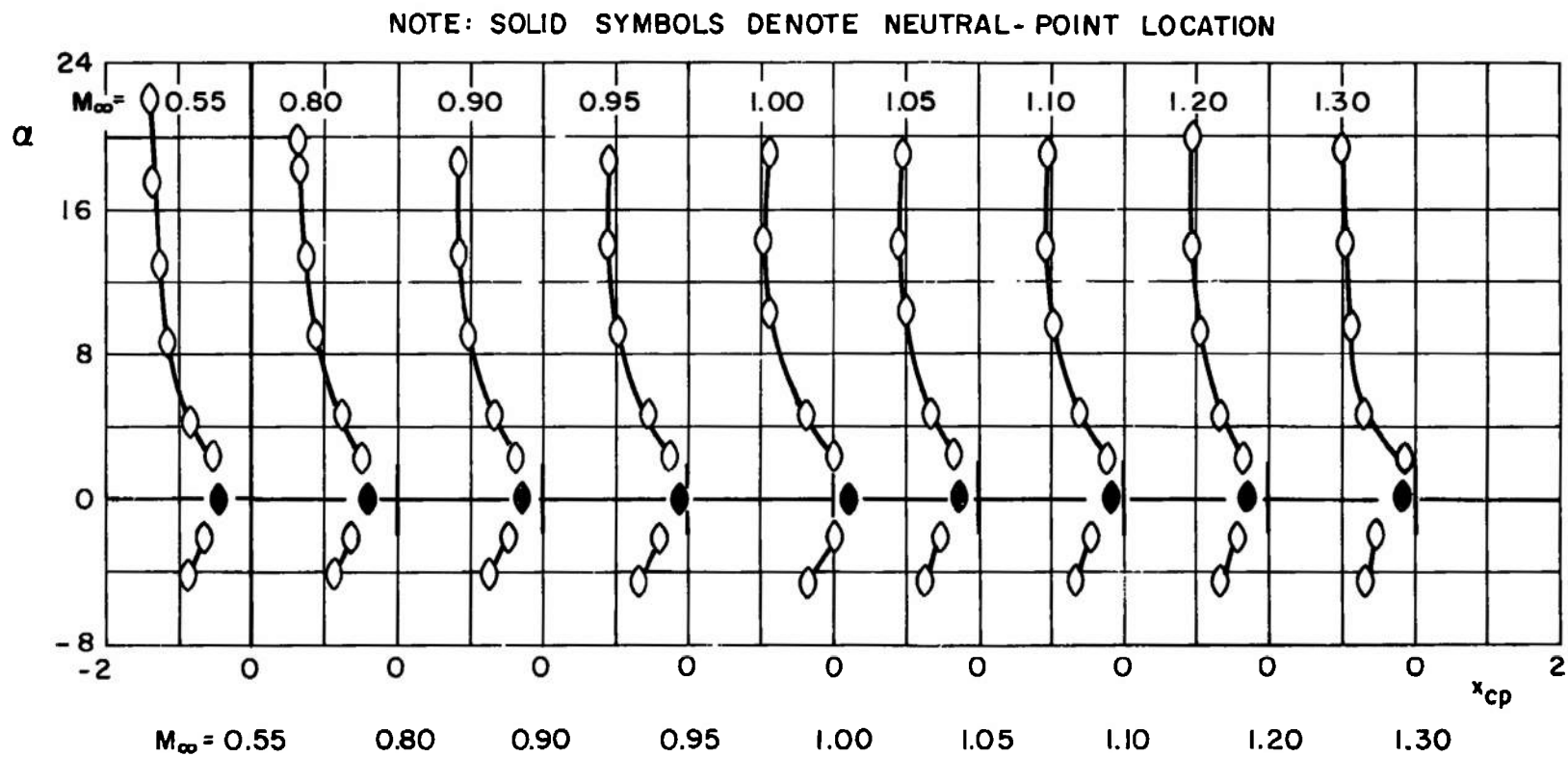


b. Configuration B

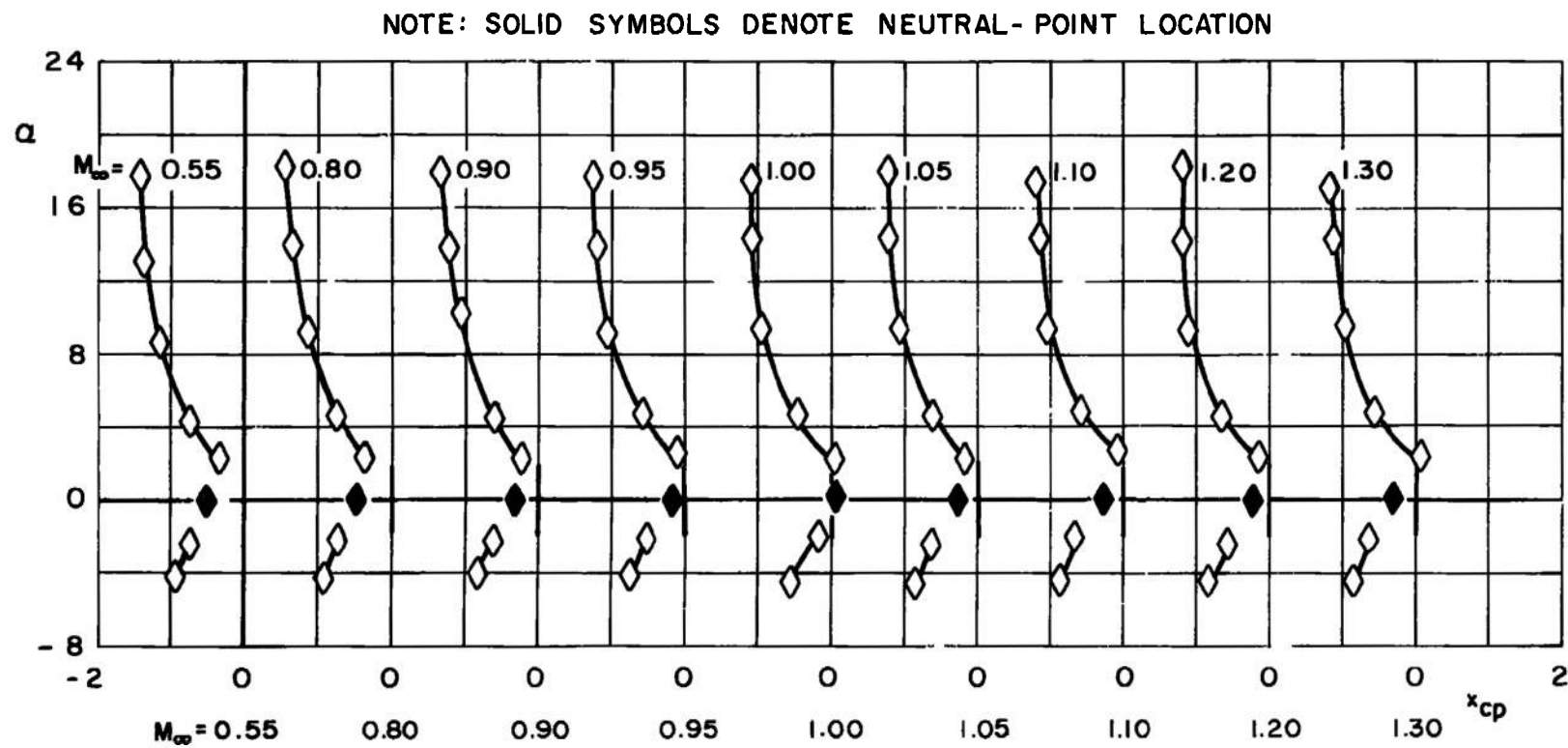
Fig. 14 Continued



c. Configuration C
Fig. 14 Continued

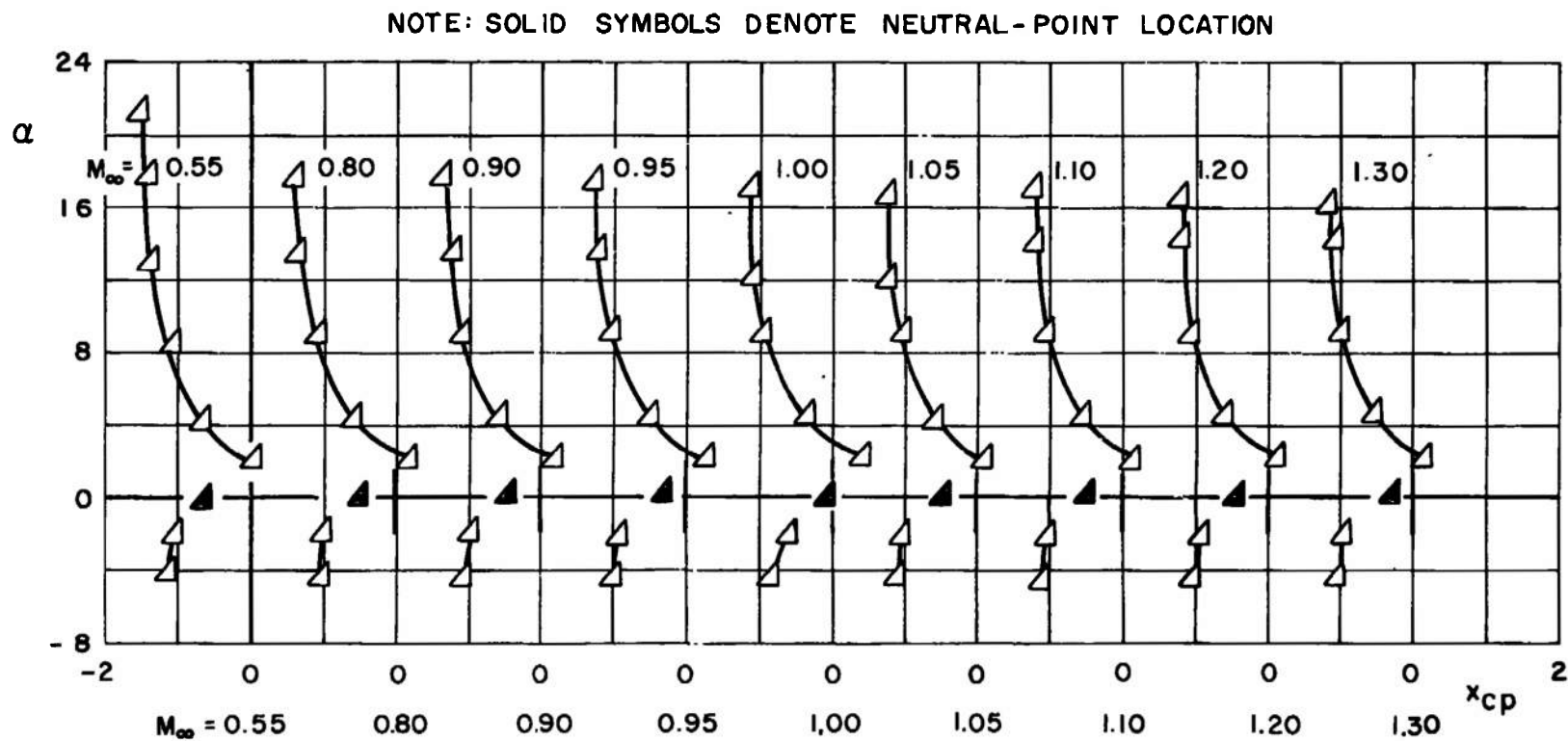


d. Configuration C-1
Fig. 14 Continued

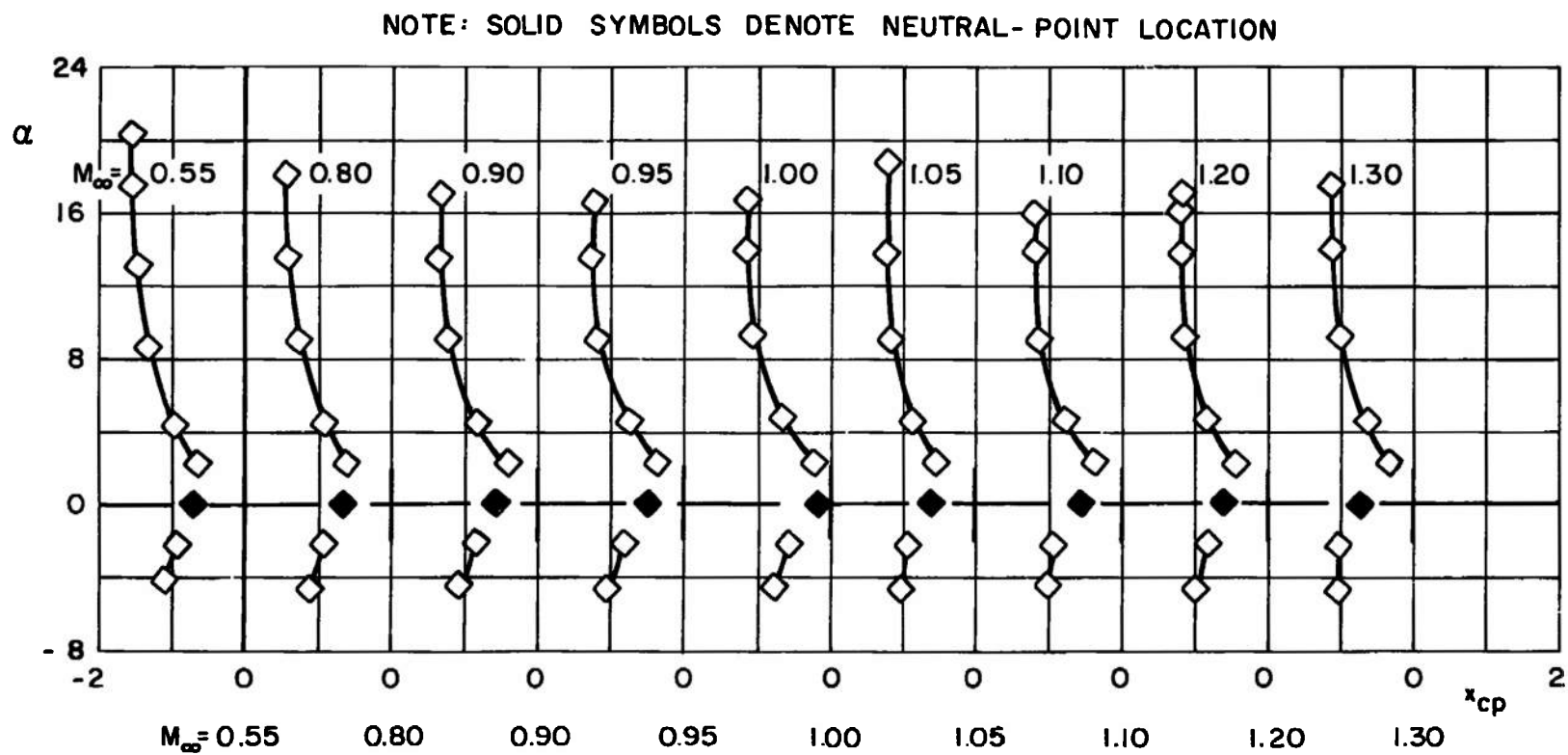


e. Configuration D

Fig. 14 Continued



f. Configuration D-1
Fig. 14 Continued



g. Configuration D-2
Fig. 14 Concluded

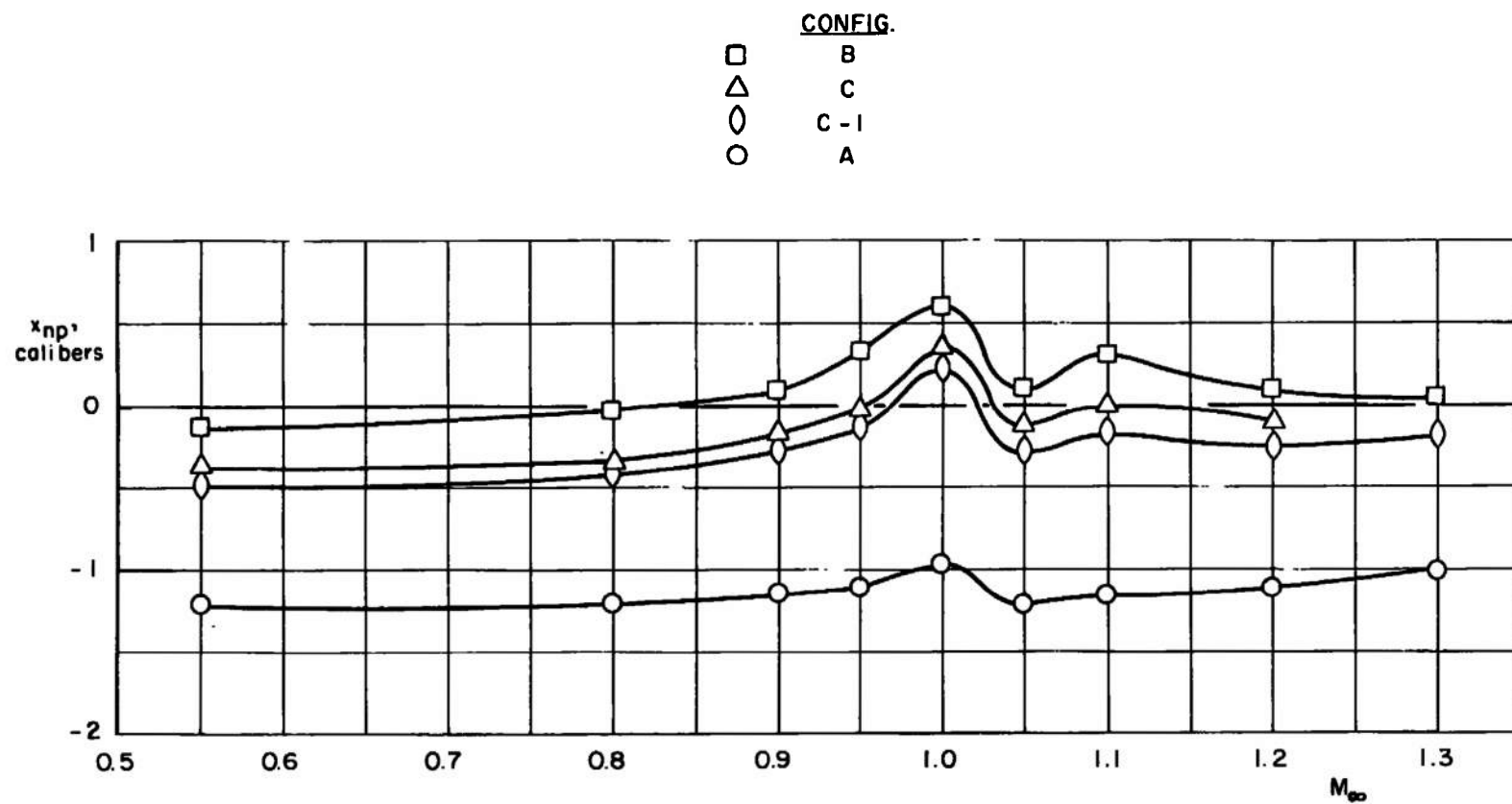


Fig. 15 Neutral-Point Location versus Mach Number Comparing Configurations B, C, C-1, and A

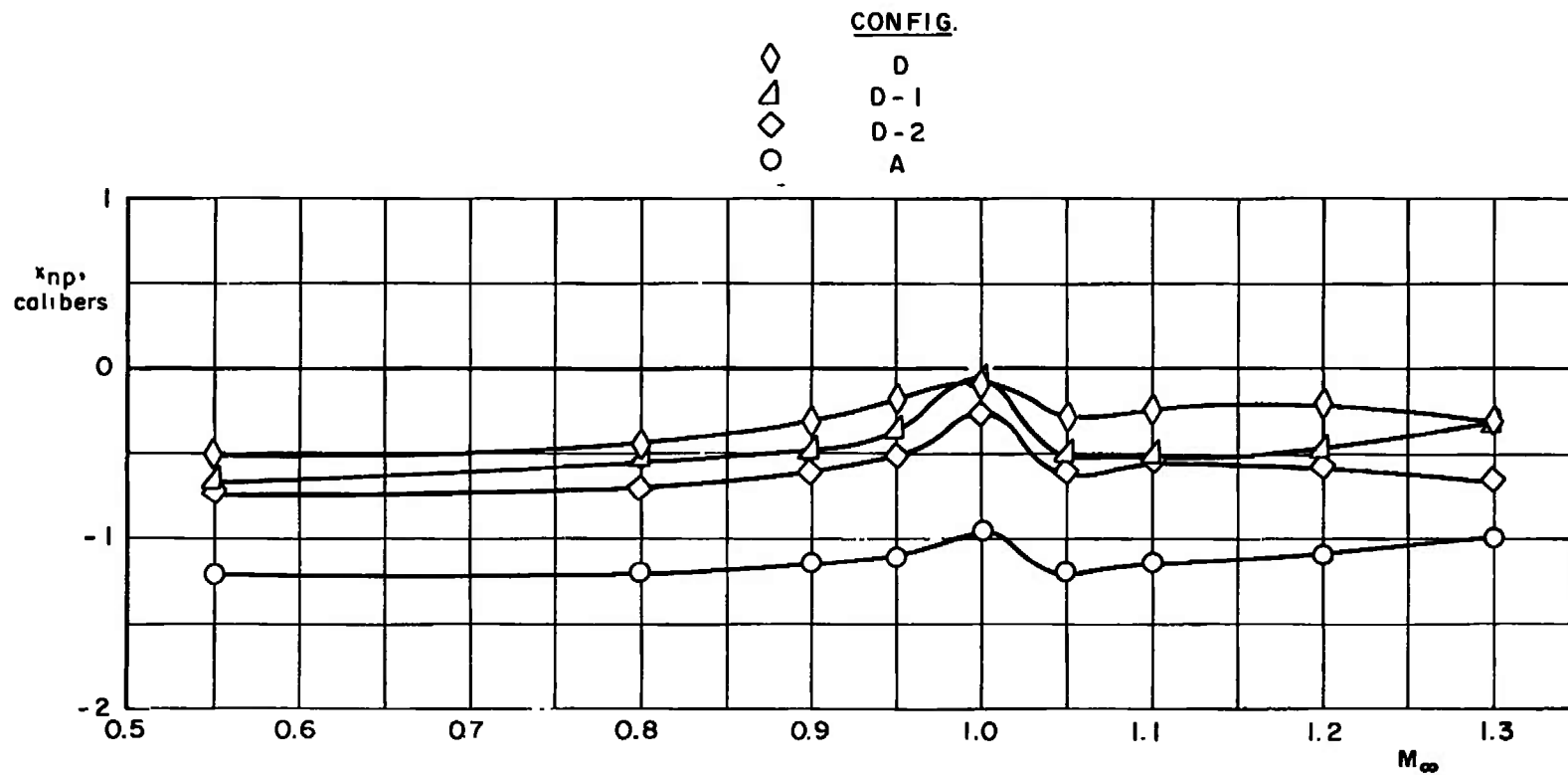


Fig. 16 Neutral-Point Location versus Mach Number Comparing Configurations D, D-1, D-2, and A

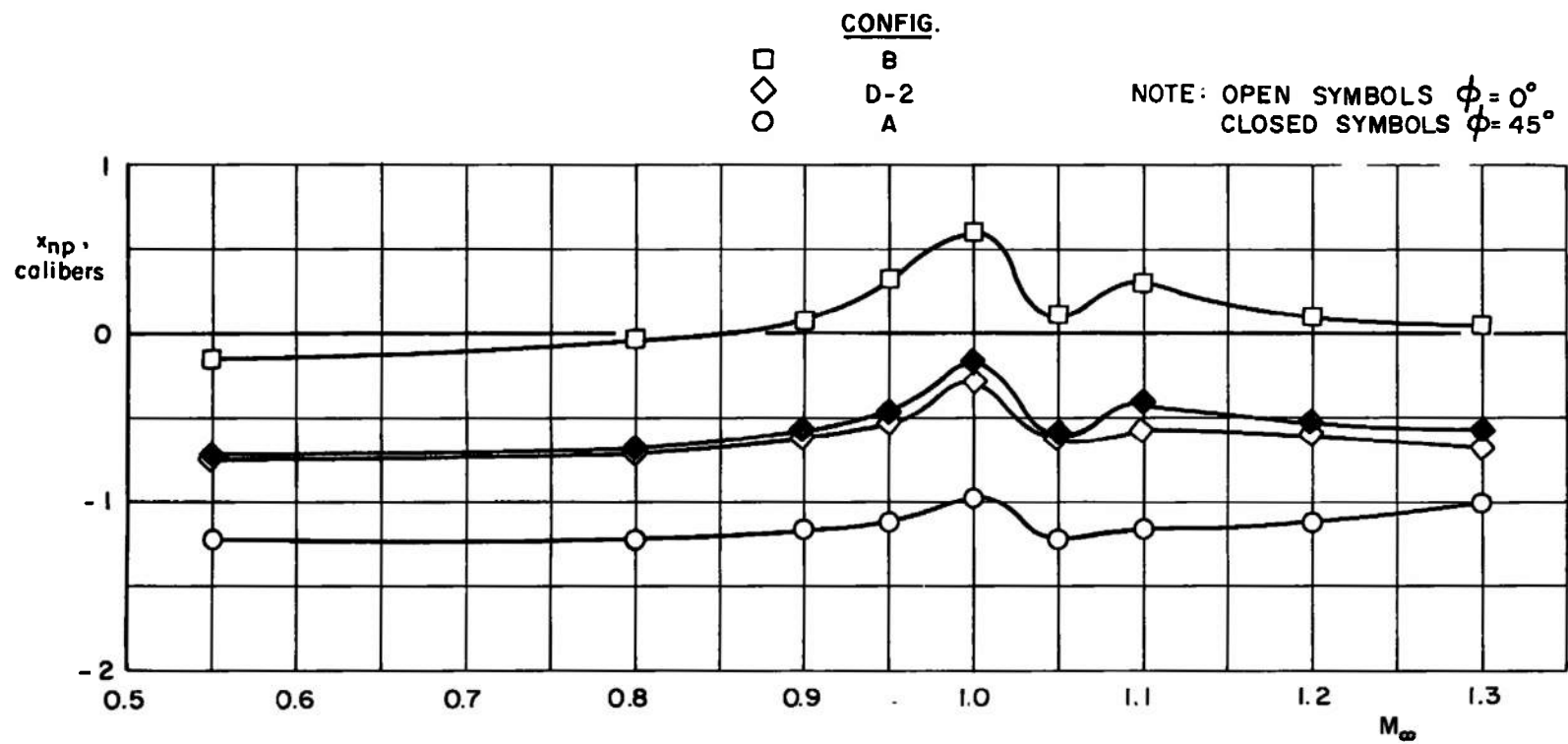


Fig. 17 Neutral-Point Location versus Mach Number Comparing Configurations B, D-2, and A

DOCUMENT CONTROL DATA - R & D

(Security classification of title, body of abstract and indexing annotation must be entered when the overall report is classified)

1. ORIGINATING ACTIVITY (Corporate author) Arnold Engineering Development Center ARO, Inc., Operating Contractor Arnold Air Force Station, Tennessee		2a. REPORT SECURITY CLASSIFICATION UNCLASSIFIED	
		2b. GROUP N/A	
3. REPORT TITLE STATIC STABILITY TESTS OF THE M-117 BOMB AT MACH NUMBERS FROM 0.55 TO 1.30 WITH SEVEN TAIL FIN CONFIGURATIONS			
4. DESCRIPTIVE NOTES (Type of report and inclusive dates) February 26 - March 1, 1968 - Final Report			
5. AUTHOR(S) (First name, middle initial, last name) Paul Lehner, ARO, Inc.			
6. REPORT DATE May 1968.		7a. TOTAL NO. OF PAGES 71	7b. NO. OF REFS N/A
8a. CONTRACT OR GRANT NO AF 40(600)-1200		9a. ORIGINATOR'S REPORT NUMBER(S) AEDC-TR-68-103	
b. PROJECT NO.		9b. OTHER REPORT NO(S) (Any other numbers that may be assigned this report) N/A	
c. Program Element 6441514F			
d.			
10. DISTRIBUTION STATEMENT This document is subject to special export controls and each transmittal to foreign governments or foreign nationals may be made only with prior approval of Ogden Air Materiel Area (OOYEC) Hill AFB, Utah 84401.			
11. SUPPLEMENTARY NOTES Available in DDC		12. SPONSORING MILITARY ACTIVITY Ogden Air Materiel Area (OOYEC) Air Force Logistics Command Hill AFB, Utah 84401	
13. ABSTRACT Wind tunnel tests at Mach numbers from 0.55 to 1.30 and angles of attack from -4 to 20 deg were conducted on a 0.18-scale model of the M-117 Bomb with seven tail fin configurations to determine the static stability characteristics of the bomb. The seven tail fin configurations consisted of the M131A1, MAU 103/B, and five variations of the MAU 103/B fin. The five variations were represented by changes in fin span, chord length, and planform shape. The stability characteristics of the seven tail fin configurations were compared on the basis of neutral-point location with respect to the center-of-gravity location. A suitable fin configuration was found that was stable throughout the range of conditions tested. This document is subject to special export controls and each transmittal to foreign governments or foreign nationals may be made only with prior approval of Ogden Air Materiel Area (OOYEC) Hill AFB, Utah 84401.			
APPROVED FOR PUBLIC RELEASE: DISTRIBUTION UNLIMITED (PER DDC-TAB-71-21, 1 Nov 71)			

14	KEY WORDS	LINK A		LINK B		LINK C	
		ROLE	WT	ROLE	WT	ROLE	WT
	<p>M-117 Bomb</p> <p>transonic flow</p> <p>tail fin configurations</p> <p>stability</p> <p>1. Bombs -- M-117</p> <p>2 " -- Stability</p> <p>3 " -- Transonic flow</p> <p>1-2</p>						